Silvio Mazziotti · Alfredo Blandino

MR Enterography

In collaboration with:
Giorgio Ascenti, Tommaso D'Angelo

Springer

MR Enterography

Silvio Mazziotti • Alfredo Blandino

MR Enterography

In collaboration with:
Giorgio Ascenti, Tommaso D'Angelo

✶ Springer

Silvio Mazziotti
Department of Radiological
Sciences
University of Messina
Messina
Italy

Alfredo Blandino
Department of Radiological
Sciences
University of Messina
Messina
Italy

Foreword

It is with great pleasure and satisfaction that I present this volume dedicated to the potential contribution of magnetic resonance to the management of inflammatory bowel diseases, which are diagnosed today more frequently than in the past.

Authors wisely describe the technical tips, diagnostic pearls, and a variety of cases that they collected over the past 7 years of daily commitment.

The volume approaches this topic in gradual steps, allowing an easy consultation also to the novice, while the expert radiologist will have the opportunity to tailor, modify, and expand his diagnostic approaches. The iconography they collected will allow identifying both the most patent and the subtle signs of the disease in order to allow accurate speculations regarding the stage, predict its evolution, and evaluate the response to therapy.

The text, of straightforward comprehension in all its sections, can offer interesting hints to the reader even if not a radiologist.

My personal appreciation for the rigorous approach of their research is widely deserved by the authors between the most motivated and skilled colleagues of the Department of Diagnostic Imaging that I have the honor to direct.

I express to them my sincere congratulations.

Emanuele Scribano,
Head of Department of Radiological Sciences,
University of Messina,
Messina, Italy

Contents

Contributors

Giorgio Ascenti Department of Radiological Sciences, University of Messina, Messina, Italy

Tommaso D'Angelo, MD Department of Radiological Sciences, University of Messina, Messina, Italy

Chapter 1
Introduction

The prevalence of small bowel diseases is low, and their clinical diagnosis is often complicated by the presence of aspecific symptoms. Moreover, the small intestine has always been a challenging area to investigate by clinical or radiographic means due to its anatomy, location, and relatively tortuosity. The upper gastrointestinal tract, comprising the esophagus, stomach, and duodenum, is accessible by direct endoscopy, as the colon is. The small bowel, however, is beyond the reach of the most flexible endoscopes.

In the past years, barium small bowel follow-through (SBFT) studies and enteroclysis were the standard radiological approaches for diagnosing gut diseases. In particular, SBFT provides information about intraluminal extension of disease and small bowel motility disorders. On the other side, small bowel enteroclysis is more accurate than SBFT at detecting early mucosal changes, but both methods provide only limited, indirect information on the state of bowel wall and of surrounding structures. Moreover, these techniques suffer from problems with overlapping bowel loops.

Nowadays, the diagnosis of Crohn's disease (CD) and the detection of disease activity are the major indications for small bowel imaging in most centers. However, there are many other conditions that may cause similar clinical symptoms or radiological signs to those of CD.

Cross-sectional imaging has a clear advantage in this aspect, and it can also depict clinically unsuspected abdominal diseases that may mimic a flare of inflammatory bowel disease (IBD), such as acute appendicitis or diverticulitis [1, 2].

In the last decade, there has been a renewed interest for small bowel imaging, using a variety of techniques such as ultrasound (US), computed tomography (CT), and magnetic resonance imaging (MRI).

US is a useful radiation-free alternative for evaluating IBD; it is widely available and is not affected by patient motion, making it particularly attractive for children examination [3–7]. In patients with CD, the most widely used criterion for the diagnosis of IBD is bowel wall thickening with increased vascularization at color or power Doppler [3–7].

Although these US findings are rather nonspecific, they can be used to guide further studies, to evaluate the response of inflamed bowel segments to therapy, and to detect postsurgical recurrence of inflammation.

Contrast-enhanced ultrasound (CEUS) of the intestinal tract is a relatively new technique that involves i.v. administration of an ultrasound contrast agent with real-time examination, providing an accurate depiction of the bowel wall microvascularization and the perienteric tissues, thus further improving the therapy planning and the monitoring of the treatment efficacy [8–10].

In small intestine contrast-enhanced ultrasonography (SICUS), performed using an oral contrast agent to distend the bowel (i.e., iso-osmolar polyethylene glycol solution), the sensitivity and specificity of US in detecting IBDs range from 78 to 90 % and 83 to 95 %, respectively [5, 11–13].

US is most effective at detecting IBD in the terminal ileum but may fail to fully delineate complications and to exclude disease elsewhere in the small and large bowel [14].

CT has become a routine examination in the evaluation of gastrointestinal disorders because of its accuracy with axial images and multiplanar reconstruction and rapid execution time. The primary role of conventional CT in patients affected by IBD

was to evaluate extraenteric manifestations and complications, such as fistulas, abscess, and bowel obstruction. Multidetector technology, enabling faster imaging and higher spatial resolution, has increased the role of CT in intestinal diagnostic. In addition to allowing direct visualization of extraenteric structures, CT enterography (CTE), performed using oral neutral contrast agents and rapid intravenous contrast infusion, can be also used to reliably identify findings of active inflammation in the small bowel: wall thickening (thickness >3 mm), mural stratification, mural hyperenhancement, increased attenuation of perienteric fat, and engorged vasa recta [15–17].

Many researchers have mentioned positive correlation between CTE findings and clinical/biochemical markers of disease activity, such as CD activity index (CDAI), C-reactive protein, and erythrocyte sedimentation rate. However, because patients with CD are often young and CD is a chronic and relapsing disease, they may have to undergo lifetime repeated imaging examinations to assess the status of their disease. Although CT is widely used in CD, one significant limitation is represented by patient exposure to ionizing radiation. Recent studies highlighted the high cumulative radiation dosages delivered to patients with CD, mainly due to an increased use of CT [18–20]. The carcinogenic effect of radiation can be particularly significant in patients with CD, who already have an increased risk of developing gastrointestinal or hepatobiliary cancer and small bowel lymphoma.

For the above mentioned reasons, it is neither recommendable to perform serial CT scans, to differentiate a stricture from a badly distended tract (this latter case could be due to slow transit of luminal contrast material or to peristalsis).

With the increasing awareness on the risk of radiation exposure, global interest in abdominal magnetic resonance (MR) imaging has generally improved. Over the last decade, the increased temporal and spatial resolution of MR images, combined with the use of large volumes of oral contrast agents to provide bowel distention, has allowed the evaluation of bowel

wall thickening, wall edema, and contrast enhancement, which are useful findings for the assessment of active ileitis, as well as extraenteric complications [21]. In addition, MRI has the potential advantage of providing functional and quantitative information about bowel wall (e.g., perfusion, diffusion, and motility) that cannot be obtained by CT [22–27]. For these reasons, a new MR technique targeted for the study of small bowel and called MR enterography (MREg) has been introduced as a radiation-free alternative method to evaluate patients with CD, and it is increasingly becoming the first line of investigation for such patients. It can be useful at both initial diagnosis and follow-up [21]; the most important issue is that MRI provides multiplanar images with high contrast resolution for soft tissue, thus enabling differential diagnosis between edema and fibrosis that represents a key issue in patients who suffer from CD.

However, MRI also has some limitations. First of all, MRI of the small bowel requires optimal MR scanner with fast imaging capabilities and a certain degree of operator's experience [21]. Secondly, a rigorous technical approach should be used to obtain satisfactory results.

Although diagnosis of CD and evaluation of disease activity are the major indications for small bowel MRI in most of centers, MREg is recently playing an evolving role in the detection of other enteric diseases, such as postoperative adhesion, celiac disease, radiation enteritis, scleroderma, and small bowel malignancy [28].

References

1. Furukawa A, Saotome T, Yamasaki M et al (2004) Cross-sectional imaging in Crohn's disease. Radiographics 24:689–702
2. Fletcher JG, Fidler JL, Bruining DH et al (2011) New concepts in intestinal imaging for inflammatory bowel diseases. Gastroenterology 140:1795–1806

3. Bremner AR, Pridgeon J, Fairhurst J et al (2004) Ultrasound scanning may reduce the need for barium radiology in the assessment of small bowel Crohn's disease. Acta Paediatr 93:479–481

4. Parente F, Macconi G, Bollani S (2002) Bowel ultrasound in the assessment of Crohn's disease and detection of related small bowel strictures: a prospective comparative study versus x-ray and intraoperative findings. Gut 50:490–495

5. Parente F, Greco S, Molteni M et al (2003) Role of early ultrasound in detecting inflammatory intestinal disorders and identifying their anatomical location within the bowel. Aliment Pharmacol Ther 18:1009–1016

6. Fraquelli M, Colli A, Casazza G et al (2005) Role of US in detection of Crohn disease: meta-analysis. Radiology 236:85–101

7. Parente F, Greco S, Molteni M et al (2005) Imaging inflammatory bowel disease using bowel ultrasound. Eur J Gastroenterol Hepatol 17:283–291

8. Paredes JM, Ripollés T, Cortés X et al (2013) Contrast-enhanced ultrasonography: usefulness in the assessment of postoperative recurrence of Crohn's disease. J Crohns Colitis 7:192–201

9. De Franco A, Marzo M, Felice C et al (2012) Ileal Crohn's disease: CEUS determination of activity. Abdom Imaging 37:359–368

10. De Franco A, Di Veronica A, Armuzzi A et al (2012) Ileal Crohn disease: mural microvascularity quantified with contrast-enhanced US correlates with disease activity. Radiology 262:680–688

11. Bozkurt T, Richter F, Lux G (1994) Ultrasonography as a primary diagnostic tool in patients with inflammatory disease and tumors of the small intestine and large bowel. J Clin Ultrasound 22:85–91

12. Hollerbach S, Geissler A, Schiegl H et al (1998) The accuracy of abdominal ultrasound in the assessment of bowel disorders. Scand J Gastroenterol 33:1201–1208

13. Tarjan Z, Toth G, Gyorke T et al (2000) Ultrasound in Crohn's disease of the small bowel. Eur J Radiol 35:176–182

14. Maconi G, Parente F, Bollani S et al (1996) Abdominal ultrasound in the assessment of extent and activity of Crohn's disease: clinical significance and implication of bowel wall thickening. Am J Gastroenterol 91:1604–1609

15. Rollandi GA, Curone PF, Biscaldi E et al (1999) Spiral CT of the abdomen after distension of small bowel loops with transparent enema in patients with Crohn's disease. Abdom Imaging 24:544–549

16. Bruining DH, Siddiki HA, Fletcher JG et al (2008) Prevalence of penetrating disease and extraintestinal manifestations of Crohn's disease detected with CT enterography. Inflamm Bowel Dis 14:1701–1706

17. Booya F, Akram S, Fletcher J et al (2009) CT enterography and fistulizing Crohn's disease: clinical benefit and radiographic findings. Abdom Imaging 34:467–475

18. Kroeker KI, Lam S, Birchall I et al (2011) Patients with IBD are exposed to high levels of ionizing radiation through CT scan diagnostic imaging: a five-year study. J Clin Gastroenterol 45:34–39

19. Palmer L, Herfarth H, Porter CQ et al (2009) Diagnostic ionizing radiation exposure in a population-based sample of children with inflammatory bowel diseases. Am J Gastroenterol 104:2816–2823

20. Desmond AN, O'Regan K, Curran C et al (2008) Crohn's disease: factors associated with exposure to high levels of diagnostic radiation. Gut 57:1524–1529

21. Mazziotti S, Ascenti G, Scribano E et al (2011) Guide to magnetic resonance in Crohn's disease: from common findings to the more rare complicances. Inflamm Bowel Dis 17:1209–1222

22. Freiman M, Perez-Rossello JM, Callahan MJ et al (2013) Characterization of fast and slow diffusion from diffusion-weighted MRI of pediatric Crohn's disease. J Magn Reson Imaging 37:156–163

23. Tielbeek JA, Ziech MLV, Li Z et al (2013) Evaluation of conventional, dynamic contrast enhanced and diffusion weighted MRI for quantitative Crohn's disease assessment with histopathology of surgical specimens. Eur Radiol. doi:10.1007/s0330-013-3015-7

24. Sharman A, Zealley IA, Greenhalgh R et al (2009) MRI of small bowel Crohn's disease: determining the reproducibility of bowel wall gadolinium enhancement measurements. Eur Radiol 19:1960–1967

25. Menys A, Atkinson D, Odille F et al (2012) Quantified terminal ileal motility during MR enterography as a potential biomarker of Crohn's disease activity: a preliminary study. Eur Radiol 22:2494–2501

26. Froelich JM, Waldherr C, Stoupis C et al (2010) MR motility in Crohn's disease improves lesion detection compared with standard MR imaging. Eur Radiol 20:1945–1951

27. Wakamiya M, Furukawa A, Kanasaki S et al (2011) Assessment of small bowel motility function with cine-MRI using balanced steady-state free precession sequences. J Magn Reson Imaging 33:1235–1240

28. Fidler J (2007) MR imaging of the small bowel. In: Carucci LR (ed) Advances in gastrointestinal imaging. Elsevier Saunders, Philadelphia, pp 317–331

Part I
MR Enterography:
Technique and Anatomy

Chapter 2
Technique

Adequate intestinal distention is the main technical prerequisite for optimal small bowel imaging, as decades of experience acquired by conventional radiology with barium contrast reveal. As a collapsed bowel loop may obscure large lesions or mimic pathological wall thickening, bowel distention is the single most important factor for any method of choice. For this purpose, a large amount of enteric contrast material is used in MR examination of small bowel to achieve luminal distention. Intraluminal contrast material does not only distend the lumen, but it also decreases the susceptibility to develop artifacts by displacing intraluminal air. Actually, MREg is only a generic term, often used to define small bowel MR examination.

The proper MREg technique consists in achieving the bowel distention by oral administration of a large amount of enteric contrast agent. Conversely, when enteric contrast agent is administered through a nasoenteric tube, the term "MR enteroclysis" (MREc) should be preferred [1–3].

2.1 Enteric Contrast Agents

Various kinds of enteric contrast agents have been investigated for MREg and MREc in an attempt to achieve uniform luminal

Enteric contrast agents   T1-W   T2-W

- *positive agents (paramagnetic)*

- *negative agents (superparamagnetic)*

- *biphasic agents (e.g. polyethylene glycol)*

Fig. 2.1 Classification of oral contrast agents. *Positive contrast agents*: high signal intensity on both T1- and T2-weighted images. *Negative contrast agents*: low signal intensity on T1- and T2-weighted images. *Biphasic contrast agents*: low signal intensity on T1-weighted images and high signal intensity on T2-weighted images

distention with minimal mucosal absorption. Other important considerations include no significant adverse effects, absence of artifacts, and low cost. The optimal contrast agent should provide adequate distention of the small bowel for the whole duration of the examination and be well tolerated by the patient.

Contrast agents can be classified into three categories, according to their signal intensity on the pulse sequences used:

(a) *Positive agents* that demonstrate high signal intensity on both T1- and T2-weighted images
(b) *Negative agents* that demonstrate low signal intensity on both T1 and T2 images
(c) *Biphasic agents* that demonstrate different signal intensities on different sequences (Fig. 2.1) [1, 4, 5]

Positive contrast agents are characterized by hyperintensity on both T1- and T2-weighted images. They consist of paramagnetic substances such as gadolinium chelates, ferrous

ammonium citrates, manganese chloride, and food products (e.g., blueberry juice, pineapple juice) [6–8]. These contrast agents reduce T1 relaxation time, while T2 relaxation time is usually not affected. However, due to high water content of the solutions, they are also seen as hyperintense on T2-weighted images [9]. Positive contrast agents are generally disfavored because their high T1 signal interferes with evaluation of inflammatory mucosal and mural enhancement or of intraluminal lesions after i.v. contrast administration.

Negative contrast agents are characterized by hypointensity on both T1- and T2-weighted sequences. They make use of superparamagnetic particles such as iron oxides, perfluorooctyl bromide, and oral magnetic particles [3, 6, 7, 10–13]. Barium sulfate can also be used as a negative agent when administered at high concentrations, but the signal loss is not as great as with the superparamagnetic particles [9]. These contrast agents induce local dishomogeneity in the magnetic field, affecting both T1 and T2 relaxation times. They may improve the conspicuity of wall edema on T2-weighted sequences as well as the detection of extraluminal fluid collections. Due to their intraluminal loss of signal intensity, bowel wall enhancement will be more remarkable on T1-weighted images.

Superparamagnetic particles have a small incidence of side effects (5–15 % of cases) mainly related to the gastrointestinal tract (suboptimal palatability, nausea, vomiting, and rectal leakage) [5]. Moreover, if negative contrast agents are not homogeneously distributed throughout the bowel loops, they can produce paradoxical high signal intensity.

The preferences of many authors are currently directed toward the use of *biphasic contrast agents* and in particular for those characterized by low signal intensity on T1-weighted images and high signal intensity on T2-weighted images [3]. Following i.v. contrast administration, the low signal intensity on T1-weighted images provides a better resolution between bowel lumen and the hyperenhancing wall inflammation or masses.

Moreover, these agents allow the assessment of fold thickness on T2-weighted images.

The biphasic category contains the largest number of available agents, including water, osmotic agents, non-osmotic bulking agents, and polyethylene glycol, each having unique advantages and limitations.

Although water is readily available, better accepted by the patients, and cheap, it is rapidly absorbed from distal bowel; therefore, adequate distention may not be obtained.

To obviate this problem, osmotic agents such as mannitol have been used, but these agents can cause osmotic effects in the small bowel such as diarrhea, meteorism, and abdominal cramps, which nonetheless are less significant when low-concentration solutions are used (mannitol 2.5 %) [14, 15].

Non-osmotic bulk agents such as locus bean gum and methylcellulose have been also evaluated; however, they are not widely available [15, 16].

Polyethylene glycol (PEG) solution is a hydrophilic molecule with a low partition coefficient, which determines an inconsistent transmembranous diffusion in the lipid phase. It also has a transversal diameter that does not allow it to pass through the intestinal mucosa, so it does not undergo intestinal absorption. Therefore, PEG simulates the properties of water with the advantage of non-absorbability, providing good distention of the entire small bowel. The main problem of PEG solution is that it can lead to rapid bowel transit and a strong urge to evacuate that can interfere with completion of the examination [3, 17–20].

Among the other biphasic agents, manganese and gadolinium chelates must be considered; in fact they are seen as low signal intensity on T2-weighted images and high signal on T1-weighted images when administered at high concentrations [6].

Barium products at lower weight per volume can also act as biphasic contrast agents being well tolerated by patients and providing good intestinal distention [5].

2.2 Patient's Preparation and Positioning

Adequate patient's preparation is mandatory because MR of the small bowel is a time-consuming technique and requires extensive hospital resources.

Patients undergoing MREg/MREc will stop ingesting solids and liquids at least 6–8 h before the examination and water up to 1–2 h prior. Instructing patients to fast before the procedure improves compliance and tolerance for ingestion of oral contrast material and ensures homogenization of bowel activity. No bowel cleansing is required.

Sedation is avoided in patients undergoing small bowel MR due to the need of patient's collaboration for assuming enteric contrast agent.

As previously said, the use of biphasic contrast agents is preferable in MREg as well as MREc.

MREc was the first dedicated MRI method for evaluating small bowel in CD and was based on the fluoroscopic enteroclysis technique. This procedure requires that the intestinal distention is achieved via the administration of contrast material through a prepositioned nasojejunal balloon-tipped catheter [3, 5]. The placement of the catheter should be preferentially obtained under fluoroscopic guidance in a separate radiology room not to slow the work of MR suite. Balloon inflation minimizes contrast reflux back to the stomach. The instillation of contrast was originally performed in the fluoroscopic suite prior to patient transfer to MR room. Using this approach, the patient was exposed to ionizing radiations.

Nowadays, with the advent of ultrafast dynamic thick-slab (e.g., 70–180 mm) MR technique (MR fluoroscopy), contrast is now routinely instilled under "real-time" MR guidance until adequate small bowel distention is obtained. Enteric contrast material can be administered by manual injection with handheld MR-compatible infusion devices or with automated pumps,

while the patient is in the MR scanner [3, 5]. The volume and the speed of infusion are crucial for the success of examination. Depending on the subject, the volume generally varies between 1,500 and 3,000 ml with an infusion rate ranging from 80 to 200 ml/min. In MREc, the contrast medium is administered in three phases:

(a) A low infusion rate of 80–100 ml/min is used during the first phase, which lasts until terminal ileum begins to distend.
(b) In the second phase, the infusion rate increases up to 200 ml/min to achieve reflex atony (note that if the infusion rate increases too fast, retrograde filling can often occur, and this may result in patient's vomiting).
(c) During the third phase, the infusion rate decreases again to 80–100 ml/min, to guarantee adequate distention of the proximal jejunum until the acquisition of cross-sectional images is performed.

MREc provides optimal distention of the bowel wall and can show detailed luminal information useful to identify early mural changes. However, these advantages have to be counterbalanced by the complexity of the procedure and by the associated patient discomfort. Moreover, an excessive distention of the bowel loops can lead to a worse assessment of the mesenteric structures, which may be compressed by nearby loops.

The MREg technique has been developed as a noninvasive alternative to MREc, due to the fact that a significant portion of patients refuses nasojejunal catheter placement. Enterography technique requires the ingestion of a large amount of fluid that fills the stomach and the small bowel in continuity.

Several different ingestion algorithms have been proposed, and they are determined by the bowel transit time of the contrast agent used and by the amount given.

In the case of PEG electrolyte solution, a total amount of 1,500–1,800 ml is generally administered within 40–60 min prior to scanning. The first 500–600 ml is ingested over the first

10–15 min and two 500–600 ml aliquots, respectively, 20–25 and 10–15 min prior to scanning, to obtain a sufficient luminal distention and to guarantee an accurate detection of lesions. Using this approach, a reasonable small bowel distention is obtained. In fact, in the majority of cases, distal small bowel is well distended in spite of proximal jejunal distention that can be variable. For this reason, some authors proposed serial acquisitions with initial imaging at 20 min after contrast medium ingestion, to assess jejunal loops in the early scans and ileum and terminal ileum in the latter scans [21].

With regard to pediatric patients, the volume of oral contrast is usually adjusted between 300 and 1,000 ml according to the weight of the subject.

Nausea and vomiting caused by oral contrast ingestion are reduced by antiemetic medication so that examination can be comfortably performed.

Although we aim for a total of 1,500–1,800 ml, some patients cannot tolerate this volume ingestion, and adequate results may be still achieved with as little as 500–600 ml. For this reason, the examination could proceed even if only a small volume of oral contrast was ingested.

Due to the poor tolerability of nasojejunal tube insertion or to excessive and uncomfortable bowel distention of MREc, in our practice we recur to enteroclysis only for the evaluation of patients unable or unwilling to ingest oral contrast for enterography.

The addition of a rectal water enema provides a better visualization of the terminal ileum and may be considered an adjunct to facilitate the evaluation of colon. However, rectal enema is not routinely performed because the colon is readily accessible at colonoscopy; anterograde filling is also possible and may be more tolerable.

To increase the signal-to-noise ratio, the patient is imaged using an abdominal phased-array radio-frequency surface coil, in either the supine or prone position (if no stoma is present).
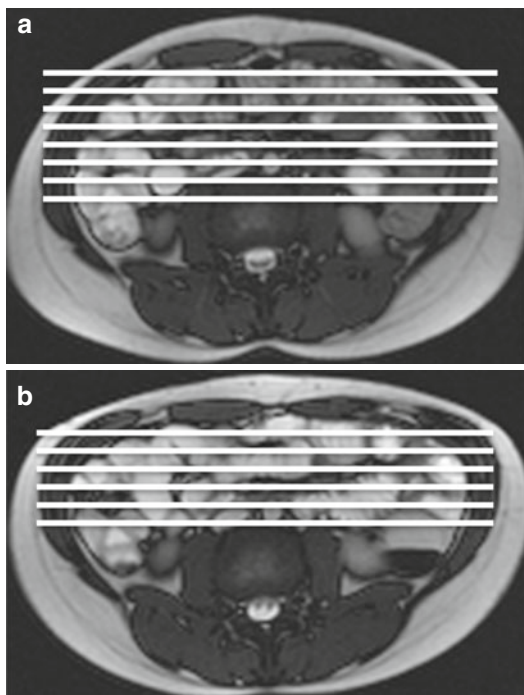
Fig. 2.2 Axial scout images obtained in supine (**a**) and prone position (**b**). Abdominal compression consequent to prone position (**b**) allows to reduce the anteroposterior diameter and to acquire a reduced number of coronal slices with respect to supine position (**a**)

Although MRI is routinely performed in supine position for a better patient's comfort, the preferred scanning position should be prone in order to facilitate elevation and separation of small bowel loops out of the pelvis. Moreover, this position produces a degree of abdominal compression, reducing the number of section required for each coronal acquisition, which in turn reduces the length of breath-hold required, resulting in improved patient compliance (Fig. 2.2). It has been also shown that it improves small bowel distention (Fig. 2.3) and that this position is safer if the patient should vomit.
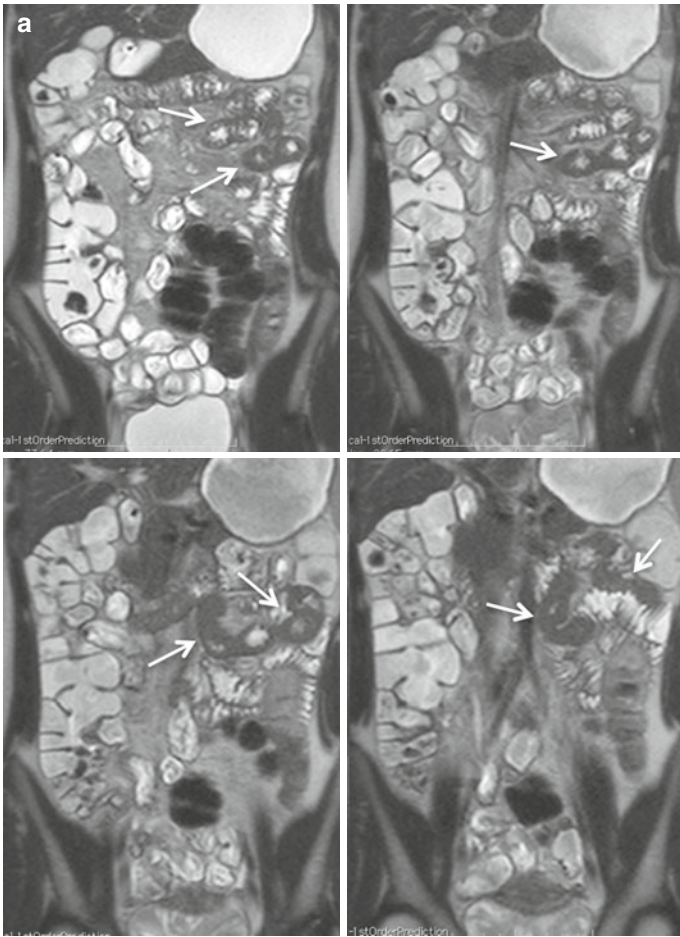
Fig. 2.3 Coronal HASTE images obtained in the same patient in supine (**a**) and prone position (**b**). In supine position (**a**), the poor distention of jejunal and proximal ileal segments can lead to difficulties of interpretation, as the result of apparent thickening of the bowel wall (*arrows*). Prone imaging (**b**) results in significantly higher small bowel distention and better bowel loops separation, excluding any pathological wall thickening
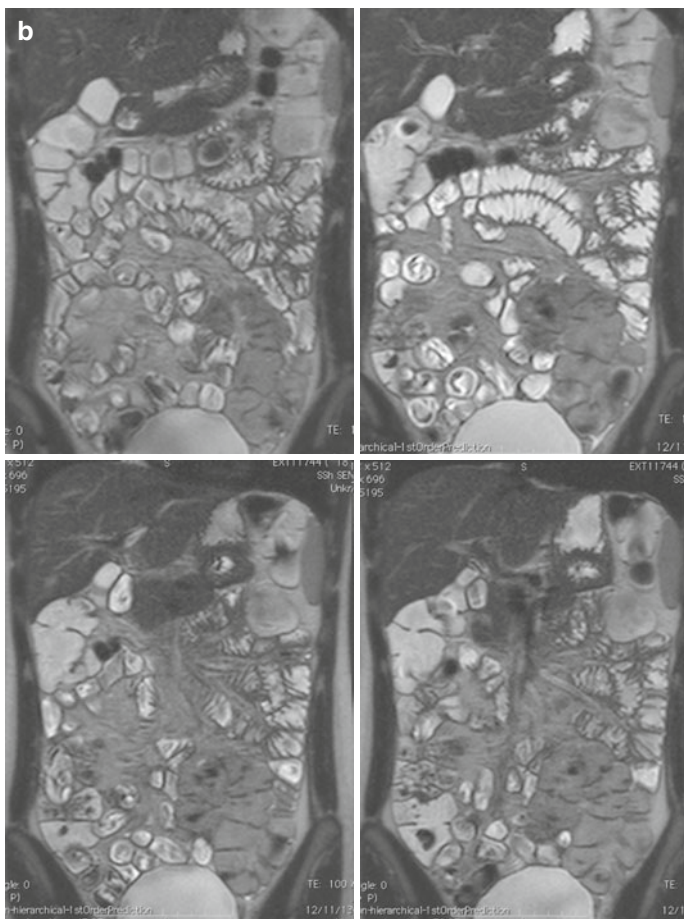
Fig. 2.3 (continued)

There are no specific contraindications to MREg/MREc, except those typical for MR (e.g., metal implants in delicate positions, aneurysm clips, shrapnel injuries, pacemakers, internal defibrillators, etc.). A relative contraindication to MR examination could be considered the inability to receive gadolinium-based contrast medium (patients with a low glomerular filtration rate, who are at risk for nephrogenic systemic fibrosis or pregnant patients). However, it should be noted that in these cases the examination could be performed without i.v. contrast material, allowing one to obtain useful findings in CD.

2.3   Protocols and Sequences

In the past, motion artifacts and poor contrast resolution precluded the use of MR for bowel imaging. Technological advances, including the use of breath-hold sequences, improved coils, fat suppression, and intravenous gadolinium, have extended the role of MRI in the evaluation of gastrointestinal tract [5]. Since then, several different pulse sequences to evaluate the small bowel have been advocated by different authors. However, non-sole sequences can be used for exhaustive imaging of CD, as each sequence has its specific advantages and drawbacks: several pulse sequences may be performed and are complementary to overcome the limitations of others.

Imaging protocols vary because of differences in available equipment and personal preferences. However, despite differences in MR equipment and software, certain basic elements are common to most imaging protocols for CD [22–24]. In general, fast sequences, capable of acquiring T2-weighted and contrast-enhanced T1-weighted images in a single breath-hold reducing motion and respiratory artifacts, are the most helpful, especially with the use of biphasic contrast agent.

Once adequate small bowel distention has been obtained, the basic MREg pulse sequence protocol is substantially the same as for MREc and includes three essential sequences acquired in coronal and axial planes:

- Half-Fourier acquisition single-shot turbo spin echo
- Balanced steady-state free precession
- Pre- and post-contrast T1-weighted ultrafast gradient echo

2.3.1   Half-Fourier Acquisition Single-Shot Turbo Spin Echo (HASTE)

HASTE sequence is an adaptation of RARE that reduces total acquisition time by acquiring only half of k-space. Different manufactures call these sequences *single-shot fast spin echo* (*SSFSE*). These sequences provide heavily T2-weighted images in less than one second with high contrast between the lumen and the bowel wall. As these sequences are highly resistant to magnetic susceptibility or chemical shift artifacts, the wall thickness may be accurately evaluated [3, 22–24]. Moreover, sinus tract, fistulas, and collections are well visualized. HASTE sequences are susceptible to motion artifacts of fluids within the visceral lumen (propulsive intestinal movements), which may result in intraluminal low-signal-intensity artifacts and appearance of "pseudo-lesions" (Fig. 2.4) [3]. Due to k-space filtering effects, visualization of the mesenteric structures such as mesenteric vessels and lymph nodes is impaired. The optional use of fat saturation allows differentiation between submucosal fat and edema which appear both bright on T2-weighted images. Fat saturation also increases the conspicuousness of edematous bowel loops and the contrast between the intestinal wall and the surrounding fat tissue. Fat-suppressed HASTE sequences are particularly useful when i.v. contrast material administration is contraindicated to assess parietal inflammatory infiltration and
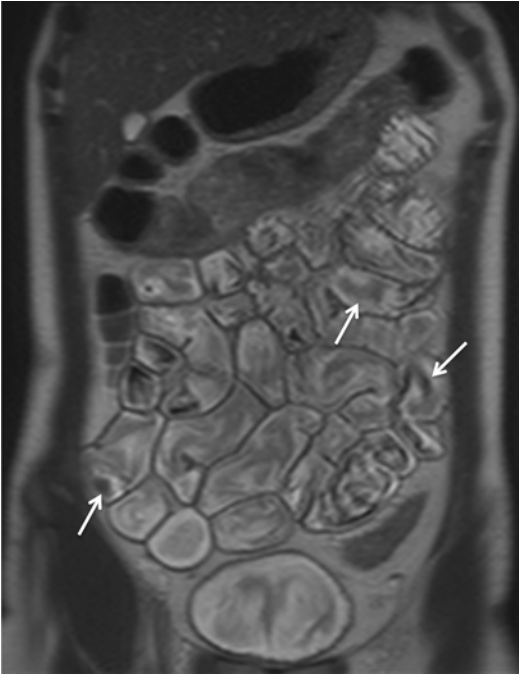
Fig. 2.4 Coronal HASTE image. Normal small bowel. Intraluminal flow voids, secondary to bowel peristalsis, are seen (*arrows*)

to reveal inflammation of the peritoneal fat tissue [3]. Moreover, the use of fat saturation allows the acquisition of thicker sections to demonstrate all bowel loops on a single image (Fig. 2.5).

2.3.2 Balanced Steady-State Free Precession (Balanced SSFP)

Another sequence promoted for imaging of the small bowel is the balanced SSFP. Other vendors call these sequences *fast*
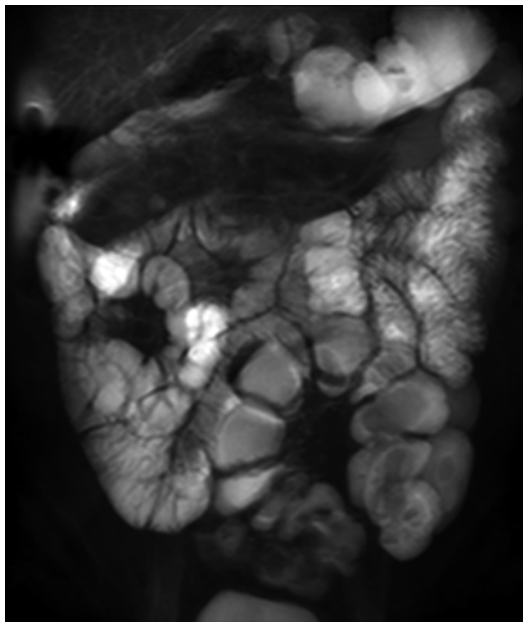
Fig. 2.5 Coronal thick-slab HASTE image (50-mm thickness) obtained with fat saturation showing several bowel loops in a single image

imaging with steady-state acquisition (*FIESTA*), *balanced fast field echo* (*balanced FFE*), and *true fast imaging with steady-state precession* (*TrueFISP*).

This sequence consists of a balanced gradient-echo sequence where image contrast is dependent on T2/T1 ratio for each tissue. The ratio of T2/T1 contrast essentially reflects the T2 differences in tissues as repetition time and echo time are so short that T1 is almost constant: tissues with a T2 value approaching their T1 value appear brightest. Moreover, these sequences eliminate phase shift caused by motion, and thus both fluid and blood appear bright. Due to the extremely short acquisition time, with each image acquired in a few hundred milliseconds,

Fig. 2.6 Coronal TrueFISP image. Normal small bowel with uniform intraluminal signal and high contrast between bowel wall and lumen. The "black-boundary" artifact may not be confused with wall thickening

they are relatively insensitive to motion artifacts, providing uniform intraluminal signal and leading to a high contrast between the bowel wall, lumen, and mesentery (Fig. 2.6). In particular, mesenteric vessels and adenopathies are better visualized on these sequences than on the HASTE sequences.

A limitation of this sequence is represented by a black-boundary artifact at the interface of the bowel wall and mesenteric fat that may mask small lesions and impede a correct assessment of bowel wall thickening due to a possible overestimation

(Fig. 2.6) [22, 23]. This cancellation of signal at boundaries is caused by opposed phases of protons in water and fat within a voxel at certain echo times (i.e., when echo times of around 2.3 ms are used at 1.5 T). Fat suppression may help in reducing the effects of the black-boundary artifact.

Susceptibility artifact occurs with the presence of intraluminal gas or ferromagnetic material, leading to image distortion.

Off-resonance artifacts occur in the presence of a nonuniform magnetic field, resulting in banding artifact at the periphery of the image. Applying built-in shimming procedures during examination can reduce them.

2.3.3   Pre- and Post-contrast T1-Weighted Ultrafast Gradient Echo

For T1 weighting, gradient-echo sequences are usually performed, as these permit short repetition times, resulting in a very short acquisition time. These can be acquired as either two-dimensional (2D) (*fast spoiled GRASS*, *fast SPGR*; *turbo fast low angle shot*, *turbo FLASH*; *turbo field echo*, *TFE*) or three-dimensional (3D) (*fast acquisition with multiphase EFGRE 3D*, *FAME*; *volumetric interpolated breath-hold examination*, *VIBE*; *T1 high-resolution isotropic volume examination*, *THRIVE*) sequences (Figs. 2.7 and 2.8a).

With a 3D sequence, a radio-frequency pulse excites a thick volume of tissue rather than a thin 2D section. If a large area is covered with 2D acquisitions, separate breath-holds will be required, which can lead to respiratory misregistration.

3D gradient-echo sequences allow thinner collimation. The volumetric data can be reconstructed in any plane, providing increased through-plane and in-plane spatial resolution as well as offering higher signal-to-noise ratio compared with 2D sequences (Fig. 2.8b, c). However, because of the relatively
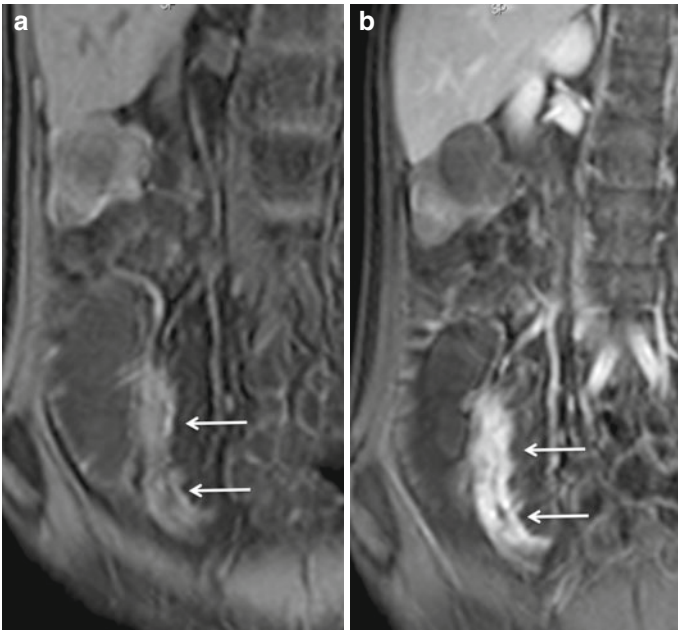
Fig. 2.7 Coronal fat-suppressed 2D GE T1-weighted image obtained before (**a**) and after i.v. contrast medium administration (**b**) in a patient with active Crohn's disease of the terminal ileum (*arrows*)

greater length of the volumetric acquisition, 3D is more sensible to motion, causing blurring (Figs. 2.9 and 2.10).

Fat saturation can be used to increase contrast resolution facilitating the visualization of the bowel wall, which has high signal intensity.

T1-weighted images are routinely obtained before and after i.v. injection of gadolinium.

After i.v. contrast administration, fat saturation also increases the conspicuity of the normal bowel wall allowing the

characterization of a lesion by assessment of its enhancement pattern [1, 3, 22–24].

A limitation of gradient-echo sequences in general is the increased sensitivity to magnetic susceptibility effects.
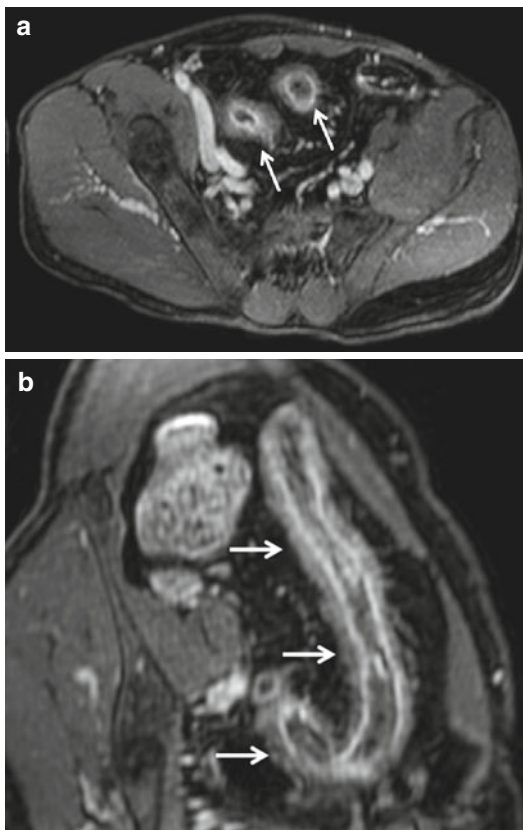
Fig. 2.8 Axial fat-suppressed 3D GE T1-weighted image obtained with i.v. contrast material (**a**) in a patient with active inflammation of the terminal ileum (*arrows*). Oblique-coronal (**b**) and sagittal (**c**) reformatted images well depict the length of the pathological ileal segment (*arrows*)
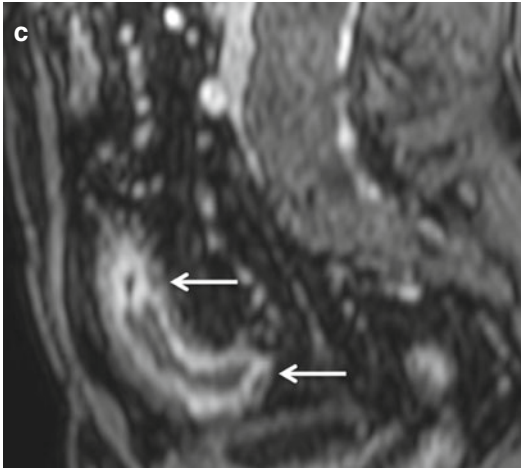
2.8 (continued)
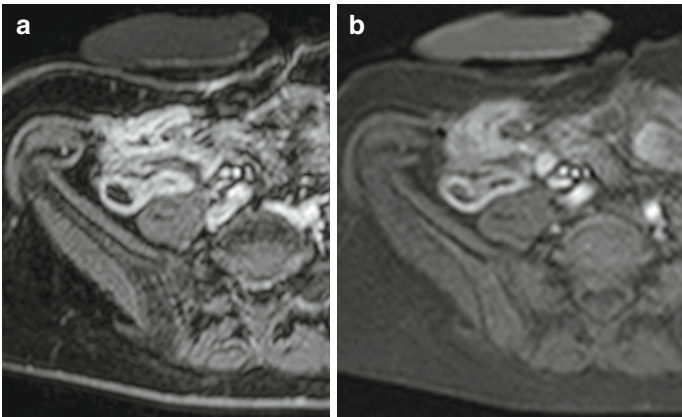
Fig. 2.9 Comparison of 2D and 3D GE T1-weighted sequences in a patient with ileo-colectomy and right ileo-cutaneous stoma. Axial 2D GE T1-weighted image (**a**) and axial 3D GE T1-weighted image (**b**) with fat suppression after i.v. contrast material administration show active inflammation of neoterminal ileum. Note the slight increased blurring of the 3D GE sequence (**b**)
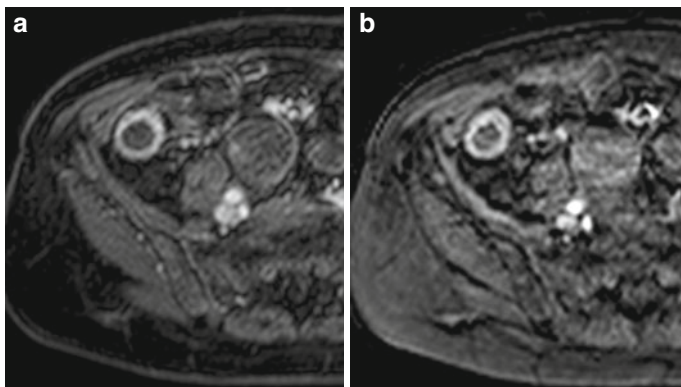
Fig. 2.10 Comparison of 2D and 3D GE T1-weighted sequences in a patient with active Crohn's disease of terminal ileum. Axial 2D GE T1-weighted image (**a**) and axial 3D GE T1-weighted image (**b**) with fat suppression after i.v. contrast material administration show active inflammation of terminal ileum. Note the slight increased blurring of the 3D GE sequence (**b**)

2.4   Spasmolytics

One of the main limitations during the MR examination of the small bowel is represented by the peristaltic motion artifacts, which are more evident in T1-weighted fast-gradient-echo sequences performed after i.v. administration of contrast material (particularly with the motion-sensitive T1-weighted 3D gradient-echo sequences).

These artifacts can potentially hide relevant findings or determine false-positive lesions, such as the intraluminal flow artifacts, previously described in HASTE sequences.

Bowel peristalsis can be reduced by i.v. administration of a spasmolytic agent. This usually consists of 20 mg intravenous hyoscine-N-butylbromide (Buscopan, Boehringer Ingelheim, Germany), or when contraindicated or not tolerated (e.g., history of cardiac arrhythmia, narrow angle glaucoma, or prostatism), 1 mg intravenous glucagon is given as alternative (unless patients have a known hypersensitivity to glucagon or a history of pheochromocytoma).

Intravenous administration of spasmolytic agents is usually performed immediately before the acquisition of contrast-enhanced T1-weighted sequences, although some centers reported the use of a double separated injection, one prior to beginning the examination and a second immediately prior to i.v. contrast administration.

It should be considered that using spasmolytics in routine MREg determines an additional amount of time, due to the patient removal from MR scanner bore, management of eventual side effects (if they occur), and examination restart.

Moreover, recent studies and our personal experience demonstrated that the administration of these agents might be not strictly necessary [25]. In fact it has to be said that the beneficial effects of spasmolytics in MR imaging are more evident in healthy bowel rather than diseased one. This is due to the fact that both fibrosis and bowel wall inflammation determine a decreased bowel motility, thus a less susceptibility to motion artifacts.

Finally, the built-in redundancy of MR examination, which allows evaluation of each bowel segment at multiple time points, can demonstrate whether a questionable segment is affected by disease or if it is just underdistended at the time of image acquisition, further reducing the usefulness of spasmolytic agent (Fig. 2.11).
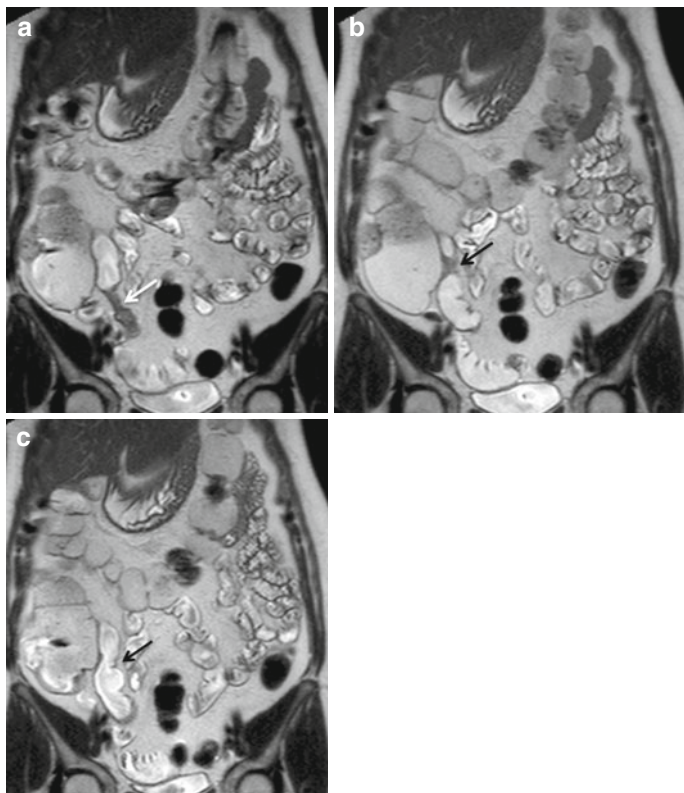
Fig. 2.11 Coronal HASTE images sequentially acquired at multiple time points (**a**–**c**). In the first image (**a**), a luminal narrowing of the terminal ileum might simulate a fibrotic stricture (*white arrow*); subsequent MR acquisitions (**b**, **c**) show the distension of the ileal segment, allowing the correct diagnosis of a functional bowel spasm (*black arrow*)

2.5   Intravenous Contrast Agent

Intravenous administration of gadolinium chelates is very important to assess parietal enhancement of inflamed bowel or lymphadenopathy, and when it occurs, it allows to better delineate sinus tracts and fistulas.

T1-weighted images are routinely obtained before and 70 s after i.v. injection of gadolinium at a dosage of 0.2 mmol/kg and a flow rate of 3.5 ml/s, which is followed by a bolus of 10–20 ml isotonic saline at 3.5 ml/s flow rate. Although pump injection of contrast material is optimal, adequate results may be achieved also with hand injection.

Fast-ultrafast gradient-echo sequences performed with both 2D and 3D acquisition are usually chosen, preferably implementing fat saturation to increase contrast resolution and to allow a better assessment of bowel enhancement.

To have a more sensitive visualization of progressive transmural bowel wall enhancement pattern, multiphasic post-contrast acquisition may be performed during the arterial (30 s), portal venous (60–75 s), and interstitial/delayed (3/10 min) phases, using bolus triggering once contrast reaches the descending aorta.

However, it has to be said that gadolinium chelates should not be given in patients with renal impairment, due to the potential long-term risk of nephrogenic systemic fibrosis. Moreover, gadolinium is a category C medication and should not be routinely administered to pregnant patients.

2.6 Advanced MR Techniques

Beyond these standard sequences, modified protocols and newer sequences are promising to further improve the diagnostic utility of MR imaging of the small bowel. Assessing small bowel motility alterations and grading the disease activity are the latest goals to reach; for this reason, there is an increasing interest to obtain additional functional information and to calculate quantitative parameters related to histopathological severity of acute inflammation, which besides correlating with clinical findings may predict the clinical course, allowing a rational use of immunosuppressive therapies.

2.6.1   MR Fluoroscopy

As it was previously mentioned, MR fluoroscopy is routinely used during MREc to evaluate oral contrast agent progression in the small bowel [26].

MR fluoroscopy can be performed with a 2D single-shot T2-weighted turbo spin-echo sequence, the same routinely employed in MR cholangiopancreatography and MR pyelography. Ultra-long echo trains in the heavily T2-weighted images provide selective static fluid visualization with complete background suppression. Fat suppression further reduces the remaining signal intensity of the fat so that exclusively fluid is displayed with high signal intensity. Moreover, the use of this sequence in the MR evaluation of the small bowel offers the further advantage of a panoramic view, similar to SBFT, with which the gastroenterologists are usually more confident.

We further developed this technique obtaining MR-fluoroscopy imaging of the small bowel also during routine MREg diagnostic protocol.

This revised technique presumes that the patient, in prone position inside MR scanner, can assume the oral contrast through a drinking straw for the whole duration of fluoroscopic acquisition (Fig. 2.12).

MR-fluoroscopy images are oriented in the coronal plane with a section thickness of 100–180 mm to include the entire intestine and the stomach. Initially, one image is acquired before the oral administration of PEG solution, and subsequent images are obtained every 1–2 min.

This technique provides real-time monitoring and documentation of gastroduodenal and small bowel filling also allowing information about the peristalsis efficiency, thus implementing MREg to better depict proximal jejunal tract (Fig. 2.13).

MR-fluoroscopy images can also be reviewed in a cine-loop format to obtain functional information concerning bowel obstruction.

Fig. 2.12 Picture showing the patient, in prone position inside the MR scanner, assuming oral contrast agent from a drinking straw during MREg

On MR-fluoroscopy images, fluid-filled bowel loops are not the only structures displayed, but other abdominal static fluid, such as the biliary system, pancreatic duct, urinary tract, as well as ascites, are also depicted.

A small amount of ascites does not impair the image quality, but large amount of ascites may obscure small bowel loops (Fig. 2.14).

2.6.2   Cine MR

In addition to morphological evaluation, MR of the small bowel allows the visualization and analysis of ileal motility with ultra-fast imaging techniques (*cine MR*) [27]. In disease states and

Fig. 2.13 Functional information provided at MR fluoroscopy with progressive filling of the normal small bowel

particularly in CD, inflammatory infiltration of the bowel wall should adversely affect motility. Moreover, additional factors over and above acute inflammation may affect motility, including drug regimens, disease duration, location, coexistence of colitis, previous surgery, and mural fibrosis.

Balanced SSFP is an ultrafast imaging sequence providing motion-free images with T2-like contrast, which has been previously used in cardiac imaging.

With technical development, a SSFP sequence now allows high temporal resolution imaging of the whole length and width of the abdomen in a coronal slice with subsecond repetition times
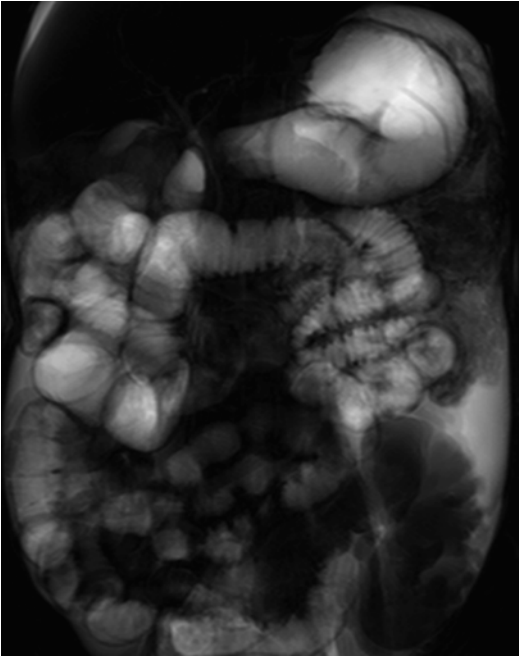
Fig. 2.14 MR-fluoroscopy image in a patient with ascites. The superimposition of hyperintense peritoneal fluid reduces the visibility of bowel loops

during a single breath-hold [22]. The resulting cine sequence is suitable to monitor the small bowel motility function.

Coronal imaging in prone position is preferably used to separate the bowel loops and also to reduce the displacement of the intestinal structures out of the imaging section.

Several cine sequences of 20 frames are performed using a 1-cm-thick coronal two-dimensional balanced SSFP. This sequence has a temporal resolution of 0.5 s indicating that in every 500 ms a new image on the same plane is acquired (Fig. 2.15).
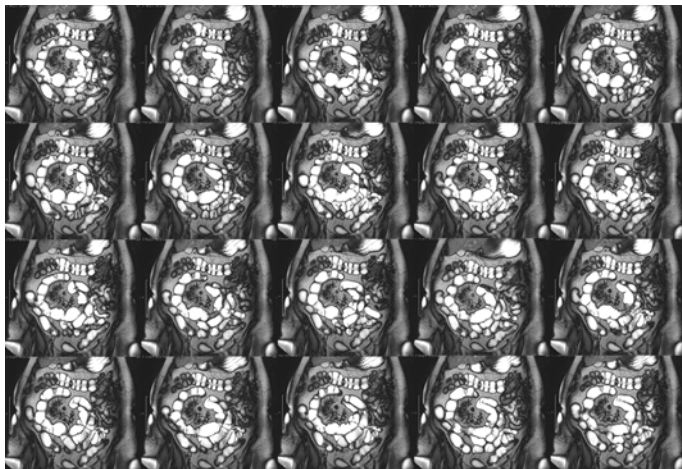
Fig. 2.15 Cine-MR sequences acquired along the same coronal plane which show functional information about small bowel motility

Depending on the size of patient, this cine sequence could be repeated stepwise in 15–25 series over the entire abdomen from anterior to posterior without a gap in between.

The cine-MR sequences can be performed repetitively anytime, with total examination time only slightly prolonged for each patient.

The evaluation of the cine sequences can be simply limited to qualitative criteria without measuring the peristaltic frequency; the motility changes are identified as zones of abnormal peristalsis in comparison with surrounding bowel segments.

Recently, software methods have been developed to automatically assess small bowel contractions as well as quantitatively analyze the motility [28, 29]. Such software can quantify changes in luminal diameter over a time series and ultimately may better characterize abnormal patterns of peristalsis in diseased bowel. Post-processing software has been elaborated to facilitate these investigations by reducing the time needed for evaluation of small bowel motility with high reproducibility.

Cine-MR sequences are becoming routine in MREg/MREc protocols. Motility, considered as a functional parameter, has been shown to significantly increase the lesion detection rate for CD-related pathological findings in comparison with only morphological MR assessment. Evaluation of small bowel motility could provide additional information about disease status or severity. However, it has to be said that cine MR cannot be used alone as a diagnostic tool. This technique is valuable for showing motility alterations, while the specific CD findings (e.g., wall thickness, stenosis, layering, or contrast enhancement) can only be detected on the static images.

2.6.3   Diffusion-Weighted Imaging

Diffusion-weighted imaging (DWI) is a noninvasive method deriving its image contrast from differences in the motion of water molecules between tissues, and it is sensitive to water molecules exhibiting restricted diffusion.

DWI is increasingly becoming a standard sequence in body MR protocol [23]. In particular, recent hardware and technical developments such as rapid echo planar imaging (EPI), high gradient amplitudes, multichannel coils, and parallel imaging have made DWI a feasible sequence for abdominal imaging.

Apparent diffusion coefficient (ADC) can be calculated as a quantitative measure of diffusion restriction.

Much of the attention has been primarily focused on the role of DWI in evaluating patients with cancer. Oncologic applications of DW imaging take advantage of restricted diffusion shown by most tumors. The higher cellularity of solid tumors and their increase in cell membranes per unit volume result in restriction of water movement and corresponding high signal intensity on b-value images.

It has long been recognized that certain inflammatory processes may cause restricted diffusion. Although this phenomenon is more challenging to explain and is likely multifactorial,

it has nevertheless led to an emerging interest in using DWI as a quantifiable indicator of abdominal inflammation.

DWI can be considered a promising diagnostic tool for detecting and assessing inflammation in the bowel affected by CD [30, 31].

DW images are routinely obtained using a diffusion factor *b* fixed at 0 and 600 or 800 s/mm^2 in the axial plane. These parameters are used in most of clinical protocols, representing the best compromise between signal-to-noise ratio (SNR) and sensitivity in detecting lesions.

Intestinal inflammatory lesions are characterized by brighter signal in the DW images and lower ADC values compared to normal segments.

Hence, DWI can be considered a well-tolerated, non-time-consuming tool to evaluate inflammation in small bowel CD.

2.6.4   Perfusion (DCE-MRI)

On conventional multiphasic contrast enhancement study, a qualitative evaluation to determine the degree of enhancement can be obtained by using a subjective categorical scale "low-mild-high" or, more objectively, by comparing bowel enhancement with the renal or hepatic one. Several authors attempt to quantify the degree of bowel wall enhancement by calculating an "enhancement ratio" (ER) obtained dividing post-contrast signal intensity by baseline signal intensity.

In perfusion imaging, analysis of the time-dependent changes of signal intensity after gadolinium chelate administration by dynamic contrast-enhanced MRI (DCE-MRI) reflects the status of tissue microcirculation and can add other feasible parameters to correlate with clinical disease grading [9, 22, 32]. In fact, compared with normal bowel, diseased bowel wall demonstrates early and intense uptake of contrast that increases over time until a plateau is reached. The difference in enhancement pattern and dynamics is also observed between active and inactive diseases [33–35].

A dynamic 3D T1-weighted fast spoiled GE sequence is performed with high temporal resolution through the abnormal bowel before, during, and after the administration of a single dose of contrast medium, injected into an arm vein at 3 ml/s and followed by 10–20 ml saline flush.

Using this technique, it is possible to evaluate the enhancement as a function of time and to calculate semiquantitative and quantitative parameters for evaluating perfusion.

In particular, semiquantitative methods refer to the use of parameters that describe the enhancement curve (i.e., initial enhancement, time to peak, slope of the enhancement curve, and such). These parameters are relatively fast and easy to calculate, and they are not directly related to any physiologic meaning. Moreover, the values obtained with semiquantitative methods cannot be compared across patients or studies performed on different scanners.

This last assumption is not true for what concerns quantitative methods, which rely on pharmacokinetic models to interpret contrast enhancement data in terms of parameters related to the underlying vascular anatomy and physiology. These quantitative parameters are generally derived using a simple two-compartmental model, which consists of an intravascular space and an extravascular-extracellular space (EES). When commonly used, contrast agents distribute in the intravascular space, and leaking into the EES, they alter MR relaxation times according to their concentration in tissues. By making certain assumptions, it is possible to calculate the concentration curve of contrast in the tissue from the signal curve. According to this, quantitative parameters can then be calculated such as volume of EES per unit volume of tissue (Ve) and volume transfer constant between intravascular space and EES in min^{-1} (*K*-trans) [36]. Inflamed bowel segments usually have faster *K-trans* values, larger Ve values, an increased contrast uptake, larger initial areas under the contrast concentration curve, and steeper initial enhancement slopes than normal bowel segments.

2.7   Perianal Imaging

MRI of the small bowel may be combined with high-resolution imaging of the perianal region to provide a comprehensive evaluation of overall disease activity in a single diagnostic session [3].

In fact, the phased-array coils used for small bowel imaging also represent a good compromise for dedicated perianal MR imaging as they can visualize the sphincter complex with a sufficient spatial resolution and a field of view large enough to permit an evaluation of extrasphincteric pelvic region [37–39].

In choosing correct orientation of scanning planes, anatomical precision is needed, so that the course of the fistula with respect to adjacent structures can be accurately visualized.

Sagittal scout image through patient's midline is used to plan oblique axial images that are truly transverse with respect to anal canal; coronal imaging is also performed at 90° to the transverse plane, so running parallel to the length of the anal canal. Alternatively, a sagittal T2-weighted sequence is firstly performed and can be used to orient sequences axially and transversally at the anal canal (Fig. 2.16).

For each plane, high-resolution T2-weighted turbo spin-echo (TSE) scans are obtained. This sequence provides good contrast between hyperintense fluid in the tract and the hypointense fibrous wall of the fistula while simultaneously enabling sufficient discrimination between the several layers of the anal sphincter.

Fat-saturated T2-weighted sequences are recommended for optimal conspicuity of active tracts and inflammatory changes.

T1-weighted TSE sequences have to be combined with fat suppression and intravenous contrast agent, to highlight the fistula and to better differentiate between fluid and inflammatory tissue.
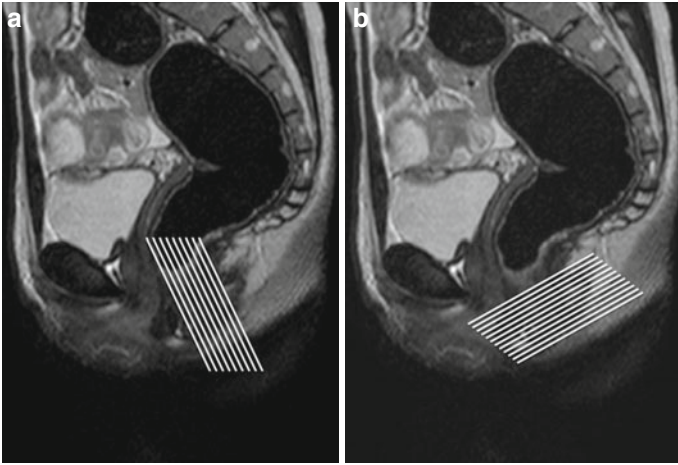
Fig. 2.16 Right orientation of coronal (**a**) and axial (**b**) scan series performed on a midline sagittal T2-weighted image

Finally, in patients where the fistula opened onto the skin, the examination could be performed with hand instillation of gadolinium and saline solution (1:10 dilution) along the fistulous tract.

References

1. Fidler JL, Guimaraes L, Einstein DM et al (2009) MR imaging of the small bowel. Radiographics 29:1811–1825
2. Leyendecker JR, Bloomfeld RS, Di Santis J et al (2009) MR enterography in the management of patients with Crohn disease. Radiographics 29:1827–1846
3. Mazziotti S, Ascenti G, Scribano E et al (2011) Guide to magnetic resonance in Crohn's disease: from common findings to the more rare complicances. Inflamm Bowel Dis 17:1209–1222
4. Siddiki H, Fidler J (2009) MR imaging of the small bowel in Crohn's disease. Eur J Radiol 69:409–417

5. Fidler J (2007) MR imaging of the small bowel. In: Carucci LR (ed) Advances in gastrointestinal imaging. Elsevier Saunders, Philadelphia, pp 317–331

6. Rieber A, Aschoff A, Nussle K et al (2000) MRI in the diagnosis of small bowel disease: use of positive and negative oral contrast media in combination with enteroclysis. Eur Radiol 10:1377–1382

7. Laghi A, Paolantonio P, Iafrate F et al (2002) Oral contrast agents for magnetic resonance imaging of the bowel. Top Magn Reson Imaging 13:389–396

8. Karantanas AH, Papanikolau N, Kalef-Ezra J et al (2000) Blueberry juice used per os in upper abdominal MR imaging: composition and initial clinical data. Eur Radiol 10:909–913

9. Kayhan A, Oommen J, Dahi F et al (2010) Magnetic resonance enterography in Crohn's disease: standard and advanced techniques. World J Radiol 2:113–121

10. Biraschi P, Braccini G, Gigoni R et al (2004) MR enteroclysis using iron oxide particles (ferristene) as an endoluminal contrast agent: an open phase III trial. Magn Reson Imaging 22:1085–1095

11. Hermann KA, Zech CJ, Michaely H et al (2005) Comprehensive magnetic resonance imaging of the small and large bowel using intraluminal dual contrast technique with iron oxide solution and water in magnetic resonance enteroclysis. Invest Radiol 40:621–629

12. Schreyer AG, Golder S, Scheibl K et al (2005) Dark lumen magnetic resonance enteroclysis in combination with MRI colonography for whole bowel assessment in patients with Crohn's disease: first clinical experience. Inflamm Bowel Dis 11:388–394

13. Faber SC, Stehling MK, Holzknecht N et al (1997) Pathologic conditions in the small bowel: findings at fat-suppressed gadolinium-enhanced MR imaging with an optimized suspension of oral magnetic particles. Radiology 205:278–282

14. Ajaj W, Goehde SC, Schneemann H et al (2004) Dose optimization of mannitol solution for small bowel distension in MRI. J Magn Reson Imaging 20:648–653

15. Lauenstein TC, Schneemann H, Vogt FM et al (2003) Optimization of oral contrast agents for MR imaging of the small bowel. Radiology 228:279–283

16. Broglia L, Gigante P, Papi C et al (2003) Magnetic resonance enteroclysis in Crohn's disease. Radiol Med 106:28–35

17. Laghi A, Carbone I, Paolantonio P et al (2002) Polyethylene glycol solution as an oral contrast agent for MR imaging of the small bowel. Acad Radiol 9(suppl):s355–s356

18. Laghi A, Paolantonio P, Catalano C et al (2003) MR imaging of the small bowel using polyethylene glycol solution as an oral contrast agent in adults and children with celiac disease: preliminary observations. Am J Roentgenol 180:191–194

19. Sood RR, Joubert J, Franklin H et al (2002) Small bowel MRI: comparison of a polyethylene glycol preparation and water as oral contrast media. J Magn Reson Imaging 15:401–408

20. McKenna DA, Roche CJ, Murphy JMP et al (2006) Polyethylene glycol solution as an oral contrast agent for MRI of the small bowel in a patient population. Clin Radiol 61:966–970

21. Lohan D, Cronin C, Meehan C et al (2007) MR small bowel enterography: optimization of imaging timing. Clin Radiol 62:804–807

22. Yacoub HJ, Obara P, Oto A (2013) Evolving role of MRI in Crohn's disease. J Magn Reson Imaging 37:1277–1289

23. Griffin N, Grant LA, Anderson S et al (2012) Small bowel MR enterography: problem solving in Crohn's disease. Insights Imaging 3:251–263

24. Sinha R, Murphy P, Hawker P et al (2009) Role of MRI in Crohn's disease. Clin Radiol 64:341–352

25. Grand DJ, Beland MD, Machan JT et al (2012) Detection of Crohn's disease: comparison of CT and MR enterography without antiperistaltic agents performed on the same day. Eur J Radiol 81:1735–1741

26. Umshaden HW, Szolar D, Grasser J et al (2000) Small bowel disease: comparison of MR enteroclysis images with conventional enteroclysis and surgical findings. Radiology 215:717–725

27. Froelich JM, Waldherr C, Stoupis C et al (2010) MR motility in Crohn's disease improves lesion detection compared with standard MR imaging. Eur Radiol 20:1945–1951

28. Odille F, Menys A, Ahmed A et al (2012) Quantitative assessment of small bowel motility by nonrigid registration of dynamic MR images. Magn Reson Med 68:783–793

29. Menys A, Atkinson D, Odille F et al (2012) Quantified terminal ileal motility during MR enterography as a potential biomarker of Crohn's disease activity: a preliminary study. Eur Radiol 22:2494–2501

30. Oto A, Kulkarni K, Karczmar GS et al (2009) Evaluation of diffusion-weighted MR imaging for detection of bowel inflammation in patients with Crohn's disease. Acad Radiol 16:597–603

31. Kiryu S, Dodanuki K, Takao H et al (2009) Free-breathing diffusion-weighted imaging for the assessment of inflammatory activity in Crohn's disease. J Magn Reson Imaging 29:880–886

32. Taylor SA, Punwani S, Rodriguez-Justo M et al (2009) Mural Crohn disease: correlation of dynamic contrast-enhanced MR imaging findings with angiogenesis and inflammation at histologic examination. Pilot study. Radiology 251:369–379
33. Del Vescovo R, Sansoni I, Caviglia R et al (2008) Dynamic contrast enhanced magnetic resonance imaging of the terminal ileum: differentiation of activity of Crohn's disease. Abdom Imaging 33:417–424
34. Horsthuis K, Nederveen AJ, de Feiter M et al (2009) Mapping of T1-values and Gadolinium-concentrations in MRI as indicator of disease activity in luminal Crohn's disease: a feasibility study. J Magn Reson Imaging 29:488–493
35. Giusti S, Faggioni L, Neri E et al (2010) Dynamic MRI of the small bowel: usefulness of quantitative contrast-enhancement parameters and time-signal intensity curves for differentiating between active and inactive Crohn's disease. Abdom Imaging 35:646–653
36. Oto A, Fan X, Mustafi D et al (2009) Quantitative analysis of dynamic contrast enhanced MRI for assessment of bowel inflammation in Crohn's disease: pilot study. Acad Radiol 16:1223–1230
37. Maccioni F, Colaiacomo MC, Stasolla A et al (2002) Value of MRI performed with phased-array coil in the diagnosis and pre-operative classification of perianal and anal fistulas. Radiol Med 104:57–67
38. Horsthius K, Stoker J (2004) MRI of perianal Crohn's disease. Am J Roentgenol 183:1309–1315
39. Halligan S, Stoker J (2006) Imaging of fistula in ano. Radiology 239:18–33

Chapter 3
Normal MR Anatomy

## 3.1 Normal MR Anatomy of Duodenum and Small Bowel

The small bowel consists of duodenum, jejunum, and ileum. It begins at the pylorus of the stomach and ends at the ileocecal junction. It is called *small bowel* because its lumen diameter is smaller than that of the large intestine, although it is longer in length than the large bowel.

The small intestine is differentiated from the large intestine also by the presence of a mesentery (exceptions being no mesentery in the duodenum and mesentery in the transverse and sigmoid colon) and the absence of taenia coli and appendices epiploicae.

The duodenum begins at the pylorus on the right-hand side of the abdominal cavity and ends at the duodenojejunal junction. Anatomically, we can divide the duodenum into four parts: superior, descending, horizontal, and ascending. Together, these parts form a *C*-shaped structure.

The jejunum and ileum are the two distal parts of small intestine. There is not a clear location at which the jejunum becomes ileum, as such they are often indicated as the jejunoileum. The jejunoileum begins at the duodenojejunal flexure and ends at the ileocecal valve (Fig. 3.1).
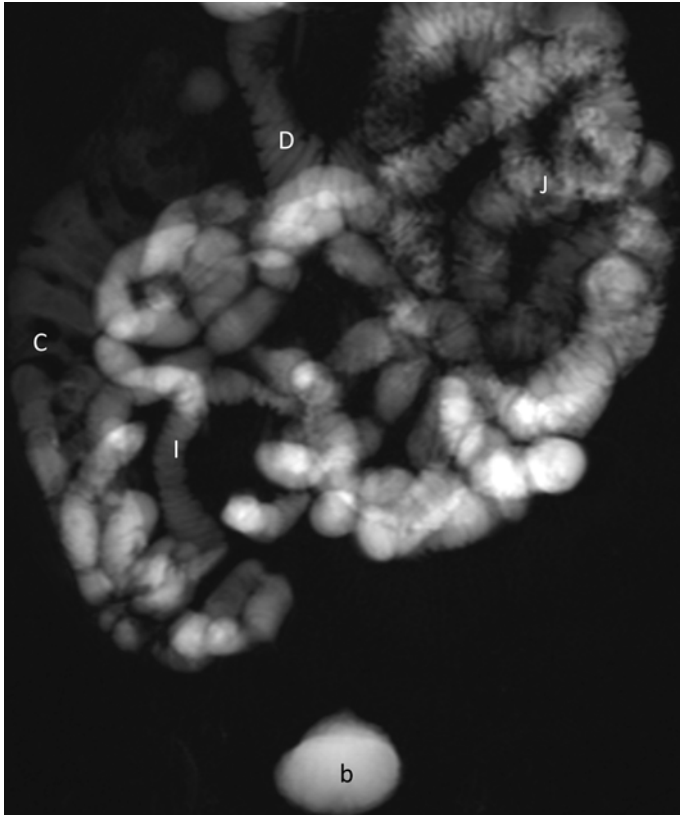
Fig. 3.1 MR fluoroscopy. A panoramic view of the small bowel. *D* duodenum, *J* jejunum, *I* ileum, *C* colon, *b* bladder

On MR images, the duodenal "C-shaped" (Fig. 3.2) as well as the duodenal and jejunal wall, lumen, and fold patterns are well demonstrated (Figs. 3.3 and 3.4). The bowel diameter,
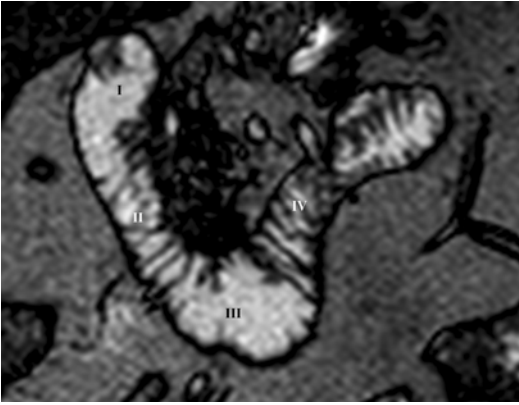
Fig. 3.2 Coronal TrueFISP image. Different parts of duodenum, which appear distended and with its characteristic fold pattern. (*I*): Superior part; (*II*): descending part; (*III*): horizontal part; (*IV*): ascending part

the fold thickness, and the number and interfold distance gradually decrease in size, reaching their smallest measurements in the terminal ileum (Figs. 3.1 and 3.5). Furthermore, the diameters of proximal, distal, and terminal ileum; its fold number; fold thickness; and interfold distances are not markedly dissimilar. The small bowel wall thickness is similar in size throughout the bowel measuring approximately 1.5 ± 0.5 mm [1].

As previously said, due to significant improvements in gradient technology, the visualization of the mesentery has become possible with the use of TrueFISP sequence. Very small mesenteric lymph nodes and vessels can be consistently detected without motion artifacts, thanks to the short acquisition time [2, 3].
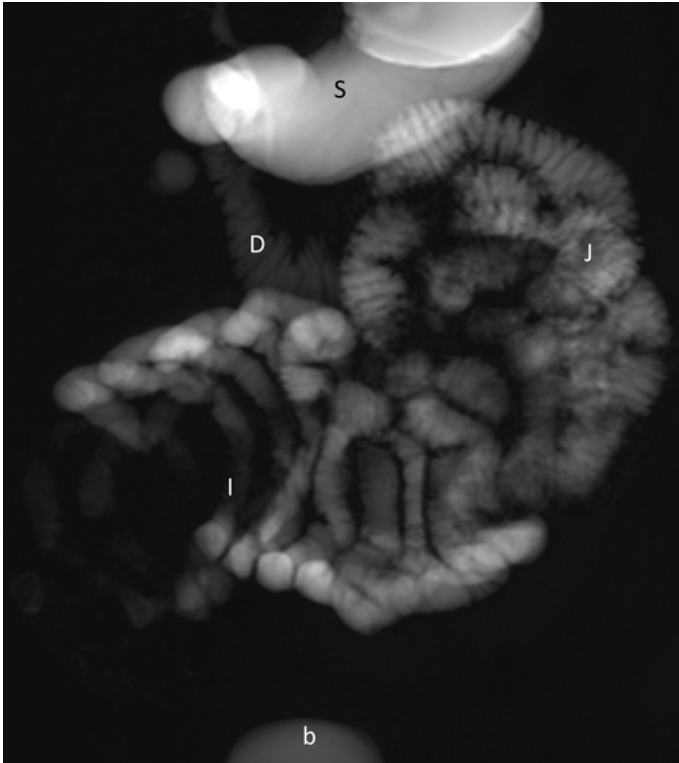
Fig. 3.3 MR fluoroscopy. Note how duodenum (*D*) and jejunum (*J*) have comparable bowel diameter and fold thickness, similar number of folds, and interfold distances. *S* stomach, *I* ileum, *b* bladder

3.2 Normal MR Anatomy of Sphincters and Perianal Region

The anal canal is the terminal portion of digestive tract, and it lies between the anal verge in the perineum below and the rectum above. It is essentially a cylinder of variable length between
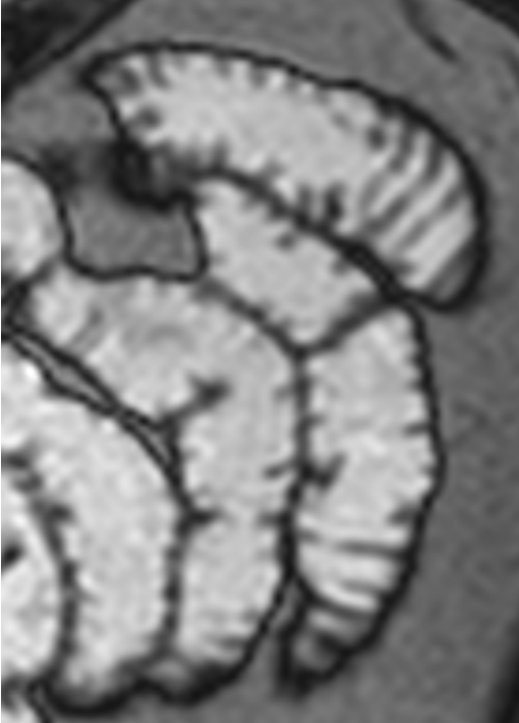
Fig. 3.4 Coronal TrueFISP image of jejunum where it is well demonstrated the normal mucosal, mural, and fold pattern

3 and 5 cm, with two-thirds of this being above and one-third below the dentate line. The anal canal is completely extraperitoneal and is delimited by two muscular sphincters, the internal and external sphincters [4–6].

The internal sphincter is part of the inner surface of the canal. It is composed of concentric layers of smooth circular muscle tissue and is not under voluntary control. The internal sphincter is the distal termination of the circular muscle of the gut tube. It is responsible for 85 % of resting anal tone. In most
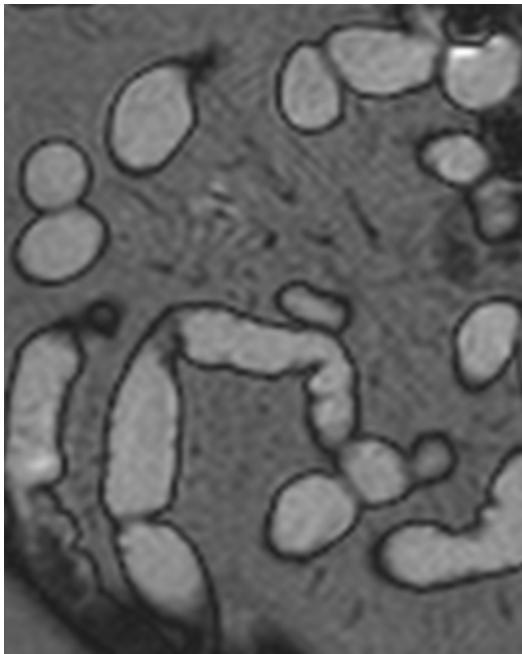
Fig. 3.5 Magnified coronal TrueFISP image of ileum with normal mucosal and mural aspect. Note how fewer folds are visualized in comparison to those of jejunum and duodenum, as seen in the previous figures

individuals, it can be divided without causing a loss of continence [6].

The external sphincter is a layer of voluntary striated muscle encircling the outside wall of the anal canal and anal opening. The external sphincter has its posterior attachment to the anococcygeal ligament and anterior attachment to the perineal body and urogenital diaphragm; it merges proximally with the sling-like puborectalis muscle which itself merges with the
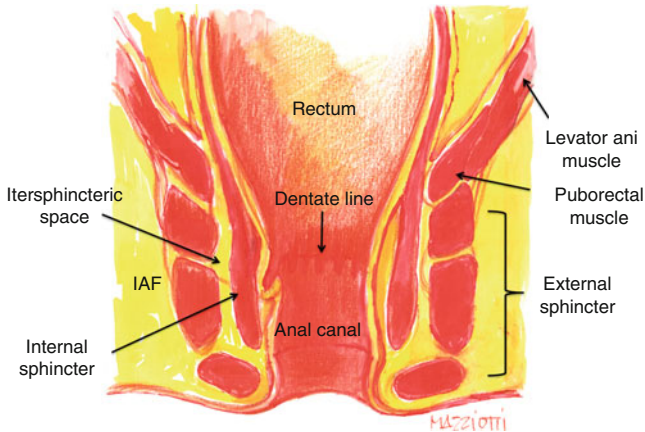
Fig. 3.6 Illustration showing the normal anatomy of the anal canal and perianal region along the coronal plane. *IAF* ischioanal fossa

levator plate of the pelvic floor. The external sphincter contributes only 15 % of resting anal tone, but its strong voluntary contractions resist defecation [6]. A division of the external sphincter can determine incontinence.

There is a fat plane between the internal and external anal sphincters, known as the intersphincteric space.

The ischioanal fossa lies laterally to the sphincteric complex. It is filled with fat and is traversed by a network of fibroelastic connective tissue. Because this space lies adjacently to the anus and immediately below the levator plate of the pelvic floor, it is preferable the term "ischioanal fossa" rather than "ischiorectal fossa" which is commonly used by surgeons. However, these two terms are interchangeable (Fig. 3.6) [5].

All these structures, due to the high contrast resolution, are well depicted in both coronal and axial MR images (Fig. 3.7).
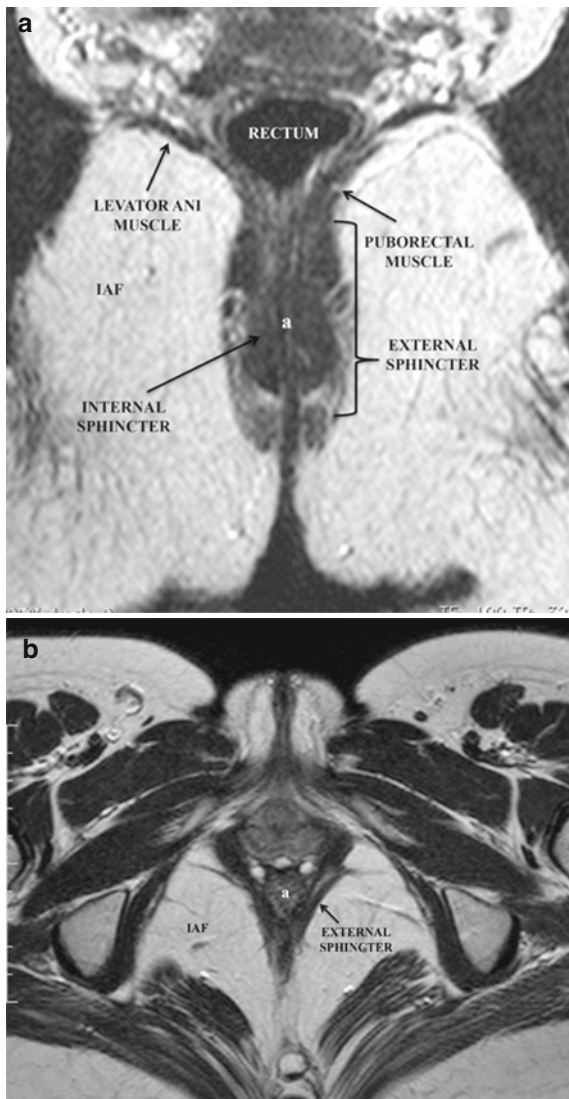
Fig. 3.7 Coronal (**a**) and axial (**b**) T2-weighted TSE images showing the normal MR anatomy of perianal region. *a* anal canal, *IAF* ischioanal fossa

References

1. Cronin C, Delappe E, Lohan DG et al (2010) normal small bowel wall characteristics on MR enterography. Eur J Radiol 75:207–211
2. Kayhan A, Oommen J, Dahi F et al (2010) Magnetic resonance enterography in Crohn's disease: standard and advanced techniques. World J Radiol 2:113–121
3. Furukawa A, Saotome T, Yamasaki M et al (2004) Cross sectional imaging in Crohn disease. Radiographics 24:689–702
4. Horsthius K, Stoker J (2004) MRI of perianal Crohn's disease. Am J Roentgenol 183:1309–1315
5. Halligan S, Stoker J (2006) Imaging of fistula in ano. Radiology 239:18–33
6. Morris J, Spencer JA, Ambrose S et al (2000) MR imaging classification of perianal fistulas and its implications for patient management. Radiographics 20:623–635

Part II
MR Enterography:
Clinical Applications

Chapter 4
MR Findings in Crohn's Disease

Inflammatory bowel disease (IBD) primarily refers to two chronic diseases that cause chronic inflammation of all or part of the digestive tract: ulcerative colitis (UC) and Crohn's disease (CD).

UC predominantly affects the colon, with the exception of "backwash ileitis," which involves the terminal ileum. In such cases, colonoscopy is therefore the most effective method to assess the activity of the disease.

CD is an idiopathic, chronic, transmural, inflammatory disease that can affect any part of the gastrointestinal tract from mouth to anus, with a tendency toward segmental distribution and often involving multiple discontinuous sites (skip lesions). Most commonly, it affects the small bowel, which is (apart from the terminal ileum) usually not accessible with conventional endoscopic techniques.

In about 70–80 % of patients with CD, there is small bowel involvement, and in about 20–30 %, the disease is limited to the small bowel. The colon can be affected either with (50 % of cases) or without (15–20 %) the involvement of the small intestine [1].

The incidence of CD seems to have a bimodal distribution, the first peak occurring in late adolescence and early adulthood while a second smaller increase in incidence can be seen between the fifth and seventh decade of life [2, 3]. Prevalence in

many developed countries is estimated at 0.1 % [4]. A familial tendency has also been described, observing an increased risk of ulcerative colitis in relatives [5].

The etiology and pathogenesis of CD are not completely understood, but there is increasing evidence that genetic as well as environmental factors may play an important role in causing a sustained activation of mucosal immune responses, which lead to cytokine overproduction and subsequently to leukocytary infiltration of the bowel wall [2, 6, 7].

Furthermore, luminal bacteria and microbiota would also likely play a major role in the pathogenesis of CD.

Microscopically, the initial lesion starts as a focal inflammatory infiltrate in the mucosa and submucosa, which leads to hyperemia and edema.

Macroscopically, the earliest feature of CD is a shallow aphthoid mucosal ulceration, histologically corresponding to initial mucosal ulceration over a mucosal lymphoid follicle. As the disease progresses, aphthoid ulcers develop and further progress into extensive linear ulcers and fissures. Advanced ulcerations with bulging of the edematous residual mucosal islands produce the typical ulceronodular or "cobblestone" appearance. In severe cases, transmural inflammation and serosal involvement are present as well. The bowel wall can also result to be thickened by a combination of fibrosis and inflammatory infiltrates. In long-standing cases, chronic obstruction due to scarring, luminal narrowing, and stricture formation may arise.

For what concerns extramural manifestations, these are fistulas, abscesses, adhesions, creeping fat, and enlargement of the lymph nodes.

Although it is not common, toxic megacolon and neoplasms such as lymphoma and carcinoma may also occur [8].

Symptoms of CD are often unpleasant and they are classically represented by abdominal pain, weight loss, diarrhea (which may include blood or mucus and may vary in frequency), and tenesmus; however, it can have different presentations and tends to have an unpredictable course marked by flares, remissions, and relapses.

The diagnosis of CD is based on a combination of clinical findings, endoscopic appearance, biopsy, radiological studies, and biochemical markers; however, most commonly, ileocolonoscopy and biopsies from the terminal ileum and colon are the ones used to determine the initial diagnosis.

With regard to the imaging of CD at initial presentation and in the setting of clinical suspicion, as previously stated in the introduction, MR of the small bowel can be considered a useful support both in patients with an incomplete ileocolonoscopy and in those with negative ileocolonoscopy, to, respectively, exclude enteric inflammation at the level of the terminal ileum or proximal to this site.

MR of the small bowel can also be used as a first-line diagnostic approach in pediatric patients with clinical suspicion for CD, or it can be performed prior to video capsule endoscopy (very sensitive to detect subtle mucosal disease), to exclude strictures.

However, in the majority of cases, MREg/MREc is primarily employed to assess the exact location and extent of inflammatory bowel disease in patients with histological diagnosis of CD.

It should also be considered that in clinical practice, CD is stratified by *disease severity* (mild, moderate, and severe), *disease location* (upper gastrointestinal, ileal, ileocolonic, colonic, or perianal), *extent of disease*, and *disease phenotype* (penetrating, structuring, or inflammatory – nonpenetrating nonstricturing disease) [9].

MR helps to categorize the relative components of inflammatory, penetrating, or structuring disease in each individual patient, and it should be used for the surveillance of patients with known CD.

The assessment of the inflammatory activity is essential in order to delineate treatment strategies and determine the optimal choice and dose of medication; at the same time, the monitoring of patient is important to evaluate the efficacy of treatment [10].

In addition to dietary approach, several medical therapies are used to induce and/or maintain remission in CD, including corticosteroids, immunomodulators (e.g., azathioprine, mercaptopurine, methotrexate), and biologic agents (e.g., TNF-alpha inhibitors). In particular, with the advent of new medication

such as infliximab, an immunomodulatory drug with considerable side effects, follow-up to determine therapy efficacy is becoming increasingly important.

Several clinical scoring systems have been developed to assess disease activity and response to therapy, the most common of which is the Crohn's Disease Activity Index (CDAI), although it is far from being a conclusive metric to evaluate the severity of the disease.

Moreover, identification of location of fibrotic restricted lumen tracts and evaluation of prestenotic dilatation may help surgeons to plan intervention [10]. However, surgery is delayed until the disease does not respond to pharmacotherapy or there are complications, such as obstruction. When performed, bowel conservation surgery is the aim.

In this context, MRI can demonstrate active small bowel inflammation recognizing wall thickening, ulcerations, increased wall enhancement, increased vascularity, perienteric inflammation, and reactive adenopathy. MR also allows more accurate identification of associated complications including penetrating and fibrostenotic disease as well as the more rare extraintestinal manifestations that are usually associated with severe and longstanding intestinal inflammation, the latter often guiding the therapeutic approach [11–16].

4.1   Wall Thickening

Bowel wall thickening is the most reported findings of CD even if not entirely specific.

In adequately distended small bowel, the normal wall thickness is 1–3 mm, while a bowel wall thickening more than 3 mm can be regarded as abnormal [17].

It has also be shown that mural thickness increases with acute inflammation, generally ranging between 5 and 10 mm (given the associated histological findings of edema and inflammatory infiltrate) and that, in patients with CD, this well correlates with
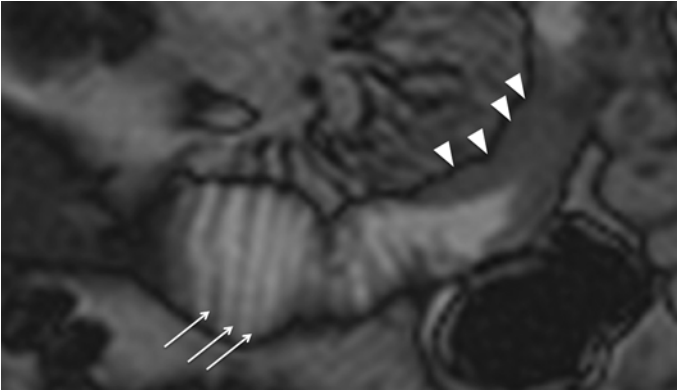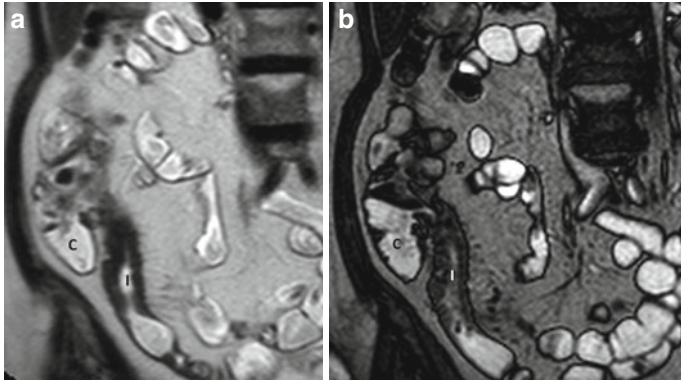
Fig. 4.1 Wall thickening. Magnified coronal TrueFISP image shows wall thickening of a proximal ileal tract (*arrowheads*) and thickening of mucosal folds in the segment next to it (*arrows*)

the presence and severity of the disease [18]. An associated thickening of the mucosal folds can be also seen (Fig. 4.1).

Although the thickness decreases during remission, the inactive but yet pathological bowel is likely to be thicker compared with the completely normal bowel [18, 19]. To help the radiologist in distinguishing between active and inactive disease, a cut-off thickness of 6 mm has been proposed [19].

The most common site of CD is the terminal ileum (Fig. 4.2), sometimes with contiguous disease in the cecum. Discontinuous skip lesions may also be seen more proximally in the small bowel (Fig. 4.3) or within the colon.

The involvement of the bowel wall may be symmetrical or asymmetrical, where greater involvement of the mesenteric border can lead to pseudosacculation. Fibrosis and shortening of the diseased mesenteric wall lead to apparent dilatation of the opposing normal bowel wall (Fig. 4.4). Because all three bowel wall layers form the sacculation (in contrast to colonic diverticular disease), such a finding may also be referred to as a pseudodiverticulum [20].

Fig. 4.2 Wall thickening. Magnified coronal HASTE (**a**) and TrueFISP (**b**) images show wall thickening of the terminal ileum (*I*). *C* cecum
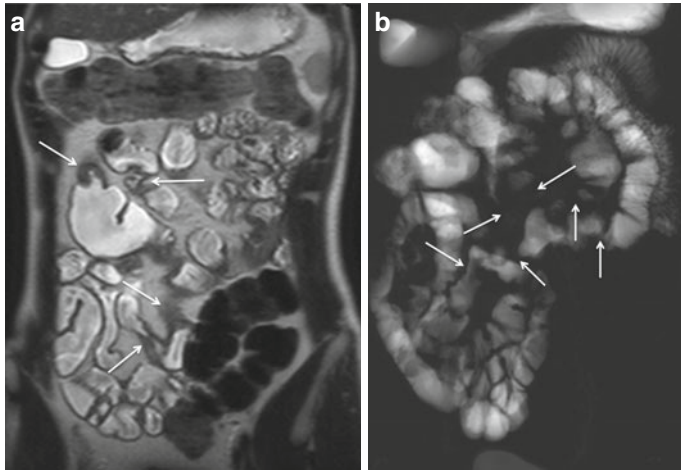
Fig. 4.3 Skip lesions. Coronal HASTE (**a**) and coronal MR-fluoroscopy images (**b**) depict multiple inflammatory strictures (*arrows*) separated by segments of both normally distended and dilated small bowel segments
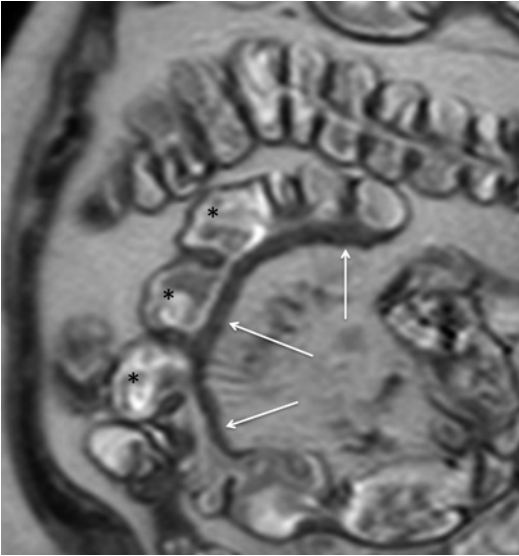
Fig. 4.4 Asymmetrical wall thickening and pseudosacculations. Magnified coronal HASTE image shows multiple pseudosacculations on the antimesenteric border (*asterisks*) due to asymmetric thickening of the bowel wall (*arrows*)

Moreover, if there is suboptimal distention (as sometimes is the case, especially with jejunal loops), the disease may be overestimated or underestimated [17]. The evaluation of all images, sequentially acquired, may help to clarify the extent of bowel involvement, as fluid distension in the small bowel will vary over time.

Mural thickening can be appreciated on all sequences. However, while thickness can be assessed with both T1- and T2-weighted sequences, balanced SSFP sequences should be avoided due to the "black border artifact," which can complicate the evaluation of bowel wall thickness. Conversely, HASTE sequence, which is insensitive to chemical shift and is
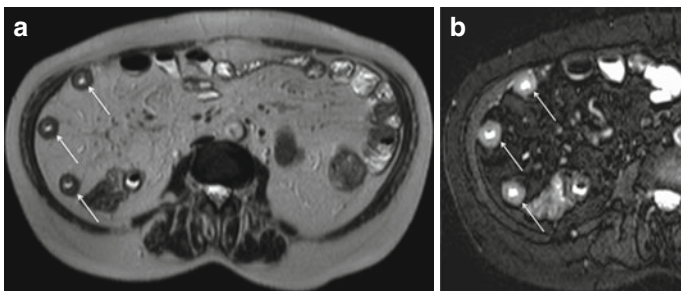
Fig. 4.5 Wall thickening in active Crohn's disease. Axial HASTE image (**a**) showing concentric bowel wall thickening in multiple segments (*arrows*). On magnified axial HASTE fat-saturated image (**b**), obtained at the same level, it is demonstrable high signal intensity of the diseased intestinal tracts, as a consistent finding of inflammatory edema in active Crohn's disease

not susceptible to black border artifact, will be indicated for more accurate measurements [16, 17].

Fat-saturated T2-weighted sequences are very helpful for characterizing the etiology of wall thickening, appearing as an area of high signal intensity in the presence of active inflammation, due to the edema (Figs. 4.5 and 4.6); this finding has been shown to well correlate with the severity of inflammation, and it can be particularly useful in patients with contraindications to contrast media administration [16].

In addition, in severe CD, the inflamed bowel wall has a layered appearance on T2-weighted sequences with a high signal intensity ring, representing the submucosal edema, between the mucosa and serosa ("target sign") [16, 21]. The hyperintensity of the submucosa also persists in the fat-saturated T2 images (Fig. 4.7).

Because on HASTE sequence, intramural fat deposition in chronic disease may result in elevated T2 signal intensity, fat-saturated T2-weighted sequences are also recommended to differentiate edema from fat: loss of signal on T2-weighted fat-saturated sequences is suggestive of chronic disease and this
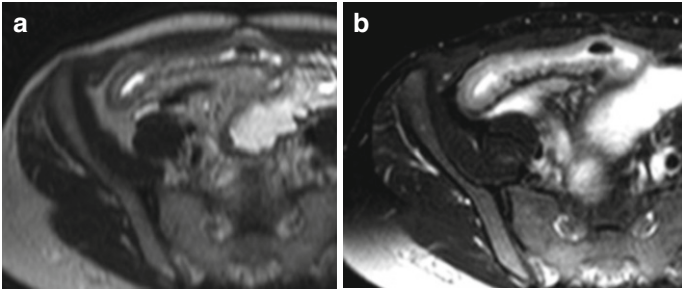
Fig. 4.6 Wall thickening in active Crohn's disease. Magnified axial HASTE image showing concentric wall thickening of the distal ileum (**a**). Magnified axial HASTE fat-saturated image, obtained at the same level (**b**), depicts high signal intensity of the diseased intestinal segment, as a consequence of inflammatory edema, a consistent finding of active Crohn's disease
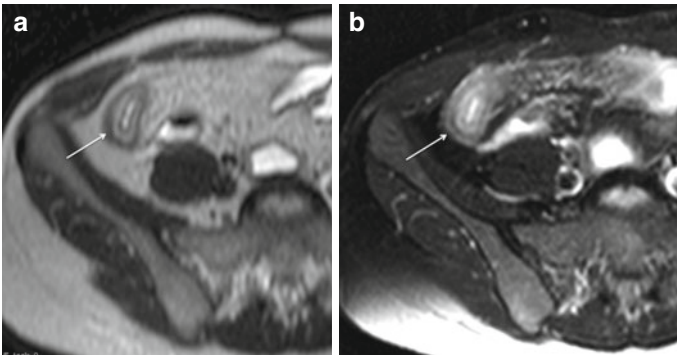
Fig. 4.7 "Target sign" in severe active Crohn's disease. Axial HASTE images in a patient with severe active Crohn's disease show a layered appearance of the inflamed terminal ileum (*arrow*), due to hyperintense submucosal edema (**a**), still visible after fat saturation (**b**)

can be a helpful feature in interpreting the significance of thickened bowel wall [16, 21]. In these cases, a target appearance may be produced by low signal intensity "ring or halo" due to

fat hypertrophy and fibrosis of the submucosa ("fat halo sign") (Fig. 4.8).

Recently, DWI, along with associated ADC measurements, has been shown to reflect abnormal activity in CD patients, helping to further characterize the bowel wall thickening and complementing the morphological information obtained by conventional MRI [22–24].

Particularly, active inflammatory thickening of the bowel wall is characterized by brighter signal in the b-value images and lower ADC values relative to normal segments (Fig. 4.9).

The visual assessment of DWI may provide higher accuracy, while calculation of the ADC may facilitate the quantitative analysis of the activity of the disease [22–24].

In the presence of a borderline thickening of the small bowel wall, dynamic cine-MR sequences can more accurately demonstrate the number of pathological intestinal segments than what static MRI can do. In fact, abnormally decreased or increased peristalsis may be an early sign of the bowel involvement by CD and can potentially help to identify affected segments that would appear with only subtle or doubtful signs of inflammation on static images. However, it should be well kept in mind that additional factors over and above acute inflammation might affect motility in CD, including drug regimens, disease duration, location, coexistence of colitis, previous surgery, and mural fibrosis [25–28].

4.2   Ulcerations

The microscopic examination of the intestinal mucosa in patients affected by CD shows active inflammation, which is usually characterized by varying degrees of injury of the neutrophilic crypts.

Intramural layer of fat and fibrosis
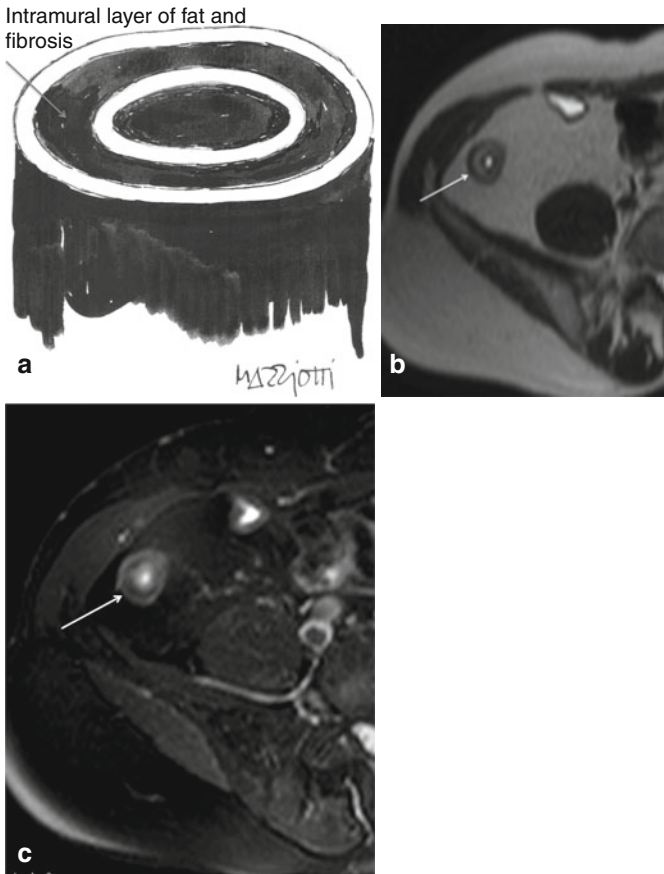
Fig 4.8 "Halo sign" in chronic Crohn's disease. Illustration showing the "halo sign" (**a**), caused by fat hypertrophy and fibrosis of the intestinal submucosa in chronic Crohn's disease. Axial HASTE image (**b**) shows a layered appearance of the terminal ileum (*arrow*), which is due to hyperintense submucosal fibrofatty proliferation, as confirmed by the lack of signal in the magnified HASTE fat-saturated image (**c**) (Note differences with active Crohn's disease, seen previously in Fig. 4.7)
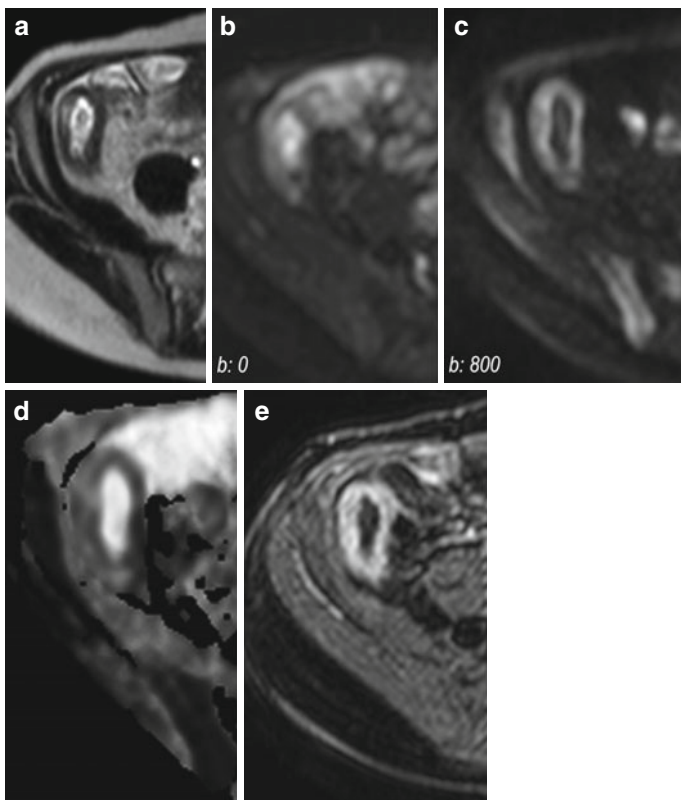
Fig. 4.9 Active Crohn's disease. Magnified axial HASTE image (**a**) shows wall thickening of the terminal ileum. Axial DW images performed at different b-values (**b**: 0 s/mm^2 and 800 s/mm^2, respectively) show persistent hyperintense signal of the pathologically thickened wall of the terminal ileum (**b**, **c**). The ADC$_{(0-800)}$ map (**d**) demonstrates restricted diffusion (*dark region*) in the site of abnormal terminal ileum, which well correlates with marked hyperenhancement on axial fat-saturated T1-weighted image obtained after i.v. administration of gadolinium (**e**)

In mild CD, only a small fraction of crypts is infiltrated by neutrophils; crypt destruction and mucin depletion can also be seen. As the degree of activity increases, there is a corresponding escalation of the involved crypts and of the severity of crypt injury, which includes the necrosis of epithelial crypts, crypts abscess, and the eventual formation of ulcers.

Two types of ulcers can be seen in CD: the superficial aphthoid ulcers and the deep fissuring ulcers, more problematic than superficial ones.

A good depiction of ulcerations is highly dependent on the quality of luminal distention.

The deep fissuring ulcers usually break through the mucosa and into the deeper layers of the bowel wall, causing initially submucosal inflammation and edema [15, 29, 30].

However, when the ulceration is initial and superficial, it is not always well demonstrable at MRI, even if full luminal distention was achieved; on the other hand, conventional fluoroscopy, if well performed, still holds this advantage.

Fissuring ulcers primarily manifest as areas of erosion in the mucosal lining, and they may finally extend into the submucosal space, damaging the mucosal lining [15, 17, 29, 30].

Larger deep ulcers are outlined by luminal contrast material and appear as thin lines of high signal intensity longitudinally or transversely oriented into the thickened bowel wall (Fig. 4.10).

HASTE and TrueFISP images, which provide high contrast between the lumen and the bowel wall, may facilitate the detection of transmural ulcers [29].

The cobblestone aspect, which results from multiple confluent and intersecting longitudinal and transverse ulcerations, with residual mucosal islands, appears as sharply demarcated and patchy areas of high signal intensity, a suggestive finding of advanced disease that may prompt a change in medical treatment (Fig. 4.11) [16, 29].
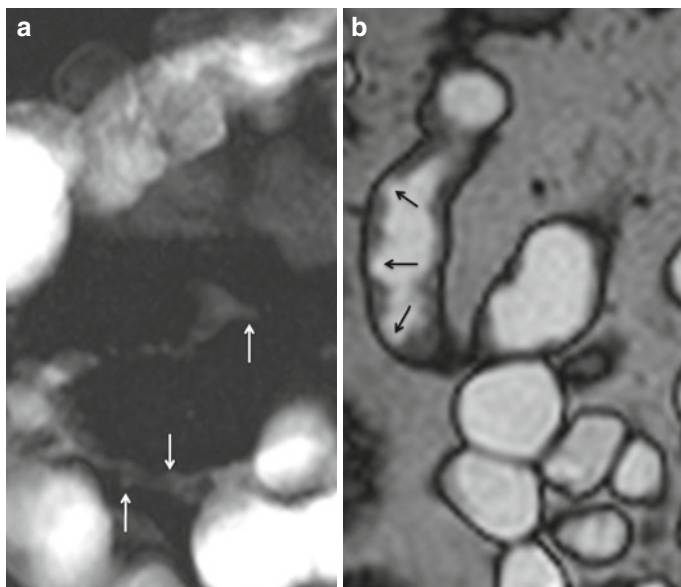
Fig. 4.10 Ulcerations. Magnified coronal MR fluoroscopy (**a**) shows ileal narrowing and ulcerations (*arrows*). Coronal high-resolution TrueFISP image (**b**) clearly depicts ulcerations as well (*arrows*)

4.3   Increased Vascularity

The increased mesenteric vascularity adjacent to inflamed bowel loops is often present in the setting of acute inflammation. In fact, when mesenteric blood flow increases, it results in engorgement of the vasa recta supplying the inflamed bowel segments, which appear as multiple tubular, tortuous opacities on the mesenteric side of the ileum, aligned like the teeth of a comb ("comb sign") [16, 17, 29].

This finding, due to contrast enhancement of the vasculature, is frequently best seen as high signal intensity parallel lines on contrast-enhanced T1-weighted fat-suppressed images (Fig. 4.12). Moreover, it can also be seen on fat-suppressed
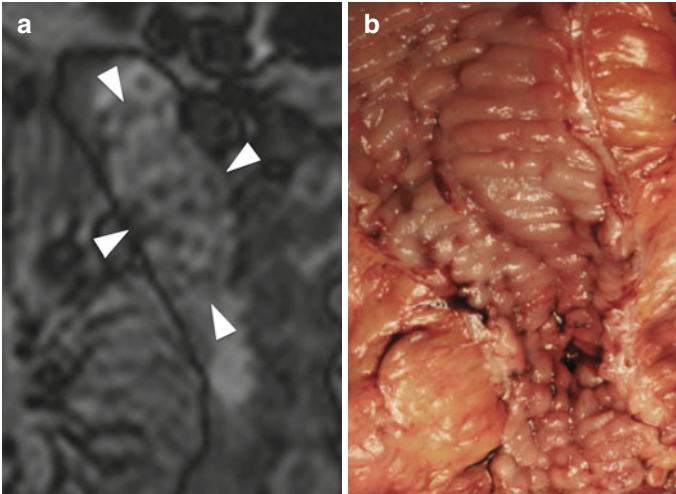
Fig. 4.11 "Cobblestone appearance" in Crohn's disease. Magnified coronal high-resolution TrueFISP image (**a**) demonstrating the cobblestone appearance of edematous mucosa between longitudinal and transverse linear ulcers (*arrowheads*). Note the good correlation with the endoscopic findings (**b**)

HASTE or TrueFISP images, respectively, as high and low signal intensity parallel lines (Figs. 4.13 and 4.14).

The identification of comb sign, however, is much more limited on the nonfat-suppressed HASTE, due to the poor contrast resolution between vessels and mesenteric fat (Fig. 4.15).

The presence of the comb sign may suggest active disease [16, 17, 29].

4.4 Patterns of Wall Enhancement

Bowel wall enhancement plays a very important role in determining disease severity, as it can be one of the earliest signs of inflammatory activity.
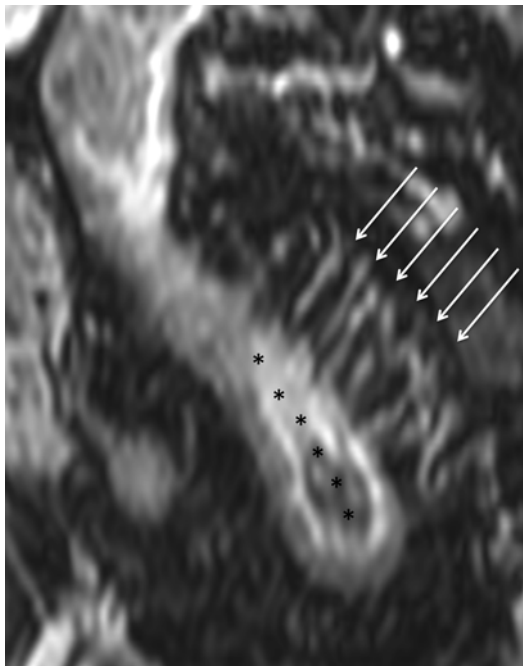
Fig. 4.12 "Comb sign" in Crohn's disease. Coronal GE T1-weighted and fat-saturated image, obtained after i.v. injection of gadolinium. Ectatic vasa recta (*arrows*) supplying a diseased bowel loop (*asterisks*)

It has been frequently reported to correlate with bowel inflammation and activity of the disease.

In CD, in fact, a marked increase in signal intensity of the inflamed bowel wall can be seen after intravenous gadolinium administration, due to increased tissue perfusion and vascular permeability.

The enhancement pattern of the inflamed bowel has also been studied to assess inflammatory activity as a comparison

Fig. 4.13 "Comb sign" Crohn's disease. Sagittal HASTE fat-saturated image showing ectatic vasa recta as hyperintense linear structures (*arrows*), directed from mesentery toward a diseased bowel segment

with clinical indices, and a significant enhancement decrease has already been correlated to good response to medical treatment [17, 18].

The assessment of enhancement should be done during several phases, based on the different scanning times, relatively to contrast injection.
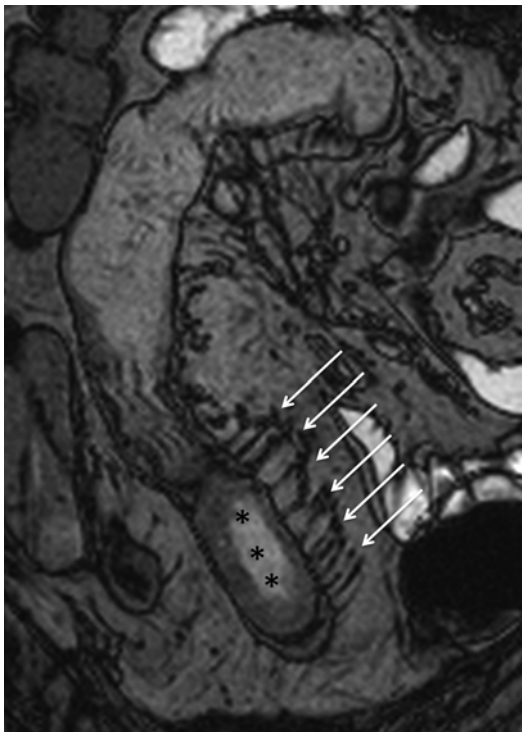
Fig. 4.14 "Comb sign" in Crohn's disease. Same patient of Fig. 4.12. Coronal TrueFISP image showing ectatic vasa recta (*arrows*), represented by multiple linear hypointensities directed toward the pathological small bowel tract (*asterisks*)

Four enhancement patterns can be described and may help the gastrointestinal radiologist to determine the likely level of inflammatory activity:

1. Pattern I – mucosal hyperenhancement may be the first sign of active inflammation, even in the absence of a substantial wall thickening (Fig. 4.16).
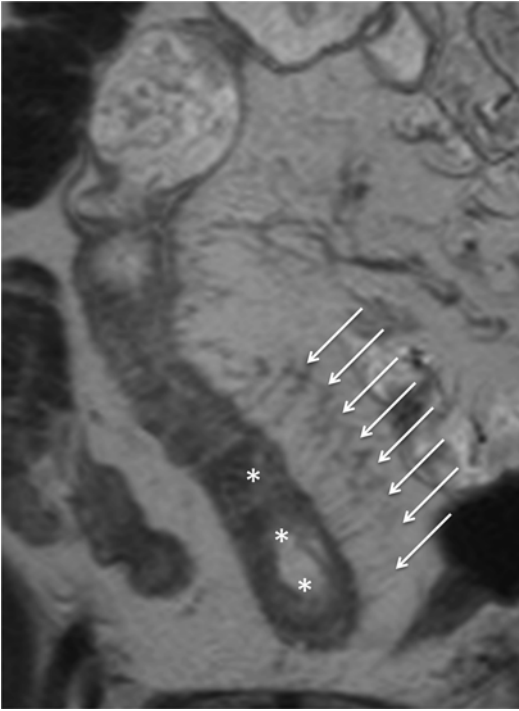
Fig. 4.15 "Comb sign" in Crohn's disease. Same patient of Figs. 4.12 and 4.14. Coronal HASTE image, without fat saturation. The minor contrast between mesenteric fat and ectatic vasa recta (*arrows*) does not allow an adequate visualization of the comb sign. Affected bowel segment (*asterisks*)

2. Pattern II – layered pattern of enhancement, termed "mural stratification," is specific for severe active inflammation. The layered appearance consists of an inner enhancing ring produced by the hyperemic mucosa and an outer ring caused by the enhancing muscularis propria and serosa, with an intermediate low-density ring produced by the submucosal edema ("target sign") (Figs. 4.17 and 4.18).
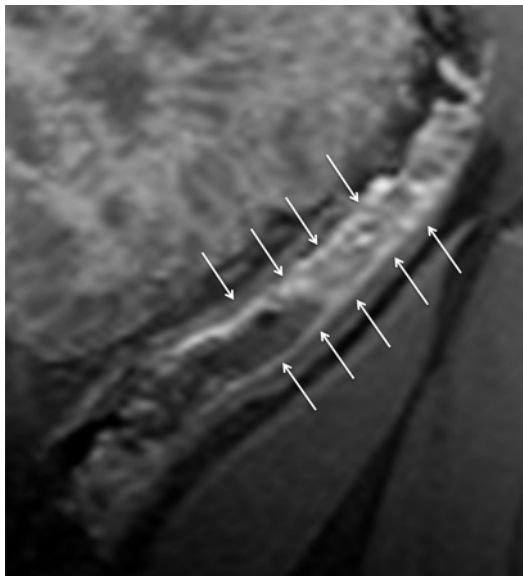
Fig. 4.16 Pattern I of mural enhancement – mucosal hyperenhancement in active Crohn's disease. Magnified sagittal GE T1-weighted fat-saturated image, obtained after i.v. injection of gadolinium, shows hyperenhancement of intestinal mucosa (*arrows*), as a sign of active inflammation

3. Pattern III – diffuse enhancement affecting the entire wall thickness, without any stratified appearance and that is a sign of transmural inflammation; it is frequently associated with early phases of CD and is very common in pediatric patients and in young adults (Fig. 4.19).
4. Pattern IV – low and inhomogeneous enhancement, more typical of chronic disease; in such cases, other findings such as low intermediate degree of transmural signal intensity on T2-weighted images or progressive transmural enhancement in delayed fat-suppressed T1-weighted images are helpful for the correct diagnosis (Figs. 4.20 and 4.21).

The degree of the bowel wall enhancement has been proposed as a marker for evaluating the activity of the disease.
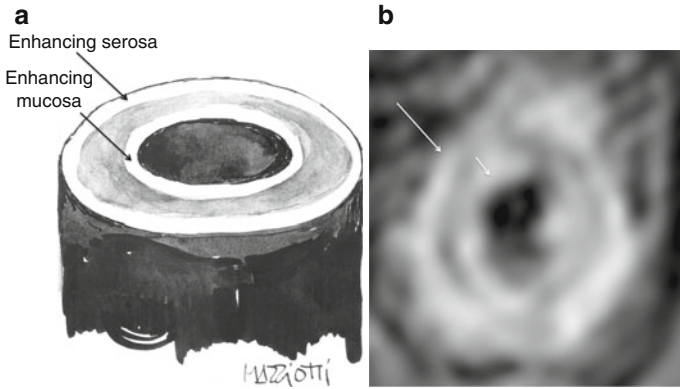
Fig. 4.17 Pattern II of mural enhancement – mural stratification ("target sign") in active Crohn's disease. Illustration showing the "target sign" (**a**). Magnified axial GE T1-weighted fat-saturated image, obtained after i.v. administration of gadolinium (**b**), shows the layered appearance of the inflamed bowel wall due to an intermediate low-density ring produced by the submucosal edema between hyperenhancing mucosa (*short arrow*) and serosa (*long arrow*)

Fig. 4.18 Pattern II of mural enhancement – mural stratification ("target sign") in active Crohn's disease. Magnified coronal GE T1-weighted fat-saturated image, obtained after i.v. injection of gadolinium. Layered enhancement pattern of inflamed terminal ileum. The enhancing mucosa (*long arrow*) and serosa (*short arrow*) are separated by an edematous submucosal layer (*asterisks*)
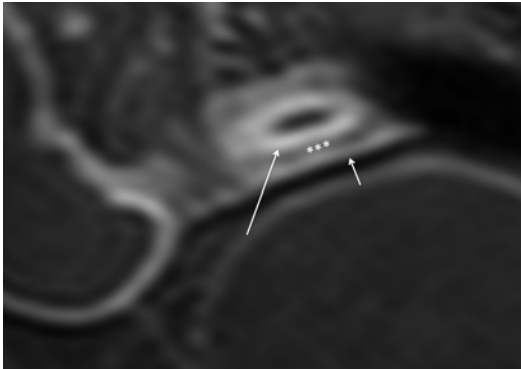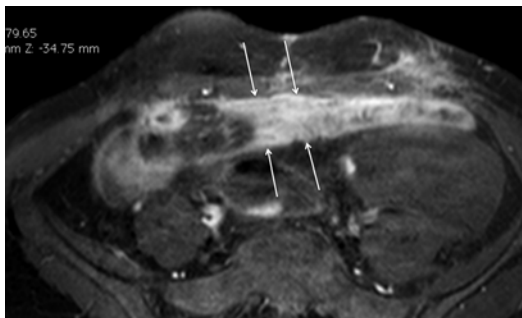
Fig. 4.19 Pattern III of mural enhancement – homogenous transmural enhancement in active Crohn's disease. Axial GE T1-weighted fat-saturated image, obtained after i.v. administration of gadolinium, shows homogeneous transmural hyperenhancement of the thickened bowel wall (*arrows*)

However, estimating the intensity of enhancement remains largely subjective and can be done by comparing the abnormally enhancing segment to an adjacent normal loop or by likening bowel loops that are at similar distance from the center of the field of view; this is to mitigate the field inhomogeneity, which may otherwise influence the apparent level of enhancement.

The degree of enhancement has been determined by using subjective categorical scales (i.e., low, mild, high) or more objective grading methods, such as the comparison with renal or hepatic enhancement [31–34].

To quantify the degree of enhancement and thus providing more objective methods of measurement, several authors have calculated several enhancement ratios obtained by dividing post-contrast signal intensity by the baseline signal intensity. However, the use of such enhancement ratios may lead to errors, not least those associated with difficulty in intra- and interobserver placement of the region of interest (ROI), whose accuracy may be ulteriorly limited in clinical practice. Moreover, there is often an overlap when assessing between active and chronic disease.
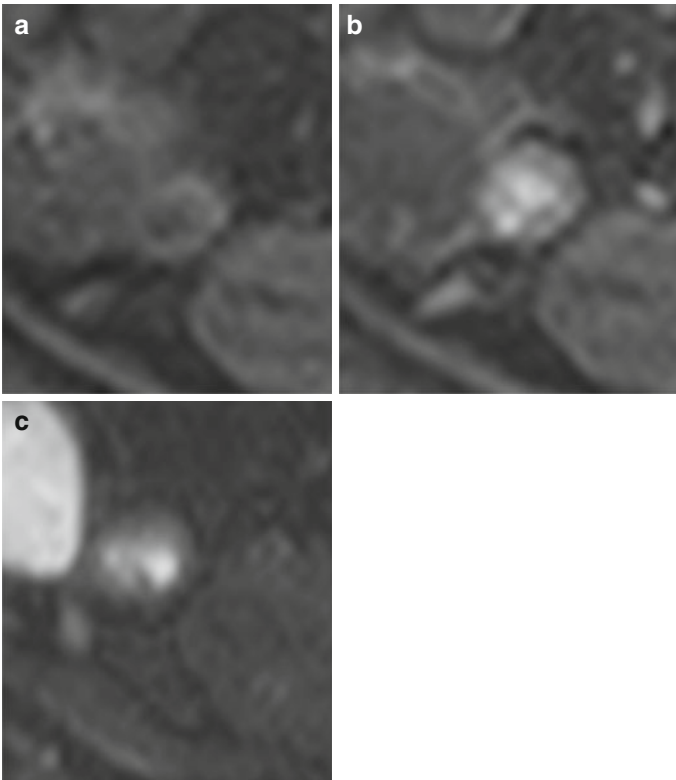
Fig. 4.20 Pattern IV of mural enhancement – chronic Crohn's disease. Magnified GE T1-weighted fat-saturated images, obtained before (**a**) and after i.v. administration of gadolinium (**b**), show inhomogeneous enhancement of the bowel. T2-weighted fat-saturated image (**c**) shows a mild, inhomogeneous hyperintensity of the bowel wall as well. Such findings are all compatible with chronic Crohn's disease

It should also be taken into account that enhancement is evaluated as a snapshot in time using standard post-contrast sequences.
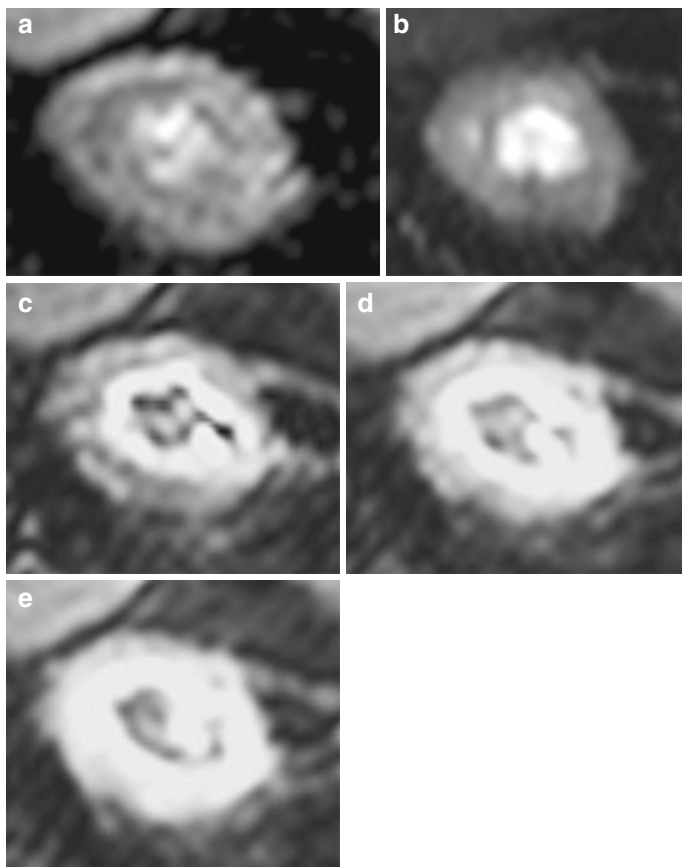
Fig. 4.21 Pattern IV of mural enhancement – mild active, progressing to chronic Crohn's disease. Bowel wall thickening is clearly seen on magnified GE T1-weighted, fat-saturated image (**a**), and a slight hyperintensity is appreciable on T2-weighted fat-saturated image as well (**b**), which is due to coexistent mild inflammation of the bowel wall. Dynamic contrast-enhanced GE T1-weighted fat-saturated images obtained at arterial, portal, and delayed phases, respectively (**c**–**e**), show mild and initial mucosal enhancement (arterial phase) and delayed submucosal enhancement (delayed phase), a finding of fibrotic degeneration

On the contrary, the emerging dynamic enhancement techniques show to be promising in quantifying enhancement, using this variable to determine inflammatory activity [10, 28, 35–37].

At DCE-MRI, the analysis of the time-dependent changes of signal intensity after gadolinium administration adds valuable information about the activity of Crohn's disease, as well as the kinetic of the signal variation reflects the status of tissue microcirculation, allowing semiquantitative (slope of enhancement) and quantitative (intravascular-extracellular transfer coefficient, volume of extracellular fluid) measurements, which may ultimately prove to be more useful in determining the level of inflammatory activity [10, 28, 35–37].

In addition, it should always be kept in mind that inadequate bowel loop distention can affect the assessment of enhancement: nondistended loops can brightly enhance, a finding that may inadvertently be interpreted as active disease.

4.5   Perienteric Inflammation

Edema and fluid in the mesenteric fat of an involved bowel segment are present in most of patients with advanced inflammatory disease, and they usually are proportionate with the activity of the disease [17].

Edema tracks along the adjacent mesentery from an inflamed bowel loop, and it is more evident on the T2-weighted fat-suppressed images [16]. The increased enhancement of the mesenteric fat around a bowel segment is another secondary sign of perienteric inflammation (Fig. 4.22).

Mesenteric inflammation may also lead to the formation of adhesions that can cause bowel kinking and obstruction. They may not be directly visualized, but their presence can be inferred on the basis of kinking, tenting, or obstruction of the bowel segments in the absence of another associated abnormality [29].
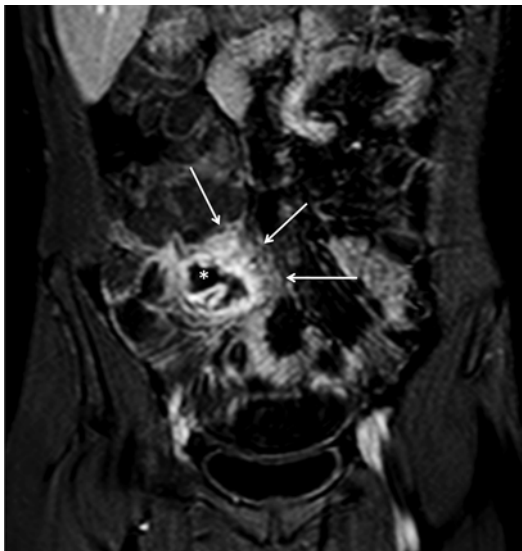
Fig. 4.22 Perienteric inflammation. Coronal GE T1-weighted fat-saturated image, obtained after i.v. administration of gadolinium, shows enhancement of both the wall of the terminal ileum (*asterisk*) and of perivisceral fat (*arrows*), as a consequence of progression of the inflammatory process to adjacent mesentery

An early detection of adhesions is important because they may require a treatment if they cause obstruction.

Thicker, fibrous adhesive bands may appear as isointense structures with enhancement similar to that of sinuses or fistulas. However, adhesions are best differentiated from sinuses and fistulas by means of MR fluoroscopy, because kinking and stretching of bowel loops may be better observed in real time. Furthermore, MR fluoroscopy is also very helpful for grading the severity of bowel obstruction.
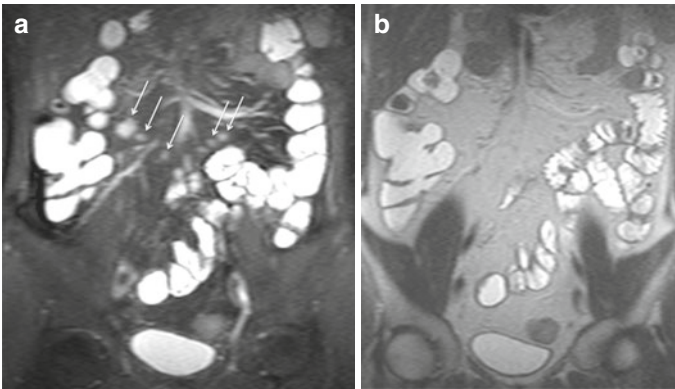
Fig. 4.23 Reactive adenopathy. Coronal T2-weighted fat-saturated image (**a**) well depicts multiple mesenteric lymphadenopathies (*arrows*), less evident on coronal T2-weighted image, performed at the same level without fat saturation (**b**)

4.6   Reactive Adenopathy

Reactive nodes and adenopathy are the rule in patients with CD, and they are usually recognizable at MRI [1, 11, 12, 16–18, 21, 28–31]. They typically lie along the vascular supply of a Crohn's diseased segment even if sometimes may be spatially remote from it.

Due to the poor contrast resolution of the extraenteric mesenteric fat tissue, lymph nodes are more easily identified on T2-weighted fat-suppressed or TrueFISP images rather than on HASTE sequences (Figs. 4.23 and 4.24) [17].

Lymph nodes of small volume can be seen adjacent to normal bowel segments and particularly those affected by active and inactive Crohn's disease. Lymph nodes that are increased in
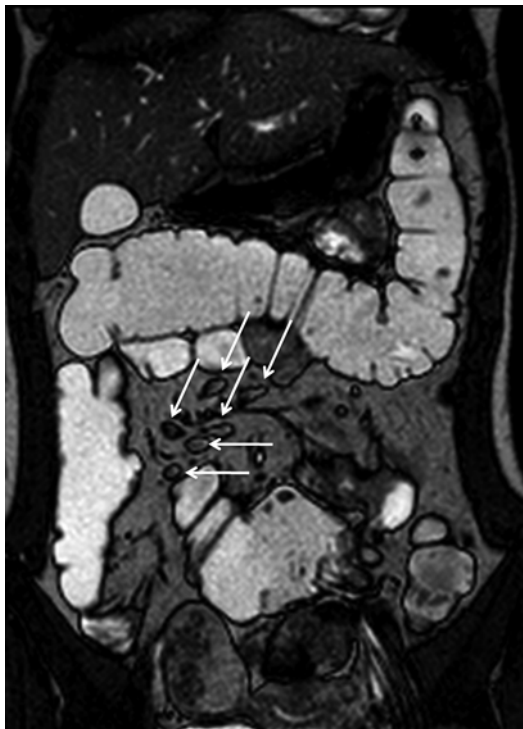
Fig. 4.24 Reactive adenopathy. Coronal TrueFISP image shows multiple mesenteric lymph nodes (*arrows*)

size can also be seen, both in active and inactive disease, and their presence alone cannot be considered as an inflammatory activity index. However, nodal edema, seen with fat-saturated HASTE sequences and homogeneous contrast enhancement, even in normal-sized nodes, is highly suggestive of active inflammation in patients in whom the diagnosis of CD has been previously established (Fig. 4.25) [38, 39].
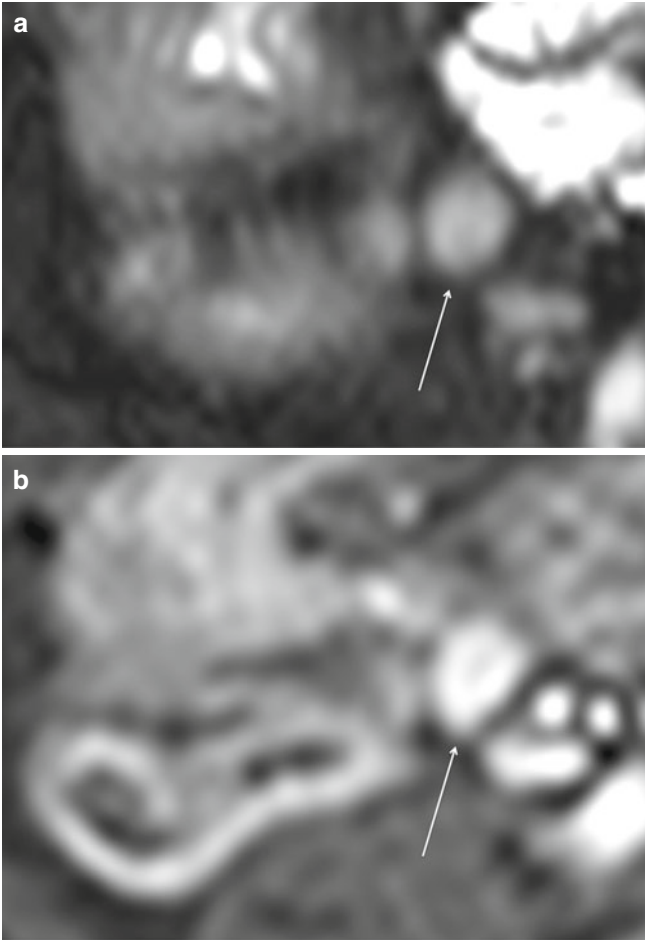
Fig. 4.25 Reactive adenopathy in active Crohn's disease. Magnified coronal HASTE fat-saturated image (**a**) shows an enlarged and hyperintense lymph node (*arrow*) that avidly enhances after i.v. administration of gadolinium, on axial GE T1-weighted image (**b**)
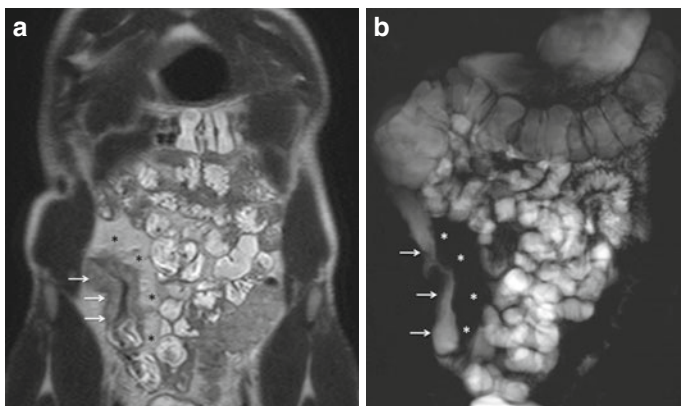
Fig. 4.26 Fibrofatty proliferation in chronic Crohn's disease. Coronal HASTE image (**a**) shows the displacement of the normal small bowel loops away from the diseased terminal ileum (*arrows*), as a consequence of mesenteric inflammation and fibrofatty proliferation (*asterisks*). Coronal MR-fluoroscopy image (**b**) clearly demonstrates the lumen narrowing of terminal ileum (*arrows*)

4.7   Mesenteric Fibrofatty Proliferation

Abnormalities of the mesenteric fat tissue, including its hypertrophy and the fat-wrapping, have been long recognized on surgical specimens and can be defined as the increased mesenteric fat tissue that produces a mass effect, separating bowel loops and displacing mesenteric vessels (Figs. 4.26 and 4.27) [10, 28, 35–37].

Frequently, it is also asymmetric, involving preferentially the mesenteric border of the bowel, even if fibrofatty proliferation often completely encircles the involved bowel loops. Fat-wrapping usually occurs in patients with long-standing, established transmural inflammation, and it is a specific distinguishing feature of chronic CD. Its presence at MR imaging is therefore indicative of CD [16].
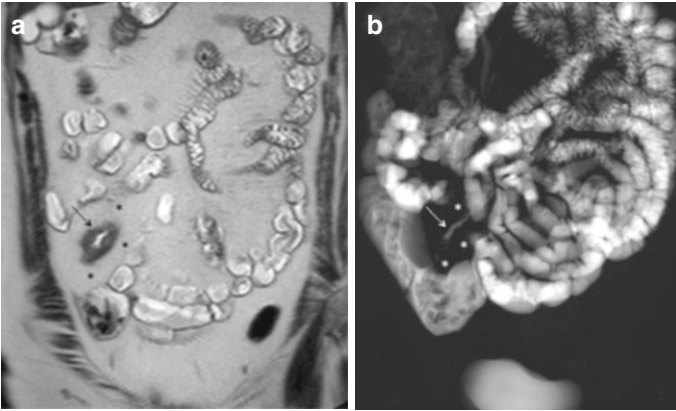
Fig. 4.27 Fibrofatty proliferation in chronic Crohn's disease. Coronal HASTE T2-weighted image (**a**) shows the normal small bowel displacement away from the diseased ileal loop (*black arrow*), caused by mesenteric inflammation and fibrofatty proliferation (*asterisks*). Coronal MR-fluoroscopy image (**b**) also shows lumen narrowing of the terminal ileum (*white arrow*)

4.8   Penetrating and Stricturing Patterns in CD

Crohn's disease is a heterogeneous entity. Clinically, the disease is classified into three categories, which are determined by pathological manifestations and symptoms, site of disease in the gastrointestinal tract, and the presence of complications, such as strictures or penetrating disease.

As previously stated in the introductive part of MRI findings regarding the phenotype of the disease, in the classification of Vienna, the behavior of Crohn's disease was separated into three prognostic relevant entities, including nonstricturing and non-penetrating disease (B1), stricturing disease (B2), and penetrating disease (B3) [40]. This classification system was later modified in the classification of Montreal, by adding perianal

penetrating disease, because perianal fistulas and abscesses have a different prognosis and outcome than intra-abdominal penetrating forms of CD [41].

Although these classification systems were originally designed to classify the patients affected by CD for clinical studies, nowadays, the behavior of the disease can also be used to determine the most correct therapeutic decision.

In fact, for what concerns the nonstricturing/nonpenetrating (or inflammatory) phenotype, it is usually medically treated.

Conversely, the presence of stricturing and penetrating disease influences the decision on surgical intervention and its timing.

The penetrating phenotype would eventually require surgical treatment in several cases. The stricturing phenotype requires intervention with mechanical treatments, such as balloon dilatation, strictureplasty, or resection, in many cases.

MR of the small bowel can offer a similar phenotypic characterization of Crohn's disease, based on the characteristic imaging findings, differentiating penetrating and stricturing disease from the inflammatory phenotype [21, 29, 42].

It is important, therefore, to report about the presence of penetrating ulcers, sinus tracts, fistulas, inflammatory masses, abscesses, and strictures/stenosis while interpreting MR enterography examinations.

4.8.1 Penetrating Disease

The fistulizing/penetrating phenotype is characterized by severe inflammation, which causes the progression of the transmural ulcerations into the surrounding mesentery, resulting in sinus tracts or fistulas.

Fistulas occur in up to 35 % of patients with CD at some time during the course of their disease and in one-third of patients within 10 years. The lifetime risk ranges from 20 % to 40 %.

The reported sensitivity of MR to detect internal fistulas ranges from 83.3 % to 84.4 %, while its specificity is approximately 100 % [11, 15, 43].

A sinus tract is defined as a blind-ending tract that arises from the bowel wall but does not reach another epithelium-lined surface. Conversely, fistulas may bridge adjacent loops of the small bowel or cross from the small bowel to the colon, stomach, and any adjacent organs, as well as the skin. Internal fistulas are more common than external enterocutaneous fistulas, and enteroenteric fistulas are usually asymptomatic [16, 21, 29, 42].

On images, sinus tracts appear as nodular irregularities and spiculations adjacent to serosal surface of the bowel. Small sinus tracts are usually difficult to identify, because of partial volume averaging, but thin-section MR images can be useful in assessing such tracts [29]. In particular, images obtained along a plane perpendicular to the bowel segment allow more accurate assessment of inflammatory perivisceral changes and of the transmural inflammation.

Large sinus tracts may be outlined by enteral contrast material and are seen on T2-weighted sequences as high signal intensity linear features.

Fistulas are usually well visualized on the TrueFISP and HASTE sequences, due to high signal of their fluid content; however, they can also be seen as rim-enhancing low-signal tracts on contrast-enhanced T1-weighted fat-suppressed images [16, 21, 29, 42]. Additionally, the multiplanar imaging capability of MR can be exploited to better depict complex fistula tracks.

When fistulas are complex, they appear as a network of intersecting linear tracts (Figs. 4.28 and 4.29). Very often in these cases, concomitant small sinus tracts can be depicted (Fig. 4.28). Typically, a complex network between multiple closely adherent and converging loops of an inflamed bowel tract may appear as a stellate configuration on contrast-enhanced MR images, the
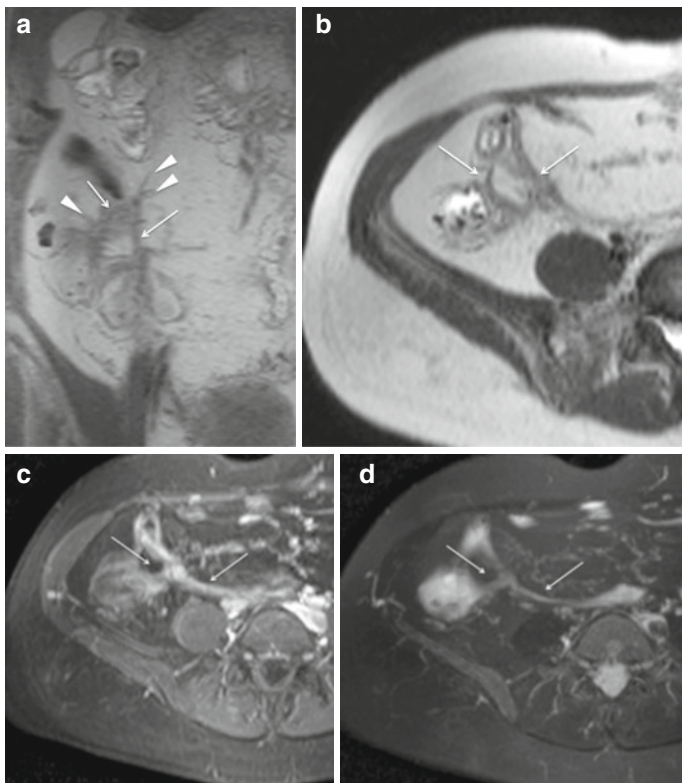
Fig. 4.28 Enterocolic fistula. Magnified coronal HASTE image (**a**) and axial HASTE image (**b**) showing enterocolic fistulas (*arrows*). On axial T2-weighted fat-saturated image (**c**), the course of fistula is well seen (*arrows*), and axial GE T1-weighted fat-saturated image, obtained after i.v. administration of gadolinium (**d**), confirms it. Note also the coexistence of of small sinus tracts (*arrowheads*) in (**a**)

"star sign," a suggestive finding of enteroenteric fistulas (Fig. 4.30) [16].

Fistulas, if associated with acute inflammation, manifest themselves as conspicuous bright signal on DWI sequences.
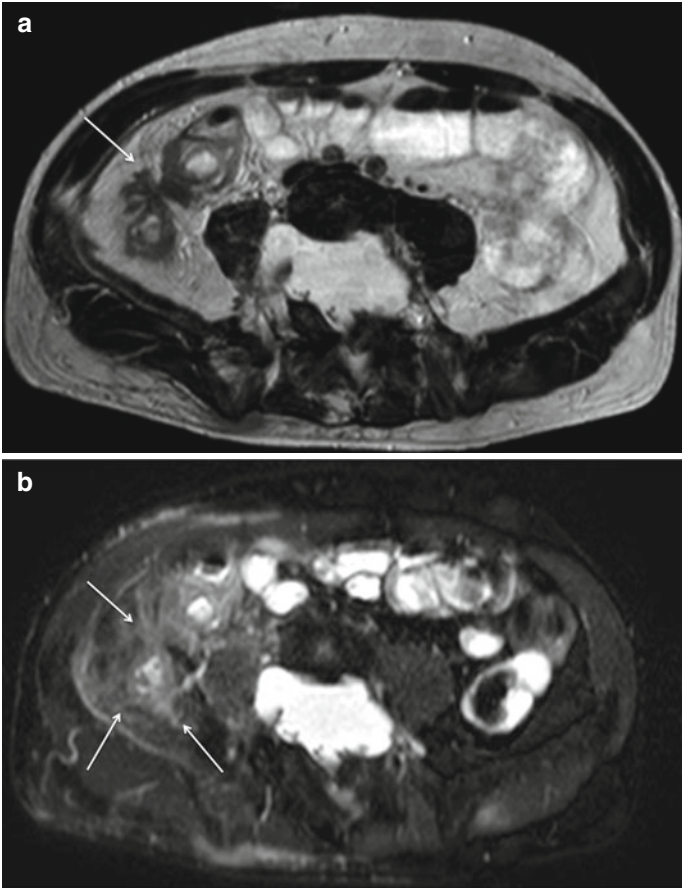
Fig. 4.29 Enterocolic fistula. Axial HASTE image (**a**) showing enterocolic fistulas (*arrow*). Perivisceral edema is more evident on axial HASTE fat-saturated image (**b**)

Both contrast-enhanced and DWI sequences have been shown to equally improve detection of fistulas when combined with a T2-weighted sequence; DWI may be especially useful in patients with risk factors for contrast agents [23, 24].
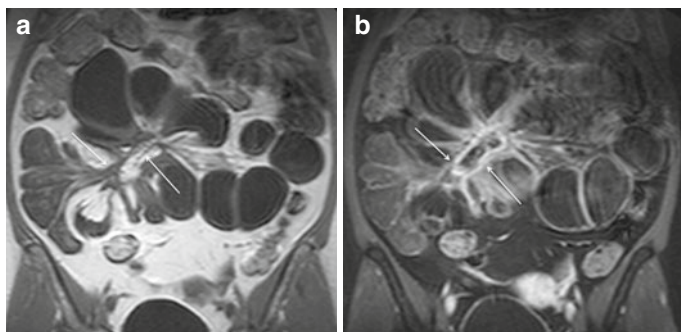
Fig. 4.30 Enteroenteral fistula. Coronal GE T1-weighted image (**a**) showing a "stellate pattern" caused by bowel loop retraction to a central area, with an associated complex enteroenteral fistula (*arrows*). Coronal GE T1-weighted fat-saturated image, obtained after i.v. injection of gadolinium, shows inflammatory hyperenhancement and "star sign" (**b**)

Intestinal fistulas by themselves are not a primary indication for surgery. In fact, surgery is indicated if fistulas involve the renal tract causing renal impairment or infection, if their drainage may cause personal discomfiture and hygiene, or if they create a significant bypass resulting in intestinal malabsorption.

Penetrating disease can also determine the formation of phlegmons or abscesses.

In fact, if deep transmural ulcers eventually penetrate the bowel muscle layers, they can cause inflammation in the adjacent mesenteric tissue, which may lead to the formation of phlegmons evolving in peri-intestinal abscesses. Moreover, deep ulcers can also form cavities within the bowel wall, which may become secondarily infected. Mural abscesses, causing bulging of the bowel wall, may also perforate it leading to the formation of intra-abdominal abscesses, just in the adjacent mesentery [16, 21, 29, 42].
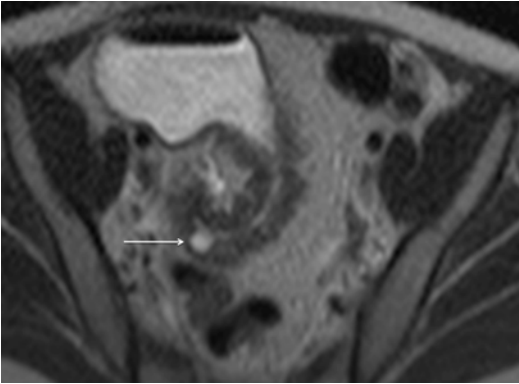
Fig. 4.31 Intramural abscess. Axial HASTE image showing a round hyperintense lesion (*arrow*) within the thickened wall of a diseased ileal segment. Of particular note, the lumen narrowing and the distention of prestenotic tract

Phlegmons appear as heterogeneous "pseudomass lesions," with low signal on T1-weighted images and intermediate to high signal on T2-weighted images.

Abscesses appear as fluid collections that show intense peripheral enhancement, with or without associated intralesional air (Figs. 4.31, 4.32, 4.33, and 4.34) [16]. However, interloop abscesses may be difficult to detect when bowel loops are retracted or matted.

On DWI, abscesses appear bright and their conspicuity on this sequence can enhance the detection and diagnostic confidence (Fig. 4.34) [23, 24].

A correct diagnosis is important, because the absence of an abscess in the presence of a penetrating disease often alters medical therapy; in fact clinicians generally avoid the use of steroids in such cases and may consider antibiotic or biologic therapy.
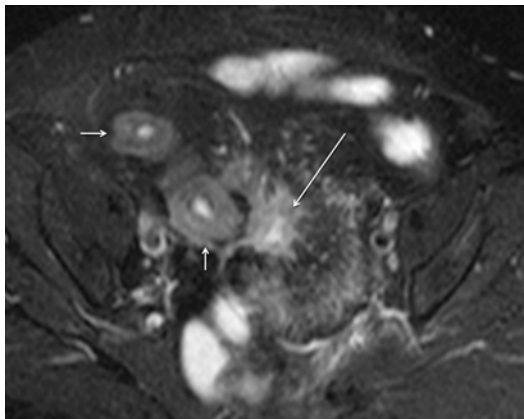
Fig. 4.32 Perivisceral phlegmon evolving toward an abscess. Axial T2-weighted fat-saturated image shows a mesenteric pseudomass (*long arrow*) adjacent to the diseased bowel segments (*short arrows*) and with a small central colliquative area

4.8.2 Fibrostenosing Disease

Over time, chronic inflammation within the bowel wall progresses to mural fibrosis. Additionally, when fibrosis is associated with stricture formation, bowel wall obstruction may develop.

Small bowel strictures can be defined as functionally significant when there is an upstream bowel dilatation greater than 3 cm. The importance of identifying fibrotic strictures with certainty is due to the fact that they are unresponsive to medical therapy [17].

Commonly, a single stricture in the terminal ileum causes the obstruction, and treatment is carried out by resection and primary anastomosis. However, recurrent disease after ileocolic resection is seen in one-third of patients within 10 years. Moreover, the presence of a fibrotic stricture does not exclude the possibility of coexistent active inflammation elsewhere in the bowel [21, 29, 42].
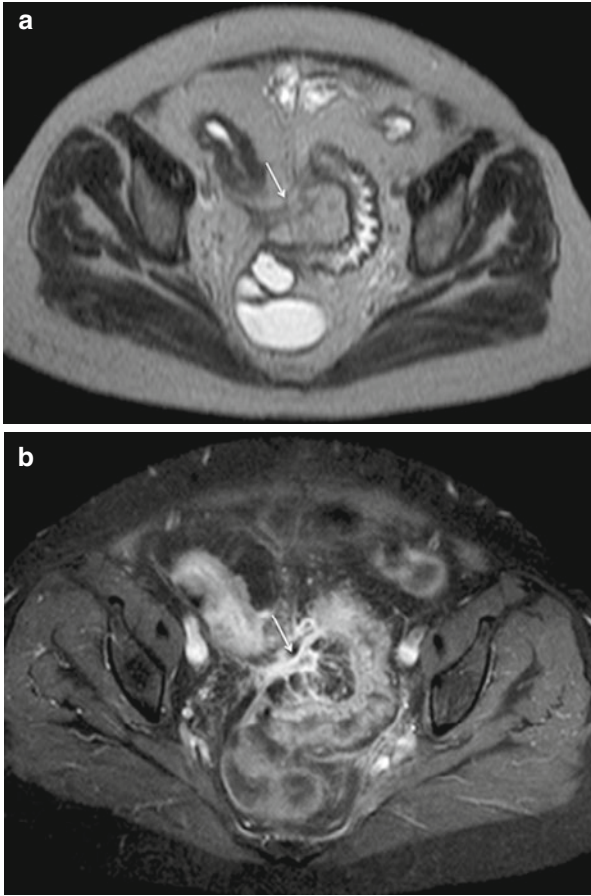
Fig. 4.33 Enterosigmoid fistula with perivisceral abscess. Axial HASTE images (**a**, **c**) and axial GE T1-weighted fat-saturated images, performed after i.v. injection of gadolinium (**b**, **d**) obtained along two different axial abdominal planes. (**a**, **b**) show an enterosigmoid fistula (*arrow*). (**c**, **d**) depict a small abscess in the adjacent mesentery, just below the fistula (*arrows*). Note also the "target sign" in the adjacent diseased bowel segment (**c**, **d**)
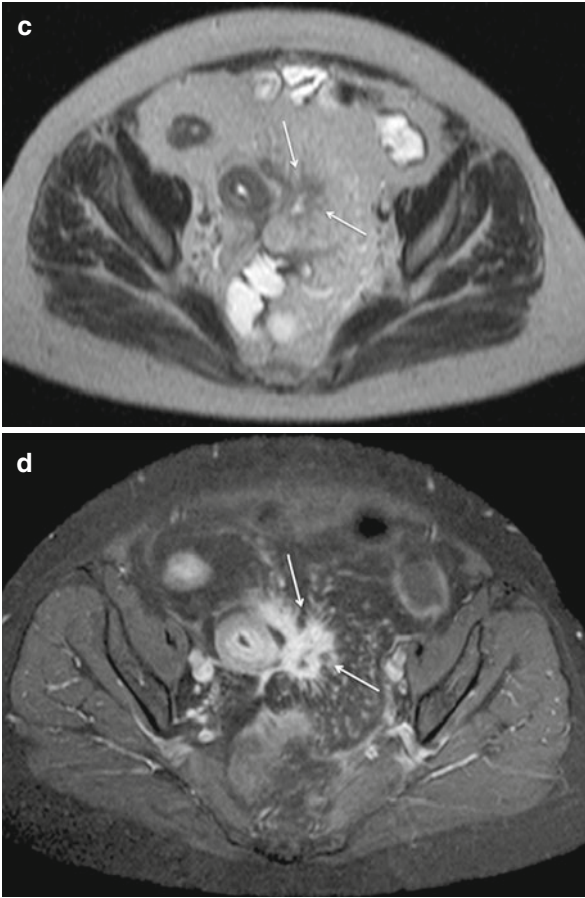
Fig. 4.33 (continued)

One of the other more common procedures is strictureplasty, which is used to open up a narrowed section of the bowel. Unlike a resection surgery, no part of the bowel is removed during a strictureplasty, making it an appealing alternative to a
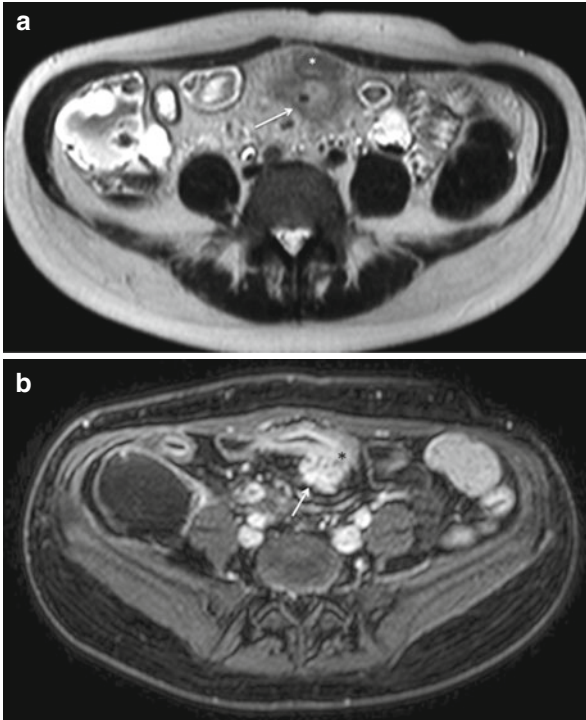
Fig. 4.34 Perivisceral abscess with gas bubble. Axial HASTE image (**a**) demonstrating a mesenteric abscess with a small gas bubble inside (*arrow*) adjacent to a diseased bowel segment (*asterisk*). Axial GE T1-weighted fat-saturated images, obtained after i.v. injection of gadolinium at different levels (**b**, **c**), demonstrate diffuse enhancement of inflamed bowel segment (*asterisk*), which appears to be undetachable from the enhancing abscess (*arrow*). On axial DW image performed at **b**: 800 s/mm^2 (**d**), abscess appears hyperintense (*arrow*), as well as the diseased bowel tract (*asterisk*). Note the loss of signal of the gas bubble

resection when possible. Strictureplasty may be done alone, or it may be done at the same time as a resection.

MRI can provide useful information in these settings by differentiating between fibrotic and inflammatory strictures.
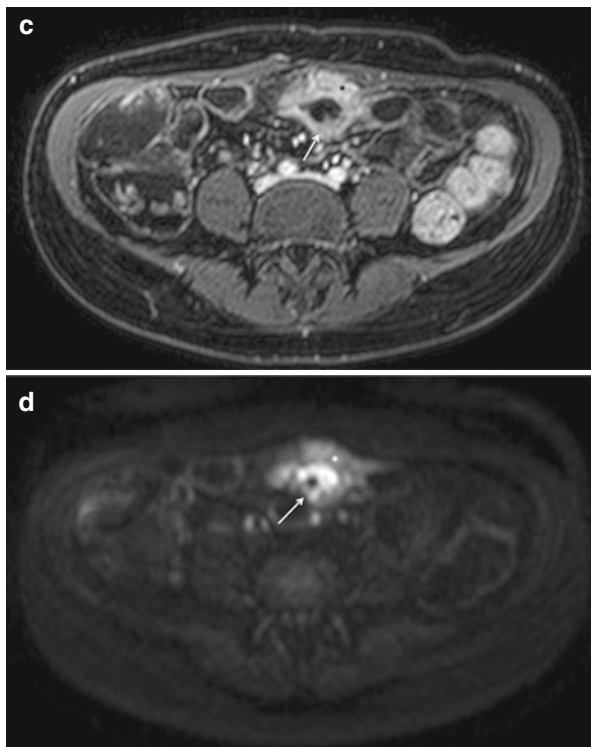
Fig. 4.34 (continued)

In the fibrostenosing disease phenotype, MRI demonstrates a fixed narrowing of the involved bowel with wall thickening associated and with a marked prestenotic dilatation. The thickened submucosa of a strictured, fibrotic bowel segment, in the absence of active disease, does not typically display any increased signal intensity on T2-weighted images, because of the lack of mural inflammation and edema [16]. Moreover, fibrotic strictures may show minor, inhomogeneous contrast enhancement without a layered pattern and without any evidence of edema, inflammation, or hyperemia of the surrounding mesentery (Fig. 4.35) [21, 29].
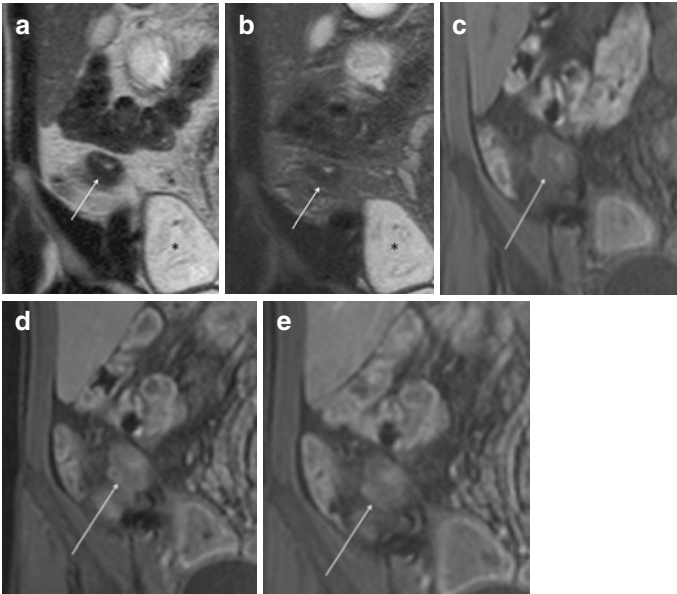
Fig. 4.35 Fibrostenosing phenotype in Crohn's disease. Magnified coronal HASTE image (**a**) showing a thickened hypointense segment at the level of the terminal ileum (*arrow*), persisting also on coronal T2-weighted fat-saturated image (**b**), expression of a fibrotic intestinal stricture, associated with marked prestenotic dilatation (*asterisk*). On oblique-sagittal GE T1-weighted fat-saturated images (**c–e**), obtained before (**c**) and after i.v. injection of gadolinium and performed during portal (**d**) and delayed (**e**) phases, no contrast enhancement could be seen (*arrow*)

Mural layered enhancement is lost also in long-standing disease if transmural fibrosis has supervened.

On MR-fluoroscopy and cine images, fibrotic strictures appear as aperistaltic bowel segments that often display a fixed mural thickening and luminal narrowing.

However, it has to be said that an isolated stricture with wall thickening in the absence of other more specific signs of CD should always imply an extensive differential diagnosis, which

includes infections, radiation enteritis, or neutropenic enteritis in immunocompromised patients (in the latter two conditions, an appropriate antecedent history would be expected) and malignancies such as carcinoid tumors and lymphoma. The clinical history always helps, therefore, to resolve the diagnostic difficulty in most cases.

References

1. Martin DR, Lauenstein T, Sitaraman SV (2007) Utility of magnetic resonance imaging in small bowel Crohn's disease. Gastroenterology 133:385–390
2. Satsangi J, Parkes M, Jewell DP et al (1998) Genetics of inflammatory bowel disease. Clin Sci (Lond) 94:473–478
3. Loftus EV Jr (2004) Clinical epidemiology of inflammatory bowel disease: incidence, prevalence, and environmental influences. Gastroenterology 126:1504–1517
4. Shanahan F (2002) Crohn's disease. Lancet 359:62–69
5. Wills JS, Lobis IF, Denstman FJ (1997) Crohn disease: state of the art. Radiology 202:597–610
6. Podolsky DK (2002) Inflammatory bowel disease. N Engl J Med 347: 417–429
7. Bosani M, Ardizzone S, Porro GB (2009) Biologic targeting in the treatment of inflammatory bowel diseases. Biologics 3:77–97
8. Bansal P, Sonnenberg A (1996) Risk factors for colorectal cancer in inflammatory bowel disease. Am J Gastroenterol 91:44–48
9. Cheifetz AS (2013) Management of active Crohn disease. JAMA 309: 2150–2158
10. Del Vescovo R, Sansoni I, Caviglia R et al (2008) Dynamic contrast enhanced magnetic resonance imaging of the terminal ileum: differentiation of activity of Crohn's disease. Abdom Imaging 33:417–424
11. Gourtsoyiannis NC, Grammatikakis J, Papamastorakis G et al (2006) Imaging of small intestinal Crohn's disease: comparison between MR enteroclysis and conventional enteroclysis. Eur Radiol 16:1915–1925
12. Masselli G, Brizi G, Parrella A et al (2004) Crohn disease magnetic resonance enteroclysis. Abdom Imaging 29:326–334
13. Chou CK, Chen LT, Sheu RS et al (1994) MRI manifestations of gastrointestinal wall thickening. Abdom Imaging 19:389–394
14. Prassopoulos P, Papanikolaou N, Grammatikakis J et al (2001) MR enteroclysis imaging of Crohn disease. Radiographics 21:s161–s172

15. Maselli G, Casciani E, Polettini et al (2006) Assessment of Crohn's dis-
    ease in the small bowel: prospective comparison of magnetic resonance
    enteroclysis with conventional enteroclysis. Eur Radiol 16:2817–2827
16. Mazziotti S, Ascenti G, Scribano E et al (2011) Guide to magnetic
    resonance in Crohn's disease: from common findings to the more rare
    complicances. Inflamm Bowel Dis 17:1209–1222
17. Tolan JM, Greenhalgh R, Zealley IA et al (2010) MR enterographic
    manifestation of small bowel Crohn disease. Radiographics 30:
    367–384
18. Sempere GA, Martinez SV, Medina CE (2005) MRI evaluation of
    inflammatory activity in Crohn's disease. Am J Roentgenol 184:
    1829–1835
19. Zappa M, Stefanescu C, Cazals-Hatem D et al (2011) Which magnetic
    resonance findings accurately evaluate inflammation in small bowel
    Crohn's disease? A retrospective comparison with surgical pathologic
    analysis. Inflamm Bowel Dis 17:984–993
20. Griffin N, Grant LA, Anderson S et al (2012) Small bowel MR enterog-
    raphy: problem solving in Crohn's disease. Insights Imaging 3:
    251–263
21. Sinha R, Murphy P, Hawker P et al (2009) Role of MRI in Crohn's
    disease. Clin Radiol 64:341–352
22. Oto A, Kulkarni K, Karczmar GS et al (2009) Evaluation of diffusion-
    weighted MR imaging for detection of bowel inflammation in patients
    with Crohn's disease. Acad Radiol 16:597–603
23. Kiryu S, Dodanuki K, Takao H et al (2009) Free-breathing diffusion-
    weighted imaging for the assessment of inflammatory activity in
    Crohn's disease. J Magn Reson Imaging 29:880–886
24. Buisson A, Joubert A, Montoriol PF et al (2013) Diffusion-weighted
    magnetic resonance imaging for detecting and assessing ileal inflam-
    mation in Crohn's disease. Aliment Pharmacol Ther 37:537–545
25. Froelich JM, Waldherr C, Stoupis C et al (2010) MR motility in
    Crohn's disease improves lesion detection compared with standard MR
    imaging. Eur Radiol 20:1945–1951
26. Odille F, Menys A, Ahmed A et al (2012) Quantitative assessment of
    small bowel motility by nonrigid registration of dynamic MR images.
    Magn Reson Med 68:783–793
27. Menys A, Atkinson D, Odille F et al (2012) Quantified terminal ileal
    motility during MR enterography as a potential biomarker of Crohn's
    disease activity: a preliminary study. Eur Radiol 22:2494–2501
28. Yacoub HJ, Obara P, Oto A (2013) Evolving role of MRI in Crohn's
    disease. J Magn Reson Imaging 37:1277–1289
29. Sinha R, Rajia P, Murphy P et al (2009) Utility of high-resolution MR
    imaging in demonstrating transmural pathologic changes in Crohn
    disease. Radiographics 29:1847–1867

30. Sinha R, Murphy P, Sanders S et al (2013) Diagnostic accuracy of high-resolution MR enterography in Crohn's disease: comparison with surgical and pathological specimen. Clin Radiol 68:917–927
31. Laghi A, Paolantonio P, Catalano C et al (2003) MR imaging of the small bowel using polyethylene glycol solution as an oral contrast agent in adults and children with celiac disease: preliminary observations. Am J Roentgenol 180:191–194
32. Low RN, Francis IR, Politoske D et al (2000) Crohn's disease evaluation: comparison of contrast-enhanced MR imaging and single-phase helical CT scanning. J Magn Reson Imaging 11:127–135
33. Maccioni F, Viscido A, Broglia L et al (2000) Evaluation of Crohn disease activity with magnetic resonance imaging. Abdom Imaging 25: 219–228
34. Laghi A, Borrelli O, Paolantonio P et al (2003) Contrast enhanced magnetic resonance imaging of the terminal ileum in children with Crohn's disease. Gut 52:393–397
35. Taylor SA, Punwani S, Rodriguez-Justo M et al (2009) Mural Crohn disease: correlation of dynamic contrast-enhanced MR imaging findings with angiogenesis and inflammation at histologic examination. Pilot study. Radiology 251:369–379
36. Giusti S, Faggioni L, Neri E et al (2010) Dynamic MRI of the small bowel: usefulness of quantitative contrast-enhancement parameters and time-signal intensity curves for differentiating between active and inactive Crohn's disease. Abdom Imaging 35:646–653
37. Oto A, Fan X, Mustafi D et al (2009) Quantitative analysis of dynamic contrast enhanced MRI for assessment of bowel inflammation in Crohn's disease: pilot study. Acad Radiol 16:1223–1230
38. Maccioni F, Bruni A, Viscido A et al (2006) MR imaging in patients with Crohn disease: MR sequences with the use of an oral superparamagnetic contrast agent. Radiology 238:157–530
39. Gourtsoyianni S, Papanikolaou N, Amanakis E et al (2009) Crohn's disease lymphadenopathy: MR imaging findings. Eur J Radiol 69:425–428
40. Gasche C, Scholmerich J, Brynskov J et al (2000) A simple classification of Crohn's disease: report of the Working Party for the world Congress of Gastroenterology, Vienna 1998. Inflamm Bowel Dis 6:8–15
41. Satsangi J, Silverberg MS, Vermeire S et al (2006) The Montreal classification of inflammatory bowel disease: controversies, consensus, and implications. Gut 55:749–753
42. Leyendecker JR, Bloomfeld RS, DiSantis DF et al (2009) MR enterography in the management of patients with Crohn disease. Radiographics 29:1827–1846
43. Schmidt S, Chevvalier P, Bessoud B et al (2007) Diagnostic performance of MRI for detection of intestinal fistulas in patients with complicated inflammatory conditions. Eur Radiol 17:2957–2963

Chapter 5
Extraintestinal Complications

Several extraintestinal complications have been associated to IBD. In particular, it has been noted that up to 36 % of patients with CD have at least one extraintestinal manifestation and 25 % have more than one extraintestinal complication. Moreover, the development of one extraintestinal complication appears to increase the risk of developing others [1].

This chapter discusses the usefulness of MREg/MREc even in detecting extraintestinal complications, which may sometimes be the initial presenting symptoms or, most commonly, be hidden by the major intestinal symptoms.

Abdominopelvic extraintestinal complications of CD, which can involve the hepatobiliary and pancreatic system, genitourinary system, musculoskeletal and cutaneous systems, as well as the peritoneum, are well depicted on MR of the small bowel [2]. It is therefore mandatory for the gastrointestinal radiologist who performs the examination to have a basic knowledge of which are the main extraintestinal complications and of their relative imaging characteristics.

Different factors may be responsible for extraintestinal organ involvement, and this can make difficult the differentiation between true extraintestinal manifestations (i.e., primary systemic affections directly caused by IBD) and secondary extraintestinal complications of the disease, caused, for

example, by malnutrition, chronic inflammation, or side effects of therapy. Furthermore, even if some of these complications may not correlate with disease activity (e.g., primary sclerosing cholangitis and ankylosing spondylitis), generally, they tend to follow the clinical course of disease and may have a high impact on the patient's life quality, morbidity, and also mortality [2, 3].

5.1 Hepatobiliary Complications

The hepatobiliary manifestations of IBD include primary sclerosing cholangitis, gallstone disease, liver abscess, and portal vein thrombosis.

Even if rare, the involvement of the biliary tract can also be caused by the presence of inflammatory disease in the duodenum or by inflammation of the lesser omentum, which can lead to obstruction of the common bile duct, to ampullary stenosis (Figs. 5.1 and 5.2), or to duodeno-biliary fistulas (Fig. 5.3).

5.1.1 Primary Sclerosing Cholangitis

One of the most serious complications of CD is primary sclerosing cholangitis (PSC), a disorder of both intrahepatic and extrahepatic bile ducts [4]. It has an unclear etiology and has a chronic and progressive course, and it manifests itself as inflammation and fibrosis of the medium and large intra- and extrahepatic bile ducts.

At least 5–10 % of PSC patients have CD. However, PSC may occur in 2–4 % of patients with CD, usually in those with colonic involvement and more likely in men than women [5]. Its clinical course bears no relationship to underlying bowel
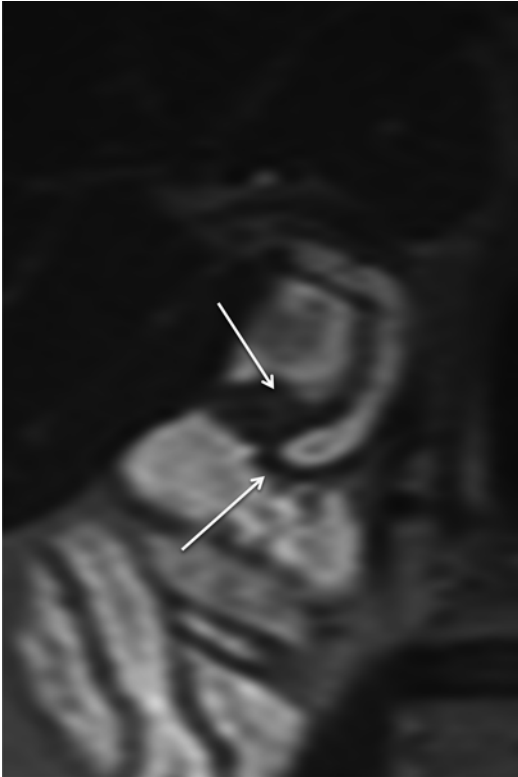
Fig. 5.1 Ampullary stenosis. Magnified coronal HASTE image shows wall thickening in the ampullary area (*arrows*) with a mild upstream dilatation of the common bile duct

disease; in fact, PSC may develop years either before or after the development of intestinal symptoms [3].

The MREg/MREc protocols, i.e. the MR fluoroscopy, well depict the typical findings of PSC, including multifocal strictures and irregularity of both intra- and extrahepatic bile ducts, leading to the classic "beads on a string" appearance (Fig. 5.4) [3, 6, 7].
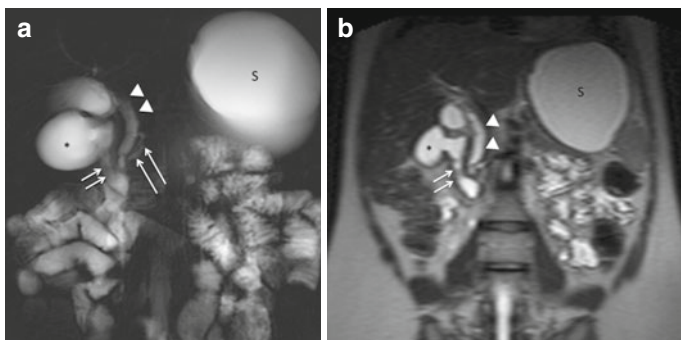
Fig. 5.2 Ampullary stenosis. Coronal MR-fluoroscopy image (**a**) and coronal HASTE image (**b**) show the narrowing of duodenal lumen (*short arrows* in **a**), due to a concentric thickening of the duodenal wall in proximity of the ampullary area (*short arrows* in **b**). The consequent dilatation of the proximal duodenal bulb (*asterisk*) and of the stomach (*S*) can also be seen. The common bile duct (*arrowheads*) and pancreatic duct (*long arrows* in **a**) are visibly dilated
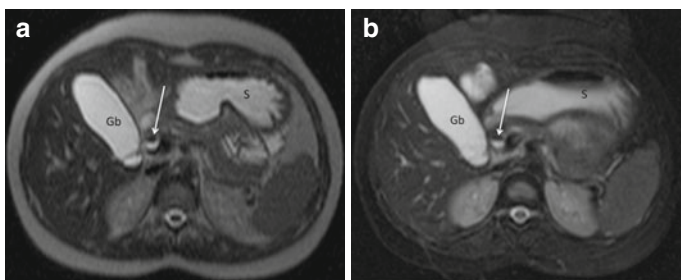
Fig. 5.3 Duodeno-biliary fistula. Axial HASTE image (**a**) and axial HASTE fat-saturated image (**b**), obtained along the same anatomical plane. Both MR images show the presence of an air-fluid level in the common bile duct (*arrow*), due to an enterobiliary fistula. *S* stomach, *Gb* gallbladder

It is the greatest risk factor for developing cholangiocarcinoma (they both present similar imaging characteristics), from which should be differentiated.
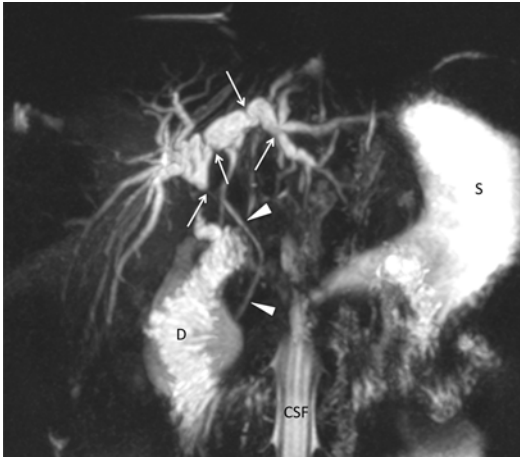
Fig. 5.4 Sclerosing cholangitis. Coronal MIP reformatted image, obtained from multislices HASTE fat-saturated sequence. Both the dilatations and strictures of intra- and extrahepatic bile ducts (*arrows*) are well seen. *Arrowheads*: common bile duct; *S* stomach, *D* duodenum, *CSF* cerebrospinal fluid

5.1.2 Gallstone Disease

Cholelithiasis is common in patients with CD. The reported prevalence of gallstone disease (GD), defined as current gallstones or previous cholecystectomy for gallstones, in patients with CD, ranges from 13 to 34 % [7–18].

In these patients, age, the site of CD at diagnosis, the number and sites of previous resections, as well as fasting and total parenteral nutrition are all independently associated with cholelithiasis, the pathogenesis of which is multifactorial.

The most important predisposing factor may be considered to be due to the malabsorption of bile acids from the inflamed terminal ileum, which leads to hepatic excretion of bile highly saturated with cholesterol; a further contributory
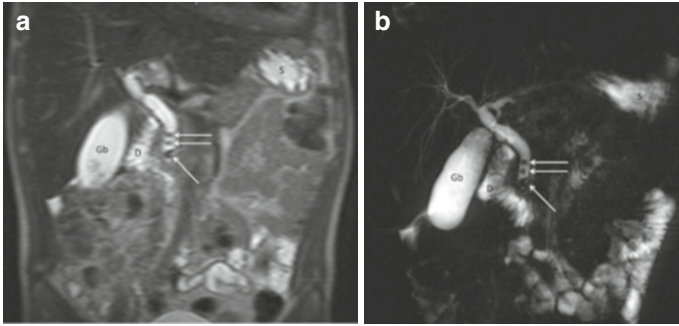
Fig. 5.5 Cholelithiasis. Coronal HASTE image (**a**) and coronal MR-fluoroscopy image (**b**) show the presence of small filling defects within the common bile duct, compatible with gallstones (*arrows*). The cholesterol composition of the CBD gallstones was demonstrated after removal by means of retrograde endoscopic cholangiopancreatography. *Gb* gallbladder, *S* stomach, *D* duodenum

role in the formation of gallstones could be played by a reduced and impaired fatty-meal-induced gallbladder motility, evidenced in most of patients with ileal and ileocolonic disease [18, 19]. Another possibility may be a decreased release and/or hypersecretion of hormones stimulating (e.g., cholecystokinin) or inhibiting (e.g., somatostatin) gallbladder motility [20].

The CD duration is another important risk factor for GD, as well as previous surgery and number of resections are, with particular regard to those involving the ileocecal region, more frequently associated with cholelithiasis and which can be explained with a reduction of transit time in the small intestine and a modification of the ileal microclimate.

The presence of cholelithiasis can be well detected at MR of the small bowel on both HASTE sequences and MR fluorography images (Fig. 5.5).

5.1.3 Liver Abscess

Most of the liver abscesses usually occur in patients who have a long-standing history of inflammatory bowel disease, even if a few reports of CD presenting de novo with hepatic abscess have been reported [21, 22]. Long-term steroid treatment, malnutrition, immunological abnormalities, and surgical interventions are additional predisposing factors that may lead to this occurrence.

The pathogenesis of liver abscess has been linked to the interruption of normal mucosal integrity by the intestinal ulcerations. In fact, the invasion of portal venous system by microorganisms facilitates these pathogens to reach the liver.

Clinical manifestations of liver abscesses are variable, and common symptoms are fever, anorexia, weight loss, and abdominal pain that may often be misdiagnosed, as their clinical presentation can resemble an exacerbation of CD.

MR findings characteristic of pyogenic abscesses are high signal intensity on T2-weighted images and low signal intensity on T1-weighted images. Pyogenic abscesses usually possess markedly thick walls and internal septations, which enhance moderately to intensely on early-phase images and demonstrate persistent enhancement on late-phase images (Fig. 5.6).

5.1.4 Portal Vein Thrombosis

A rare complication in the nonsurgical clinical setting is represented by portal vein thrombosis.

Generally, patients with IBD are three times more likely to experience thromboembolic events, compared with the general population, with incidence reported to be between 1 and 41 % [7].

The exact cause of the prothrombotic state is still unknown, even if it is likely multifactorial. Risk factors include active
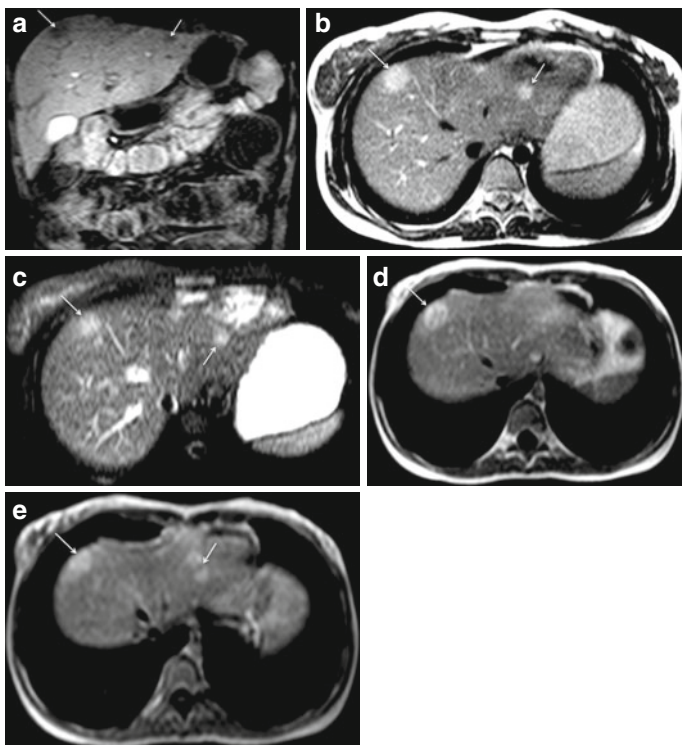
Fig. 5.6 Pyogenic liver abscesses in a febrile patient with Crohn's disease. Coronal GE T1-weighted fat-saturated image (**a**). Axial HASTE image (**b**) and axial HASTE fat-saturated image (**c**). Axial GE T1-weighted fat-saturated images, obtained after i.v. administration of gadolinium (**d**, **e**). MR shows two peripheral hepatic abscesses (*arrows*) hypointense on T1-weighted image (**a**) and hyperintense on T2-weighted sequences (**b**, **c**) characterized by marked peripheral enhancement on T1-weighted images obtained after contrast medium administration (**d**, **e**). The follow-up MR examination, performed after antibiotic therapy, demonstrated the complete resolution
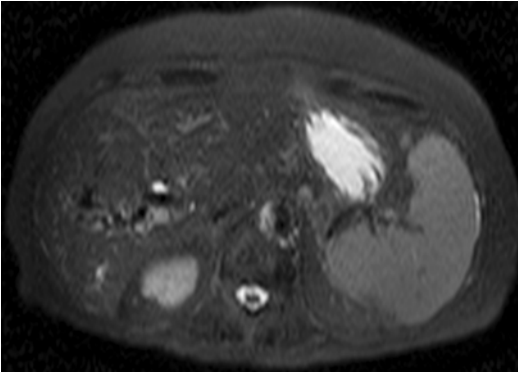
Fig. 5.7 Portal vein thrombosis. Axial HASTE fat-saturated image depicts right portal vein thrombosis with signs of periportal cavernomatosis. Because the patient had contraindications to contrast medium administration (allergy and nephropathy), diagnosis of thrombosis of the portal vein was confirmed by means of ultrasonography

inflammation, immobility, surgery, and central venous catheters as well as IBD itself.

During MRE, the signs of abdominal thromboembolic complication can and should be recognized (Fig. 5.7) [3].

5.2 Pancreatic Complications

Although infrequent, acute pancreatitis and less often chronic pancreatitis may occur in patients affected by IBD as a result of the disease itself or secondary to the medications used during the treatment [23–28]. Many drugs in IBD treatment have the potential to induce acute pancreatitis; in particular, sulfasalazine, 5-aminosalicylic acid, azathioprine,
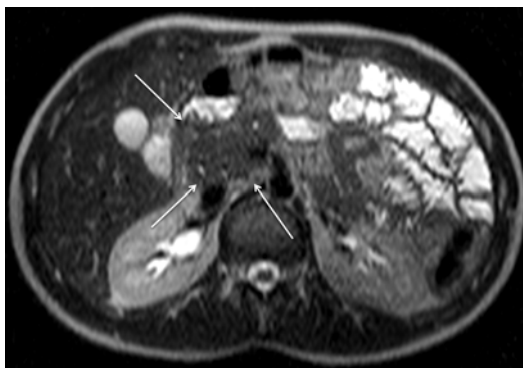
Fig. 5.8 A patient with CD in treatment with sulfasalazine and with a mild edematous form of head pancreatitis. Axial HASTE image shows mild enlargement of the pancreatic head (*arrows*) without any peripancreatic fluid collection

6-mercaptopurine, and rarely corticosteroids are well known to cause acute pancreatitis as a result of a possible idiosyncratic mechanism. Drug-induced pancreatitis typically occurs within the first weeks after drug therapy begins; the course is usually mild and resolves quickly after discontinuing the drug (Fig. 5.8) [25].

The IBD-pancreas association is further reflected in many reports of exocrine as well as endocrine pancreatic insufficiency.

The regional inflammatory complications due to duodenal and papillary involvement or biliary complications should also be considered when evaluating the pancreas at MRE.

For what concerns the pathogenesis of *chronic pancreatitis*, it still remains unclear. It has been considered to be caused by circulating inflammatory mediators rather than directly involved pancreatic tissue. Anyhow, autoantibodies against pancreatic tissue may also play a role in the development of exocrine insufficiency [29–32].

5.3 Genitourinary Complications

The topic of urogenital complications in inflammatory bowel disease is fairly narrow in its spectrum, and it is the expression of the metabolic interrelationships between the two organ systems. The most frequent conditions that fall under this list include ureteral obstruction, nephrolithiasis, fistulous disease involving the genitourinary tract, intrinsic renal disease associated with CD, and some considerations in those who have had surgical procedures that may alter the normal pelvic anatomy.

5.3.1 Ureteral Obstruction

Ureteral involvement is caused predominantly by transmural inflammation of the bowel, which can affect the retroperitoneum and results in ureter and bladder inflammation, fibrosis, or fistula formation [2]. The right ureter is involved most commonly because of the high incidence of CD in the ileocecal region.

Urinary symptoms are often minimal because of the more evident intestinal symptoms, giving evidence of the important role of imaging for early diagnosis.

Heavily T2-weighted sequences, performed in MREg/MREc protocols, help to determine the degree and the location of ureteral obstruction, a valuable method to noninvasively assess the urinary tract of patients affected by CD. Moreover, T1-weighted sequences, performed after intravenous injection of contrast medium, can also provide information about the renal excretory function (Fig. 5.9).

5.3.2 Nephrolithiasis

Kidney stones are a common manifestation of CD, occurring up to 19 % of patients with IBD, and should always be a part of the
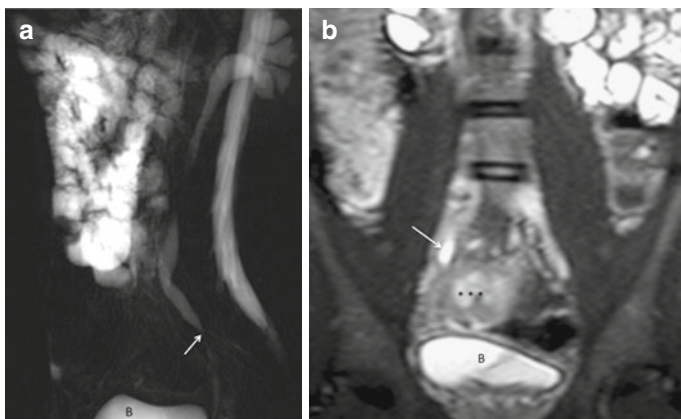
Fig. 5.9 Right ureterohydronephrosis due to pelvic ureter stenosis. Sagittal MR-fluoroscopy image (**a**) shows tapering of the pelvic ureter with mild degree of upstream dilation of ureteral and renal cavities (*arrow*). Coronal HASTE image (**b**) confirms the tapering of the ureter, which is caused by the diseased intestinal segment and the associated perivisceral inflammation (*asterisks*). *B* bladder

differential diagnosis when the patient presents with localized pain. Patients with severe intestinal involvement and a long disease course or who previously underwent extensive ileal resection or ileostomy formation are the ones with higher risk [32–35].

The causes of lithogenesis in CD are believed to be dehydration associated with chronic diarrhea, decreased urine volume, aciduria, bowel resection, abnormal metabolism of oxalic acid, and oral administration of steroids or salazosulfapyridine [36].

In fact, in patients with IBD, there is a tendency of chronic volume contraction, due to loss of water and salt in diarrhea stool, which leads to decreased urine volumes.

They also have a decreased intestinal absorption and a diminished urinary excretion of citrate and magnesium, which normally act as inhibitors of calcium oxalate crystallization. Moreover, in the intestinal lumen of these patients, less oxalate
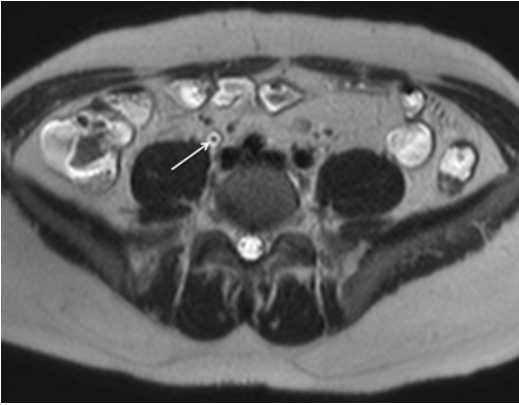
Fig. 5.10 Nephrolithiasis. Axial HASTE image shows a filling defect in the right ureter due to a stone (*arrow*)

is bound to luminal calcium, as the calcium preferentially binds to unabsorbed fatty acids, leading to an increased colonic absorption of oxalate and a decreased intraluminal component of insoluble calcium oxalate. For both these reasons, calcium oxalate stones are the most common type of stone encountered in patients with IBD, and for the same reasons, the treatment is supplemental calcium, rather than calcium restriction, as is commonly and erroneously recommended.

Uric acid stones can also occur, usually in patients with ileostomies and high ileostomy outputs. In fact in this case, there is a loss of a large volume of alkaline fluid from the stoma, which gives rise to a low volume of acidic urine favoring the precipitation of uric acid. To prevent this type of nephrolithiasis, the correct strategy is to increase the fluid intake, maintaining the patient on a low oxalate diet, and substituting medium-chain fatty acids for fats in the diet [33].

On MREg/MREc, the dilated ureter and the site of urinary stone obstruction can be readily demonstrated with the use of heavily T2-weighted sequences, which are routinely performed (Fig. 5.10).

5.3.3   Genitourinary Tract Fistulas

Patients with fistulous disease may present with urinary complaints prior to gastrointestinal abnormalities. It can involve several anatomical sites: upper urinary tract (kidney, ureter), lower urinary tract (bladder, urethra), or the female reproductive tract (vagina, uterus).

Enterovesical fistulas are the most common CD-related urinary fistula, affecting 2–8 % of patients [37–39].

They can arise as a manifestation of the transmural inflammation or as a complication of surgical resection, in the setting of anastomotic breakdown. Even if it can be difficult to diagnose, the most common symptoms include pneumaturia, dysuria, and frequency. Enterovaginal fistulas can arise from the ileum or colon. Patients affected by CD who underwent hysterectomy appear to be associated with the increased risk for the inception of a de novo fistula (Fig. 5.11).

Radiologists should be familiar with findings of genitourinary fistulas for both accurate diagnosis and, in many cases, guidance of management planning.

The direct identification of fistulas is not always possible, even if progressive filling with PEG-water solution of the uterine or vaginal cavity, observed at MRE performed with several sequential acquisitions, represents a reliable sign of enterovaginal or enterouterine fistula (Fig. 5.12).

5.4   Musculoskeletal and Cutaneous Manifestation

IBD-related arthropathy is part of a subset of diseases broadly termed "seronegative spondyloarthropathies." Arthritis occurs equally in males and females and is generally more common in

Fig. 5.11   Post-hysterectomy enterovaginal fistula. Sagittal HASTE image showing an enterovaginal fistula (*white arrows*). *Black arrow*: vaginal stump; *asterisk*: diseased ileal segment

patients with colonic disease than those with small bowel disease [40–42]. Approximately 12.8–23 % of patients have peripheral arthritis that typically runs a parallel disease activity course to that of the bowel [43, 44]. Axial arthropathies instead are not associated with disease activity.

The articular involvement can precede, be synchronous with, or develop following the diagnosis of IBD [40–42].
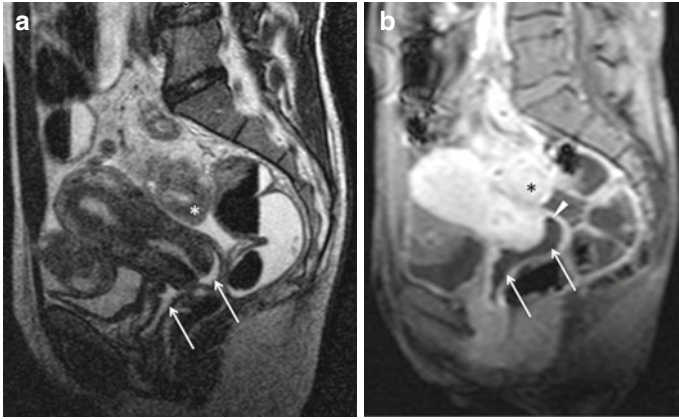
Fig. 5.12 Enterovaginal fistula. Sagittal HASTE image (**a**) shows the presence of fluid (*arrows*) within the vaginal channel; on sagittal GE T1-weighted image obtained after i.v. administration of gadolinium (**b**) and acquired 15 min after (**a**), a further filling of the vaginal cavity (*arrows*) is seen, as well as a suspicious gas bubble in the posterior vaginal fornix (*arrowhead* in **b**); both these signs are highly suggestive for enterovaginal fistula. *Asterisk*: inflamed bowel segment

Progressive ankylosing spondylitis and sacroiliitis, sometimes paucisymptomatic, may both occur.

MR is generally characterized by high sensitivity in detecting signs of sacroiliitis, and considering that as many as 27 % of patients with CD eventually have radiographic evidence of sacroiliitis, at MRE, attention has to be paid to detect any early signs.

MR signs of sacroiliitis are characterized by increased signal intensity in the sacroiliac joints and subchondral bone marrow on fat-suppressed T2-weighted images, as well as by enhancement of the joint space and subchondral region on fat-suppressed T1-weighted images obtained after intravenous injection of contrast medium (Fig. 5.13).
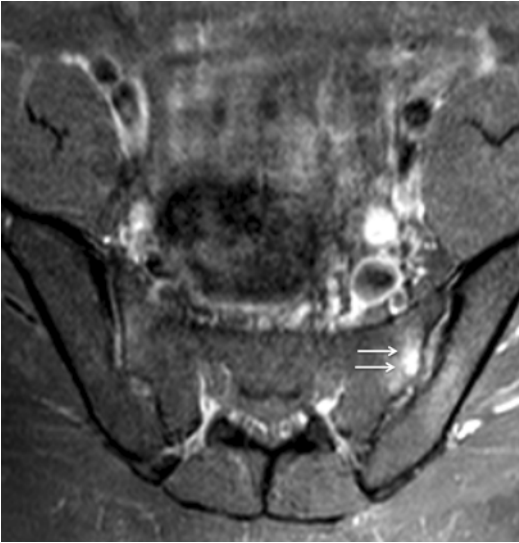
Fig. 5.13 Sacroiliitis. Axial GE T1-weighted fat-saturated image obtained after i.v. injection of gadolinium shows enhancement of both the sacroiliac joint spaces as well as a mild subchondral enhancement of the sacral bone. Such findings are more evident on the left side (*arrows*)

Osteoporosis is nowadays recognized as a common complication of IBD and in particular of CD. Beyond age-related risk factors that are present in the general population, there are multiple IBD-specific risk factors; these include corticosteroid therapy, inflammatory-mediated bone resorption, calcium and magnesium dietary malabsorption, poor dietary calcium intake (related to lactose intolerance), vitamin D deficiency, decreased serum albumin levels, and a reduced physical activity. Patients with IBD are therefore at increased risk of sustaining insufficiency fractures at several sites, such as the spine and pelvis (Fig. 5.14).
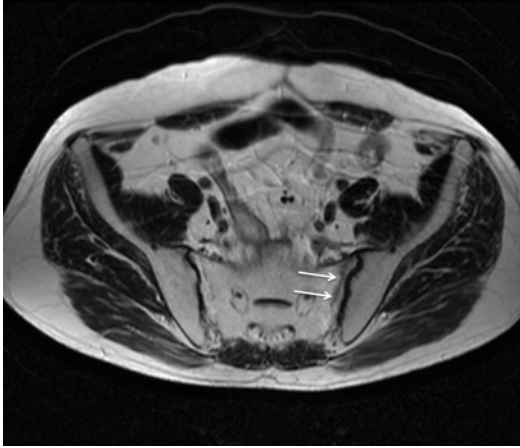
Fig. 5.14 Insufficiency fracture. Axial HASTE image showing a linear hypointensity (*arrows*) in the left sacralis ala that runs parallel to the sacro-iliac joint

Cutaneous CD may be contiguous with the gastrointestinal tract or distant ("metastatic cutaneous CD"). The classic extraintestinal manifestations are erythema nodosum, pyoderma gangrenosum, psoriasis, oral aphthous stomatitis, and Sweet's syndrome. These manifestations, related to systemic disease itself, are usually recognized at physical examination [45]. Anyhow, enterocutaneous fistulas can be routinely well demonstrated at MRE (Fig. 5.15).

5.5   Peritoneal Involvement

Normally, the peritoneum easily absorbs fluid; when inflamed or mechanically injured, the serosal properties are changed and fluid absorption is slower [36]

Fig. 5.15 Enterocutaneous fistula. Sagittal HASTE image shows the presence of enterocutaneous fistula (*arrows*)

Moreover, in females, peritoneal fluid is formed by exudation from an active ovary as suggested by the higher concentration of ovarian steroid hormones in peritoneal fluid than in plasma [46, 47]. When chronic peritoneal inflammation or
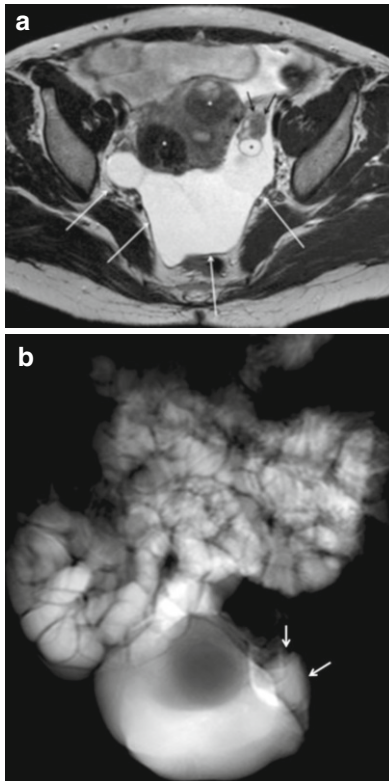
Fig. 5.16 Peritoneal pseudocyst. Axial HASTE image (**a**) showing a large peritoneal fluid collection outlined by peritoneum (*white arrows*). Note the left ovary at the periphery of the peritoneal pseudocyst (*black arrows*) with a small functional cyst (*black asterisk*). Uterine fibroids (*white asterisks*) can be seen. The same findings (the large peritoneal pseudocyst and the ovary with the cystic lesion) are also well showed on coronal MR fluoroscopy (**b**)

previous surgery leads to formation of adhesions that envelop an active ovary, ovarian fluids accumulate and a peritoneal pseudocyst may develop [48, 49].

MRE is particularly useful in detecting peritoneal pseudocysts in CD, because of its high contrast resolution to soft tissues. On MR imaging, pseudocysts appear irregular in shape, and the cyst walls may reflect the invaginations of the surrounding structures, because they do not have any true walls (walls are formed by the surrounding structures).

MR characteristics of peritoneal inclusion cysts are low signal intensity on T1-weighted images and high signal intensity on T2-weighted spin-echo images, suggesting that the fluid is serous. T2-weighted sequences performed during MRE allow the correct diagnosis in the right clinical setting, useful in treatment planning and considering the risk of recurrence after surgical resection (30–50 %) (Fig. 5.16) [47].

References

1. Bernstein CN, Blanchard JF, Rawsthorne P et al (2001) The prevalence of extraintestinal disease in inflammatory bowel disease: a population based study. Am J Gastroenterol 96:1116–1122
2. Mazziotti S, Ascenti G, Scribano E et al (2011) Guide to magnetic resonance in Crohn's disease: from common findings to the more rare complicances. Inflamm Bowel Dis 17:1209–1222
3. Mazziotti S, Blandino A, Scribano E et al (2013) MR enterography findings in abdominopelvic extraintestinal complications of Crohn's disease. J Magn Reson Imaging 37:1055–1063
4. Wee A, Ludwig J, Hellers G et al (1990) Extracolonic diagnosis of ulcerative colitis: an epidemiological study. Am J Gastroenterol 85:711–716
5. Ramussen HH, Fallinborg JF, Mortensen PB et al (1997) hepatobiliary dysfunction and primary sclerosing cholangitis in patients with Crohn's disease. Scand J Gastroenterol 32:604–610

6. Alexopoulou E, Xenophontos PE, Economopoulos N et al (2012) Investigative MRI cholangiopancreatography for primary sclerosing cholangitis-type lesions in children with IBD. J Pediatr Gastroenterol Nutr 55:308–313

7. Navaneethan U, Shen B (2010) Hepatopancreatobiliary manifestations and complications associated with inflammatory bowel disease. Inflamm Bowel Dis 16:1598–1619

8. Cohen S, Kaplan MM, Gottlieb L et al (1971) Liver disease and gallstones in regional enteritis. Gastroenterology 60:237–245

9. Baker AL, Kaplan MM, Norton RA et al (1974) Gallstones in inflammatory bowel disease. Am J Dig Dis 19:109–112

10. Hill GL, Mair WS, Goligher JC (1975) Gallstones after ileostomy and ileal resection. Gut 16:932–936

11. Whorwell PJ, Hawkins R, Dewbury K et al (1984) Ultrasound survey of gallstones and other hepatobiliary disorders in patients with Crohn's disease. Dig Dis Sci 29:930–933

12. Bluth EI, Merritt CR, Sullivan MA et al (1984) Inflammatory bowel disease and cholelithiasis: the association in patients with an ileostomy. South Med J 7:690–692

13. Andersson H, Bosaeus I, Fasth S et al (1987) Cholelithiasis and urolithiasis in Crohn's disease. Scand J Gastroenterol 22:253–256

14. Lorusso D, Leo S, Mossa A et al (1990) Cholelithiasis in inflammatory bowel disease: a case-control study. Dis Colon Rectum 33:791–794

15. Kangas E, Lehmusto P, Matikainen M (1990) Gallstones in Crohn's disease. Hepato-Gastroenterology 37:83–84

16. Hutchinson R, Tyrrell PMN, Kumar D et al (1994) Pathogenesis of gall stones in Crohn's disease: an alternative explanation. Gut 35:94–97

17. Lapidus A, Bangstad M, Astrom M et al (1999) The prevalence of gallstone disease in a defined cohort of patients with Crohn's disease. Am J Gastroenterol 94:1261–1266

18. Fraquelli M, Losco A, Visentin S et al (2001) Gallstone disease and related risk factors in patients with Crohn disease: analysis of 330 consecutive cases. Arch Intern Med 161:2201–2204

19. Dowling RH, Bell GD, White J (1972) Lithogenic bile in patients with ileal dysfunction. Gut 13:415–420

20. Fraquelli M, Bardella MT, Peracchi M et al (1999) Gallbladder emptying and somatostatin and cholecystokinin plasma levels in celiac disease. Am J Gastroenterol 94:1866–1870

21. Filik L, Ulker A, Tunc B et al (2004) Liver abscess: a rare but an important complication that must be considered in Crohn's disease. Acta Gastroenterol Belg 67:303–305

22. Karaca C, Pinarbasi B, Danalioglu A et al (2004) Liver abscess as a rare complication of Crohn's disease: a case report. Turk J Gastroenterol 15:45–48

23. Meyers S, Greenspan J, Greenstein AJ et al (1987) Pancreatitis coincident with Crohn's ileocolitis. Report of a case and review of the literature. Dis Colon Rectum 30:119–122

24. Ball WP, Baggenstoss AH, Bargen JA (1950) Pancreatic lesions associated with chronic ulcerative colitis. Arch Pathol 50:347–358

25. Axon AT, Ashton MG, Lintott DJ (1979) Chronic pancreatitis and inflammatory bowel disease. Clin Radiol 30:179–182

26. Pitchumoni CS, Rubin A, Das K (2010) Pancreatitis in inflammatory bowel diseases. J Clin Gastroenterol 44:246–253

27. Moolsintong P, Loftus EV Jr, Chari ST et al (2005) Acute pancreatitis in patients with Crohn's disease: clinical features and outcomes. Inflamm Bowel Dis 11:1080–1084

28. Inoue H, Shiraki K, Okano H et al (2005) Acute pancreatitis in patients with ulcerative colitis. Dig Dis Sci 50:1064–1067

29. Barthet M, Hastier P, Bernard JP et al (1999) Chronic pancreatitis and inflammatory bowel disease: true or coincidental association? Am J Gastroenterol 94:2141–2148

30. Ransford RA, Langman MJ (2002) Sulphasalazine and mesalazine: serious adverse reactions re-evaluated on the basis of suspected adverse reaction reports to the Committee on Safety of Medicines. Gut 51:536–539

31. Maconi G, Dominici R, Molteni M et al (2008) Prevalence of pancreatic insufficiency in inflammatory bowel diseases. Assessment by fecal elastase-1. Dig Dis Sci 53:262–270

32. Gschwantler M, Kogelbauer G, Klose W et al (1995) The pancreas as a site of granulomatous inflammation in Crohn's disease. Gastroenterology 108:1246–1249

33. Worcester EM (2002) Stones from bowel disease. Endocrinol Metab Clin North Am 31:979–999

34. Caudarella R, Rizzoli E, Pironi L et al (1993) Renal stone formation in patients with inflammatory bowel disease. Scanning Microsc 7:371–379

35. McConnell N, Campbell S, Gillanders I et al (2002) Risk factors for developing renal stones in inflammatory bowel disease. BJU Int 89:835–841

36. Stote RM, Smith LH, Dubb JW et al (1980) Oxypurinol nephrolithiasis in regional enteritis secondary to allopurinol therapy. Ann Intern Med 92:384–385

37. Ishii G, Nakajima K, Tanaka N (2009) Clinical evaluation of urolithiasis in Crohn's disease. Int J Urol 16:477–480
38. Greenstein AJ, Sachar DV, Tzakis A et al (1984) Enterovesicular fistulae in Crohn's disease. Am J Surg 147:788–792
39. Schwartz DA, Loftus EV, Tremaine WJ et al (2002) The natural history of fistulizing Crohn's disease in Olmsted County, Minnesota. Gastroenterology 122:875–880
40. Herrmann KA, Michaely HJ, Zech CJ et al (2006) Internal fistulas in Crohn's disease: magnetic resonance enteroclysis. Abdom Imaging 31:675–687
41. Peeters H, Vander Cruyssen B, Mielants H et al (2008) Clinical and genetic factors associated with sacroiliitis in Crohn's disease. J Gastroenterol Hepatol 23:132–137
42. de Vlam K, Mielants H, Cuvelier C et al (2000) Spondyloarthropathy is underestimated in inflammatory bowel disease: prevalence and HLA association. J Rheumatol 27:2860–2865
43. Mielants H, Veys EM, De Vos M et al (1995) The evolution of spondyloarthropathies in relation to gut histology. Clinical aspects. J Rheumatol 22:2266–2272
44. Dekker-Saeys BJ, Meuwissen SGM, Van Den Berg-Loonen EM et al (1978) Prevalence of peripheral arthritis, sacroiliitis, and ankylosing spondylitis in patients suffering from inflammatory bowel disease. Ann Rheum Dis 37:36–41
45. Weiner SR, Clarke J, Taggart NA et al (1991) Rheumatic manifestations of inflammatory bowel disease. Semin Arth Rheum 20:353–366
46. Tavarela Veloso F (2004) Review article: skin complications associated with inflammatory bowel disease. Aliment Pharmacol Ther 20:50–53
47. Maathuis JB, Van Look PFA, Michie EA (1978) Changes in volume total protein and ovarian concentrations of peritoneal fluid throughout the human menstrual cycle. J Endocrinol 76:123–133
48. Komickx PR, Renaer M, Brosens IA (1980) Origin of peritoneal fluid in women: an ovarian exudation product. Br J Obstet Gynaecol 87:177–183
49. Kim JS, Lee HJ, Woo SK et al (1997) Peritoneal inclusion cysts and their relationship to the ovaries: evaluation with sonography. Radiology 204:481–484

Chapter 6
Perianal Complications

Crohn's disease is commonly complicated by a variety of perianal manifestations. Perianal fistulas and abscesses can result in substantial morbidity, including scarring, continual seepage, and fecal incontinence [1].

Perianal abscess occurs in up to 80 % of patients with CD [2], as the frequency of perianal fistulas varies from 17 to 43 % [3–9]. A distal involvement of the gastrointestinal tract increases itself the incidence of perianal manifestations. In fact, patients with disease confined to the colon have a higher incidence of perianal fistulas, and their rate of incidence approaches 100 % in patients with CD that involves the rectum [4, 10].

For what concerns the pathogenesis of perianal abscess, it may result from a cryptoglandular infection or an obstructed sinus tract [1].

The exact pathogenesis of perianal fistula is instead unidentified. The first theory suggests that fistulas may be due to the elongation of deep penetrating ulcers in the anus or distal rectum; over time, feces collect in these ulcers, and the pressure of evacuation forces the fecal matter into the subcutaneous tissue, extending the ulcer and creating fistula [1, 11]. The second theory suggests that fistulas result from an anal gland abscess that serves as the point of origin for a fistulous tract; the complexity of fistula that follows depends on the type of abscess drained [12].

Perianal CD may herald the development of intestinal manifestations by several months to several years. About two-thirds of patients with perianal disease will be diagnosed with intestinal disease within 1 year and another third within 1–5 years, with only a few patients being diagnosed after more than 5 years. Only a small proportion of patients with Crohn's disease may persist in having isolated perianal involvement [13, 14].

Surgical management of perianal CD depends on the extent of the primary fistula and of any secondary fistulous tracks or associated abscesses, being usually more aggressive with larger fistulas and conservative in the case of smaller lesions. Consequently, an accurate preoperative classification with adequate imaging techniques is required to clearly identify the fistula and its intra- and extrasphincteric extent and, as far as possible, to avoid aggressive procedures and/or recurrences that may result from any undiagnosed secondary branches.

Moreover, preservation of fecal continence is the principal consideration, and all treatment strategies should aim to preserve the integrity of the external sphincter.

6.1   Classification of Fistulas

Classification systems for perianal fistulizing disease are useful in determining what surgical procedure (if any) should be performed. Several classifications have been used to define the different types of fistulas. The most anatomically detailed classification system, and the most widely used, is that one formulated by Parks and his colleagues; it encompasses the external anal sphincter as anatomical landmark, and with reference to the coronal plane, it distinguishes four different kinds of fistula: intersphincteric, trans-sphincteric, supra-sphincteric, and extrasphincteric (Table 6.1) [15]. A superficial, subcutaneous fistula, instead, has no relation to the sphincter or the perianal gland and therefore is not part of the Parks' classification (Fig. 6.1).

Table 6.1 Parks' classification [15]

Intersphincteric: within the intersphincteric space, between the internal and external sphincters

Trans-sphincteric: extends through both the internal and external sphincters

Supra-sphincteric: from the skin surface to the ischiorectal fossa, without communication with the anal sphincter

Extrasphincteric: above the levator ani muscle, within the pelvic region
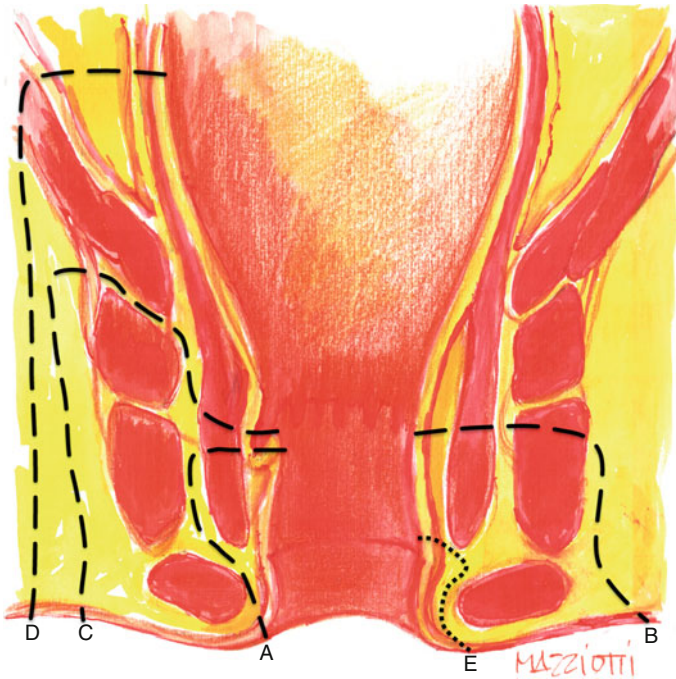
Fig. 6.1 Parks' classification (for anatomical correlation, see Fig. 3.6): *A* intersphincteric fistula, *B* trans-sphincteric fistula, *C* supra-sphincteric fistula, *D* extrasphincteric fistula, *E* subcutaneous fistula (not part of Parks' classification)

Table 6.2 St. James University Hospital classification [15]

Grade 0	Normal aspect
Grade 1	Simple linear intersphincteric fistula
Grade 2	Complex intersphincteric fistula with abscess or secondary track
Grade 3	Trans-sphincteric fistula
Grade 4	Trans-sphincteric fistula with abscess or secondary track within the ischioanal or ischiorectal fossa
Grade 5	Supralevator and translevator fistula

More recently, new MR imaging-based classifications have been proposed, such as the classification of St. James Hospital [16]. It consists of five grades and relates the Parks' surgical classification to MRI anatomy seen on both axial and coronal planes (Table 6.2) [16].

6.2   MRI in Perianal CD

The role of imaging in perianal complications of CD is to identify the primary fistulous track, even in the absence of cutaneous openings, the possible secondary tracks, and the sites of any abscess cavities, and to define their relations with the sphincters, the levator ani muscle, and the ischiorectal and ischioanal fossa [17].

As mentioned in Chap. 1, MRI performed along the coronal and axial planes demonstrates fistulous tracks in relation to the sphincteric complex, ischiorectal and ischioanal fossae, and levator plate.

Tracts are described in accordance with the terminology illustrated by Parks et al. [15].

In particular, in order to describe the exact site and direction of fistulous tract according to the surgical view, radiologist should correlate the axial MRI findings to the "anal clock."

Abscesses and active tracts filled with pus and granulation tissue appear as hyperintense structures on T2-weighted and STIR images (Figs. 6.2, 6.3, and 6.4). In particular, identification
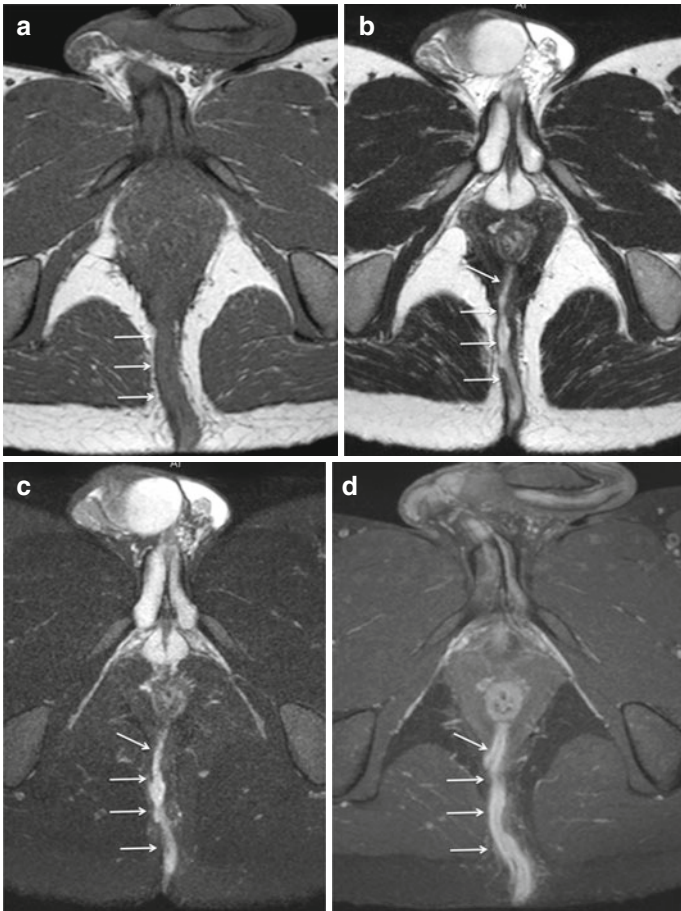
Fig. 6.2 Trans-sphincteric fistula. Axial-oblique T1-weighted TSE (**a**) and T2-weighted TSE images, performed without (**b**) and with fat saturation (**c**), show a posterior midline trans-sphincteric fistula, hypointense on T1-weighted image, and hyperintense on T2-weighted images (*arrows*). Contrast enhancement of the inflamed wall of the fistula is well depicted after i.v. injection of gadolinium (**d**)
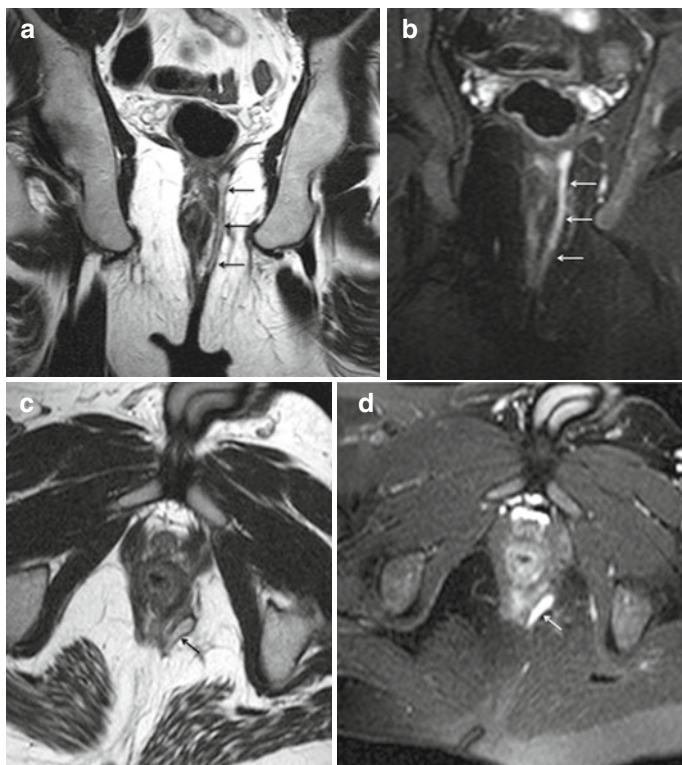
Fig. 6.3 Extrasphincteric fistula. Coronal-oblique (**a, b**) and axial-oblique (**c**, **d**) T2-weighted TSE images, performed without (**a**, **c**) and with fat saturation (**b**, **d**), show a left hyperintense extrasphincteric fistula (*arrows*). On coronal-oblique (**e**) and axial-oblique (**f**) T1-weighted TSE fat-saturated images, performed after gadolinium administration, enhancement of the fistulous walls is well depicted (*arrows*)
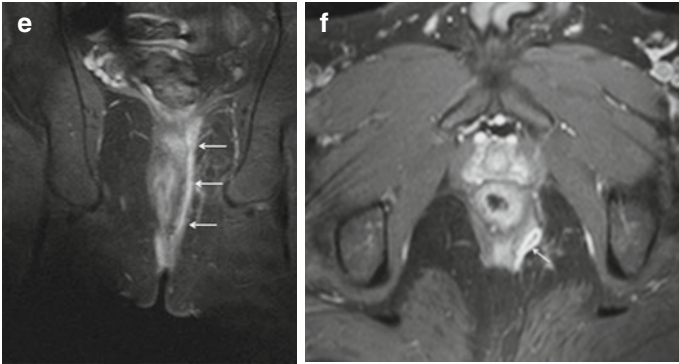
Fig. 6.3   (continued)

of the tract is most easily performed on fat-saturated sequences, whereas the T2-weighted sequences without fat suppression give more detailed information about the relationship of the tract with surrounding anatomical structures (Fig. 6.5).

Active tracts are often surrounded by hypointense fibrous walls, which can be relatively thick, especially in cases of recurrent disease and/or previous surgery (Fig. 6.6). Some hyperintensity in this fibrous tissue may seldom be seen, probably due to associate inflammatory edema. This hyperintensity may also extend beyond the tract and its fibrous sleeve, reflecting adjacent inflammation (Fig. 6.7).

On contrast-enhanced T1-weighted images, active fistulous tracks brilliantly enhance, as do the walls of abscess cavities (Figs. 6.2, 6.3, and 6.8). Retained pus remains unenhanced, with resulting ring enhancement, an appearance that is typical of abscess formation elsewhere in the body.
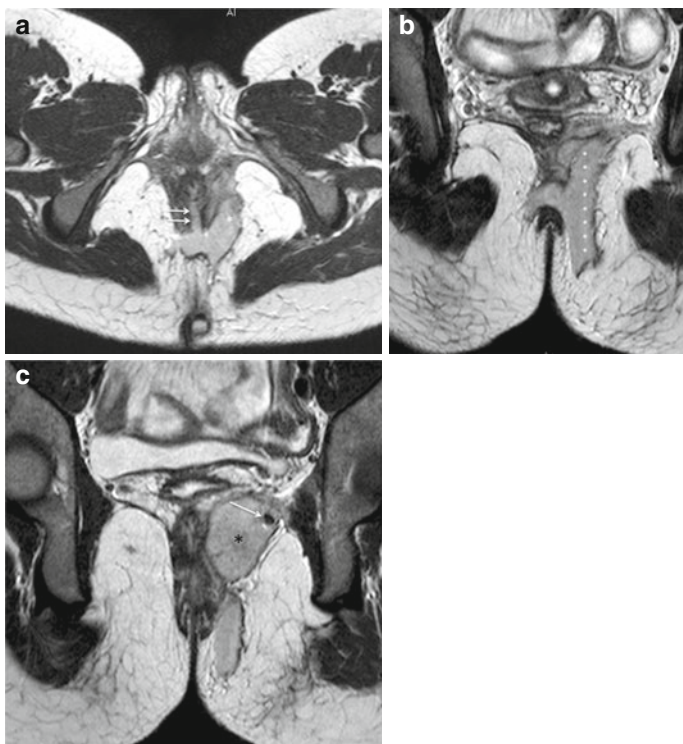
Fig. 6.4 Trans-sphincteric fistula with abscess. Axial-oblique (**a**) and coronal-oblique (**b**, **c**) T2-weighted TSE images show a posterior midline trans-sphincteric fistula (*arrows* in **a**) with its course in left ischioanal fossa (*white asterisks* in **a** and **b**). A voluminous perianal abscess can also be seen (*black asterisk* in **c**), showing a small gas bubble in its context (*arrow*)

The fistulous tract should be identified and followed throughout its entire course, and in case of multiple tracts, a verification of communication among the tracts is very relevant.

In particular, some considerations have to be done to determine whether a fistula is contained by the external sphincter or has extended beyond it.
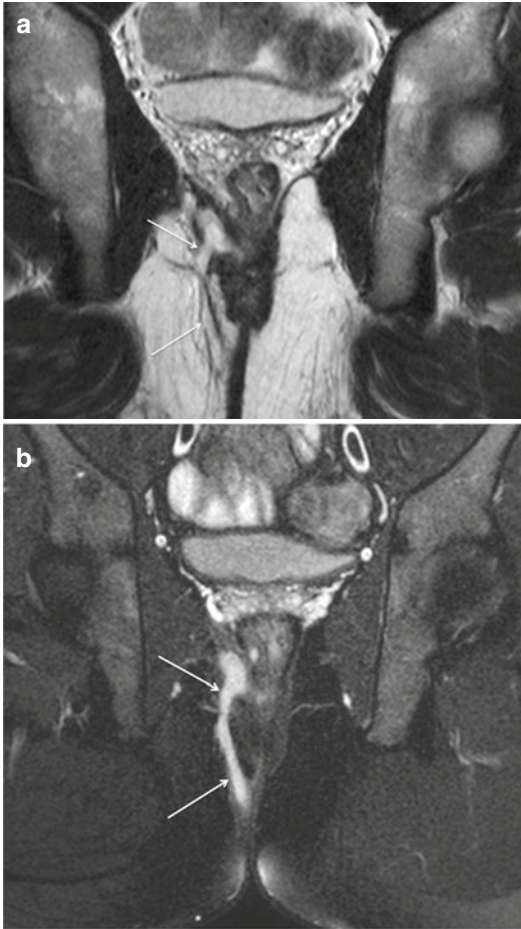
Fig. 6.5 Trans-sphincteric fistula. Coronal-oblique T2-weighted TSE image (**a**) shows a right trans-sphincteric fistula, involving the ischioanal fossa (*arrows*). Fat-saturated image (**b**) clearly shows the fistulous tract (*arrows*) because bright signal of fat, in which the fistula is located, is suppressed
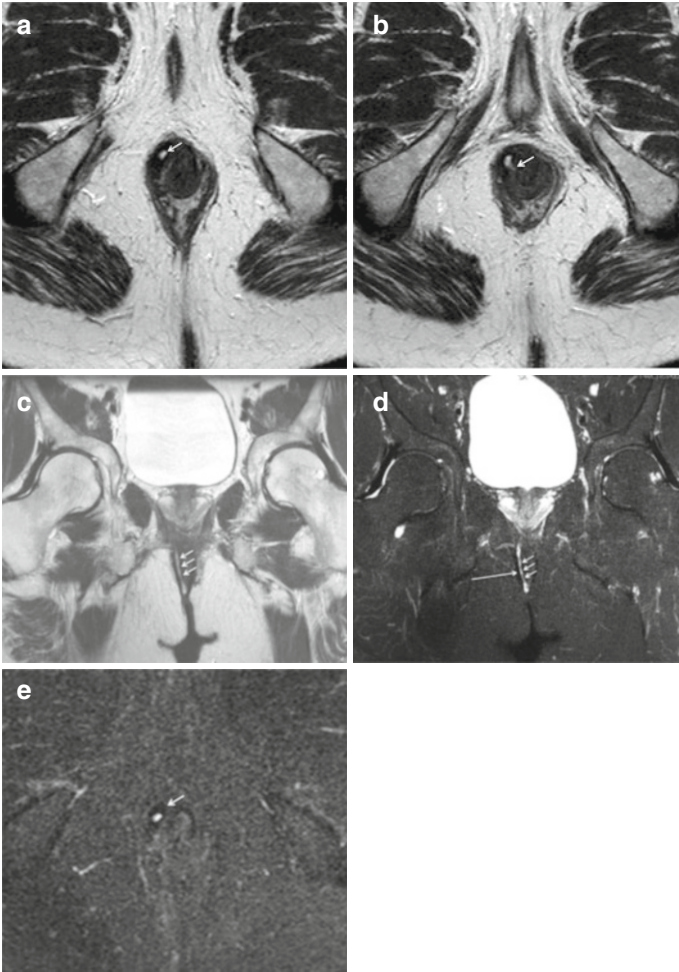
Fig. 6.6 Intersphincteric fistula. Axial-oblique T2-weighted TSE images (**a**) show intersphincteric fistula at 11 o'clock (*arrow*). In a more cranial image (**b**), the internal opening is demonstrable (*arrow*). Coronal-oblique T2-weighted TSE images performed without (**c**) and with fat saturation (**d**) show right intersphincteric fistula, traceable along most of its course (*short arrows*), with sparing of ischioanal fossa. Note the hypointense fibrous wall surrounding the active fistula (*long arrow* in **d**), also confirmed in the axial T2-weighted TSE fat-saturated image (**e**) obtained through its middle part (*arrow*)
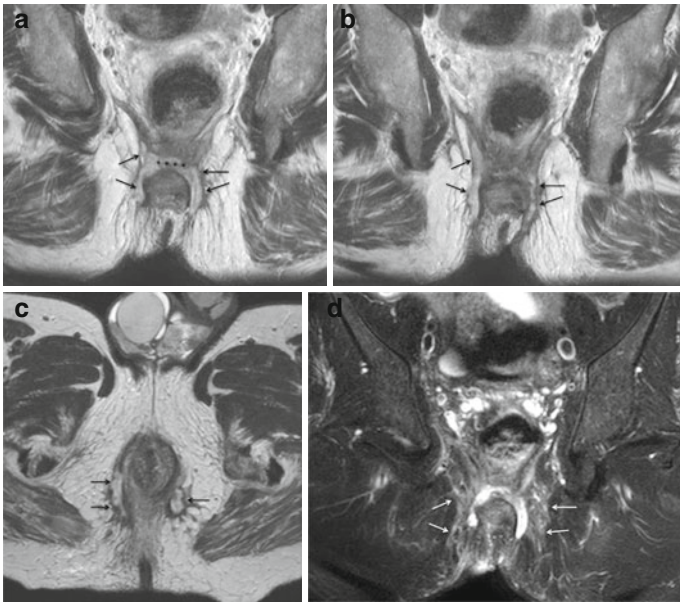
Fig. 6.7 Complex perianal fistula. Coronal-oblique T2-weighted TSE images (**a**, **b**) and axial-oblique T2-weighted TSE image (**c**) show a horse-shoe-like intersphincteric fistulous tract (*asterisks* in **a**), which extend bilaterally toward the ischioanal fossa through the external sphincter (*arrows*). Coronal-oblique T2-weighted TSE fat-saturated image (**d**) well demonstrates perifistulous inflammatory edema (*arrows*)

In fact, if a fistula remains contained by the external sphincter, it is highly likely to be intersphincteric (Fig. 6.6).

On the contrary, any evidence of a fistulous tract in the ischioanal fossa effectively excludes an intersphincteric fistula.

Moreover, it should also be considered that trans-, supra-, and extrasphincteric fistulas share the common feature of a tract that lies beyond the confines of the external sphincter. Although trans-sphincteric fistulas are the most common cause of a tract in the ischioanal fossa (Fig. 6.9), it must be remembered that a differentiation between these three fistulas is possible only by
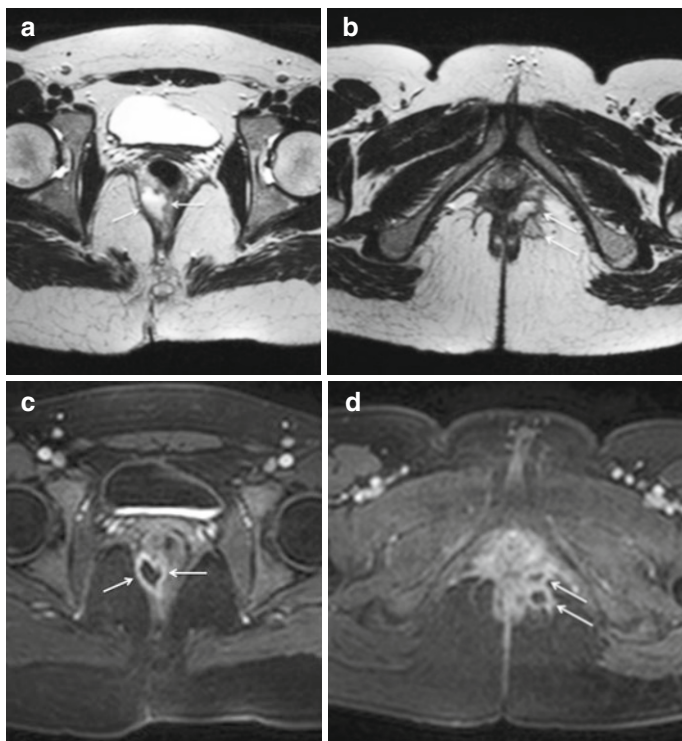
Fig. 6.8 Perianal fistula with multiple abscesses. Axial-oblique T2-weighted TSE image (**a**) shows a supralevatoric right-sided abscess (*arrows*). A more caudal scan (**b**) demonstrates other two small abscesses in the left ischioanal fossa (*arrows*). Axial-oblique T1-weighted TSE fat-saturated images, obtained after i.v. injection of gadolinium (**c**, **d**), show peripheral contrast enhancement of abscesses, containing a central focus of non-enhancing pus (*arrows*)
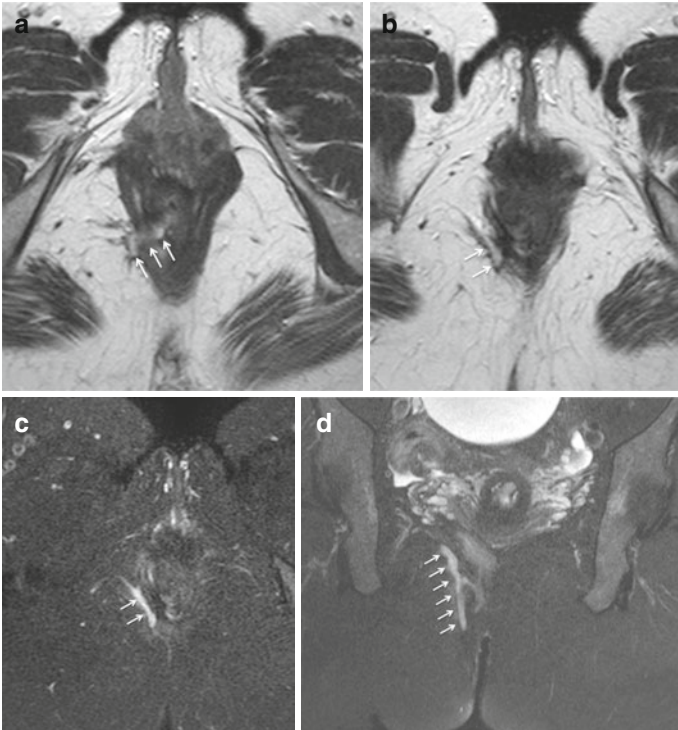
Fig. 6.9 Trans-sphincteric fistula. Axial-oblique T2-weighted TSE image, showing the internal opening of fistula at 7 o' clock (*arrows*). More caudally, T2-weighted TSE images, performed without (**b**) and with fat saturation (**c**), show a fistulous tract in the right ischioanal fossa (*arrows*). Coronal-oblique T2-weighted TSE fat-saturated image (**d**) clearly traces the craniocaudal extent of fistula (*arrows*)

Fig. 6.10 Perianal abscess. Axial-oblique (**a**), coronal-oblique (**b**), and sagittal (**c**) T2-weighted TSE images show a voluminous perianal abscess (*arrows*) that displaces to right side the sphincteric complex (*asterisks*)

locating the internal opening and clearly determining the course between this and the primary tract [18].

Finally, in presence of voluminous perianal abscesses, eventual fistulous tracts can be hidden, due to the compression or dislocation of the sphincter complex itself and, in more severe cases, large dehiscence with nearby pelvic viscera may also be found (Figs. 6.10 and 6.11).
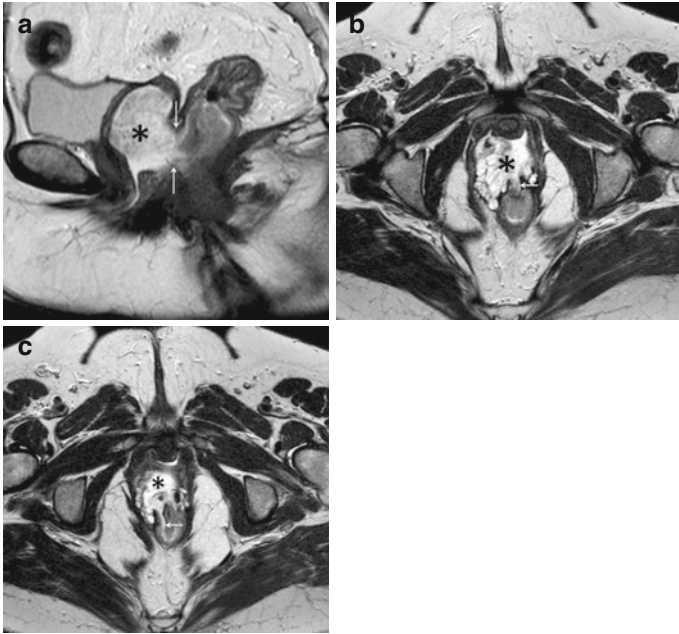
Fig. 6.11 Rectovaginal communication. Hysterectomied patient. Sagittal (**a**) and axial-oblique (**b**, **c**) T2-weighted TSE images clearly depict a wide defect of the posterior vaginal wall (*arrows* in **a**). On axial-oblique images (**b**, **c**), some fistulous tracts demonstrate a communication with the anterior wall of the rectum (*arrows*). Vaginal lumen is filled by fecaloid material (*asterisk*)

References

1. Schwartz DA, Pemberton JH, Sandborn WJ (2001) Diagnosis and treatment of perianal fistulas in Crohn disease. Ann Intern Med 135:906–918
2. Makowiec F, Jehle EC, Becker HD et al (1997) Perianal abscess in Crohn's disease. Dis Colon Rectum 40:443–450

3. Rankin GB, Watts HD, Melnyk CS et al (1979) National Cooperative Crohn's Disease Study: extraintestinal manifestations and perianal complications. Gastroenterology 77:914–920

4. Williams DR, Coller JA, Corman ML et al (1981) Anal complications in Crohn's disease. Dis Colon Rectum 24:22–24

5. Buchmann P, Keighley MR, Thompson H et al (1980) Natural history of perianal Crohn's disease. Ten year follow-up: a plea for conservatism. Am J Surg 140:642–644

6. van Dongen LM, Lubbers EJ (1986) Perianal fistulas in patients with Crohn's disease. Arch Surg 121:1187–1890

7. Goebell H (1990) Perianal complications in Crohn's disease. Neth J Med 37(Suppl 1):S47–S51

8. Fielding JF (1972) Perianal lesions in Crohn's disease. J R Coll Surg Edinb 17:32–37

9. American Gastroenterological Association (2003) AGA technical review on perianal Crohn's disease. Gastroenterology 125:1508–1530

10. Hellers G, Bergstrand O, Ewerth S et al (1980) Occurrence and outcome after primary treatment of anal fistulae in Crohn's disease. Gut 21:525–527

11. Safar B, Sands D (2007) Perianal Crohn's disease. Clin Colon Rectal Surg 20:282–293

12. Parks A (1961) The pathogenesis and treatment of fistula-in-ano. Br Med J 1:463–469

13. Lockhart-Mummery HE (1975) Symposium. Crohn's disease: anal lesions. Dis Colon Rectum 18:200–202

14. Alabaz O, Weiss EG (1999) Anorectal Crohn's disease. In: Beck D, Wexner SD (eds) Fundamentals of anorectal surgery, 2nd edn. WB Saunders, Philadelphia, pp 498–509

15. Parks AG, Gordon PH et al (1976) A classification of fistula-in-ano. Br J Surg 63:1–12

16. Morris J, Spencer JA, Simon N et al (2000) MR imaging classification of perianal fistulas and its implications for patient management. Radiographics 20:623–635

17. Maccioni F, Colaiacomo MC, Stasolla A et al (2002) Value of MRI performer with phased-array coil in the diagnosis and pre-operative classification of perianal and anal fistula. Radiol Med 104:58

18. Halligan S, Stoker J (2006) Imaging of fistula in ano. Radiology 239:18–33

Chapter 7
Other Indications for MRE

The potential of MREg/MREc to evaluate Crohn's disease patients has been investigated extensively in the previous chapters. Nowadays, technological developments have extended the role of MRI in the evaluation of the gastrointestinal tract.

In fact, both these techniques are assuming an interesting role also in the detection of other small bowel diseases, including tumors [1, 2].

Moreover, the gastrointestinal radiologist should take into account that an increasingly large spectrum of bowel and mesenteric diseases can be incidentally diagnosed by performing MR of the small bowel.

An example can be seen in patients with suspicion of *gastrointestinal tract congenital rotation and fixation anomalies*. In such cases, symptoms are not caused by the abnormal position of the bowel, but they are due to complications that occur when an abnormal position or fixation of the mesentery may cause volvulus. Symptoms can vary from mild (e.g., nonspecific complaints that could lead to the incorrect diagnosis of gastric ulcerations or irritable bowel syndrome) to acute (i.e., midgut volvulus), rare in adults [3, 4]. Some highly suggestive signs of midgut rotation and fixation anomalies are the position on the right-hand side of the abdomen of the duodenojejunal junction

(ligament of Treitz) and proximal loops of the jejunum, as well as the lack of the normal midline position of the horizontal part of the duodenum. A rotation of the superior mesenteric and adjacent mesenteric fat around the superior mesenteric artery (*whirl sign*), even if not specific to midgut volvulus, can also be related [5].

A primarily pediatric condition, rarely seen in adults, is *intussusception*, defined as the invagination of a bowel loop with its mesenteric fat into the lumen of the adjacent bowel [6]. The use of a cross-sectional imaging technique as MR of the small bowel frequently allows the recognition of this condition, which presents with a pathognomonic target-like (bowel-into-bowel) mass, due to the telescoping of the bowel and its trapped mesenteric fat and vessels into an adjacent bowel tract [6–8], a condition that may finally cause bowel obstruction.

Sometimes, protrusion of the viscera within the peritoneal cavity through a normal or abnormal peritoneal or mesenteric opening (congenital or acquired) can be seen during MR of the small bowel, allowing the diagnosis of *internal hernias*. Clinical manifestations may be not specific, with only mild abdominal complaints if the hernia is reducible. Naturally, in case of incarcerated hernia, acute small bowel obstruction is very frequent [9–11]. There can be different types of internal hernias (paraduodenal, pericecal, transmesenteric, intersigmoid, paravesical, and Winslow's foramen hernias), and they all can be seen by performing a MREg/MREc [9–12].

A congenital anomaly most common in the gastrointestinal tract and particularly in patients affected by Crohn's disease is *Meckel's diverticulum* [13]. It is the result of incomplete atrophy of the omphalomesenteric duct, and it has to be considered as a true diverticulum on the antimesenteric side of the distal ileum containing three layers of the bowel wall. Ectopic gastric or pancreatic mucosa is present in 50 % of all Meckel's diverticula; in fact, the most frequent complication is represented by peptic ulceration and bleeding from heterotopic mucosa [13, 14].

On MREg/MREc, Meckel's diverticulum is diagnosed when a saccular, blind-ended structure continuous with the ileum is identified; when inflamed, it usually has a distended lumen and surrounding inflammatory infiltration.

Multiple polypoid lesions in the gastrointestinal tract may be detected on high-resolution MR imaging of the small bowel in *Peutz-Jeghers syndrome*. Polyps may vary in location, appearance (sessile or pedunculated), and size (from small to large) and tend to enhance after injection of gadolinium, helping to differentiate them from bowel content. MREg/MREc may be performed to detect and monitor polyps of the gastrointestinal tract (polyps larger than 1.5–2 cm are considered potentially malignant and should be removed) and in patients with Peutz-Jeghers syndrome, in the suspicion of intussusception. Although multiple polyps of the gastrointestinal tract are typical of Peutz-Jeghers syndrome, they are not specific and may be found also in other syndromes such as *juvenile polyposis*, *familial adenomatous polyposis*, and *Cronkhite-Canada syndrome* [15]. Naturally, the diagnosis must be based not only on radiological findings but also on clinical and histopathology results [16].

For what concerns the neoplastic disease, *gastrointestinal stromal tumors* (*GIST*) are mesenchymal neoplasms affecting the gastrointestinal tract, with the highest prevalence in the stomach (70 %). In rare cases, they may be found in the omentum, mesentery, or retroperitoneum. The clinical presentation is variable, also depending on the involvement of adjacent organs, metastases, or peritoneal seeding.

They usually appear as well-circumscribed, heterogeneous, and exophytically growing masses with peripheral contrast enhancement. The degree of signal intensity on MRI and its homogeneity depend on tumor necrosis and hemorrhage. Solid parts of the tumor may appear hyperintense on T2-weighted images and enhance after intravenous injection of gadolinium [17–19].

Lymphoma is considered to account for 20 % of all primary small bowel malignancies.

The terminal ileum is considered to be the most frequently affected site in the small bowel, as there is a relative abundance of lymphoid tissue, and patients affected by inflammatory bowel disease are associated with a small but measurable increased risk of lymphoma due to medications, disease activity, and underlying disease-related immune alterations [20].

Infiltrative and polypoid forms are the two main growth patterns of primary gastrointestinal lymphoma. Infiltration is usually circumferential, homogeneous, and over a different length. Multifocal involvement of the small bowel is possible and is thought to be more common in primary T-cell lymphoma [21]. Preservation of the surrounding fat tissue and a long involved segment helps to differentiate lymphoma from adenocarcinoma, even if a high-grade lymphoma may infiltrate the mesenteric fat. Lymphoma may also ulcerate, perforate, or create fistulas into the adjacent mesenteric or adjacent bowel loops, which makes it hard to distinguish from Crohn's disease on MREg/MREc [21–23].

Adenocarcinoma is a malignant neoplasm of the glandular epithelium. Despite its low incidence (<1 % of all primary malignancies), it is the most common primary malignant tumor of the small bowel and usually occurs in the proximal intestine, duodenum, and jejunum. It often metastasizes to regional lymph nodes, liver, or peritoneum [24–26]. At MREg/MREc, it may appear as an infiltrative lesion that causes luminal stenosis and obstruction, with pre-stenotic dilatation or as polypoid intraluminal masses, less common. MR fluoroscopy shows circumferential and sharply demarcated narrowing of the lumen, with shouldering of the margins due to mucosal destruction. A moderate and heterogeneous enhancement is typically demonstrable on post-gadolinium images. Usually, adenocarcinomas tend to

infiltrate the entire bowel wall and extend into the surrounding mesenteric fat tissue, causing a desmoplastic reaction, which is easily assessed at MRI. Other typical features of adenocarcinomas include the proximal location, the solitary presentation, and the involvement of short segments of bowel with infiltration of perivisceral fat [27].

Carcinoids are well-differentiated endocrine tumors arising from the enterochromografin cells at the base of the Lieberkühn's crypts and account for nearly 25 % of primary malignant neoplasms of the small bowel [26]. At MREg/MREc, such tumors appear as mural thickening, usually associated with linear soft tissue strands radiating toward the surrounding mesentery in a stellate appearance. On T1-weighted images, these lesions are isointense to muscle and mildly hyperintense to muscle on T2-weighted images. After intravenous injection of gadolinium, the primary lesion shows hypervascular contrast enhancement. MR fluoroscopy shows a solitary or multiple round, intramural, or intraluminal filling defects that encroach on the intestinal lumen. Usually, these neoplasms cause kinking of the bowel wall and secondary narrowing of the lumen, rather than annular stenosis [28–31].

Among the benign neoplasms of the small bowel, *adenomas* are considered to be the most common [27]. They can present as a polypoid pedunculated mass on a stalk, as a sessile mass, or as a mural nodule within the mucosa. Adenomatous polyps appear as intraluminal homogeneous enhancing masses on post-contrast and fat-suppressed T1-weighted images, confined within the boundaries of intestinal lumen. On both HASTE and TrueFISP sequences, they appear as rounded low signal intensity intraluminal masses, while MR fluoroscopy shows an intraluminal filling defect, with mild narrowing of the lumen and without any proximal dilatation [32].

References

1. Masselli G, Polettini E, Casciani E, Bertini L, Vecchioli A, Gualdi G (2009) Small-bowel neoplasms: prospective evaluation of MR enteroclysis. Radiology 251:743–750
2. Tolan DJ, Greenhalgh R, Zealley IA, Halligan S, Taylor SA (2010) MR enterographic manifestations of small bowel Crohn disease. Radiographics 30:367–384
3. Berrocal T, Lamas M, Gutieérrez J, Torres I, Prieto C, del Hoyo ML (1999) Congenital anomalies of the small intestine, colon, and rectum. Radiographics 19:1219–1236
4. Kanazawa T, Kasugai K, Miyata M, Miyashita M, Mizuno M, Nagase F et al (2000) Midgut malrotation in adulthood. Intern Med 39:626–631
5. Lee NK, Kim S, Jeon TY, Kim HS, Kim DH, Seo HI et al (2010) Complications of congenital and developmental abnormalities of the gastrointestinal tract in adolescents and adults: evaluation with multimodality imaging. Radiographics 30:1489–1507
6. Kim YH, Blake MA, Harisinghani MG, Archer-Arroyo K, Hahn PF, Pitman MB et al (2006) Adult intestinal intussusception: CT appearances and identification of a causative lead point. Radiographics 26:733–744
7. Guillén Paredes MP, Campillo Soto A, Martín Lorenzo JG, Torralba Martínez JA, Mengual Ballester M, Cases Baldó MJ (2010) Adult intussusception – 14 case reports and their outcomes. Rev Esp Enferm Dig 102:32–40
8. Renzulli P, Candinas D (2010) Idiopathic small-bowel intussusception in an adult. CMAJ 182(3):E148
9. Takeyama N, Gokan T, Ohgiya Y, Satoh S, Hashizume T, Hataya K (2005) CT of internal hernias. Radiographics 25:997–1015
10. Zissin R, Hertz M, Gayer G, Paran H, Osadchy A (2005) Congenital internal hernia as a cause of small bowel obstruction: CT findings in 11 adult patients. Br J Radiol 78:796–802
11. Selçuk D, Kantarci F, Oğüt G, Korman U (2005) Radiological evaluation of internal abdominal hernias. Turk J Gastroenterol 16:57–64
12. Mathieu D, Luciani A, GERMAD Group (2004) Internal abdominal herniations. AJR Am J Roentgenol 183:397–404
13. Levy AD, Hobbs CM (2004) From the archives of the AFIP Meckel diverticulum: radiologic features with pathologic correlation. Radiographics 24:565–587

14. Malik AA, Shams-ul-Bari WKA, Khaja AR (2010) Meckel's diverticulum – revisited. Saudi J Gastroenterol 16:3–7
15. Rufener SL, Koujok K, McKenna BJ, Walsh M (2008) Small bowel intussusception secondary to Peutz-Jeghers polyp. Radiographics 28:284–288
16. Kopacova M, Tacheci I, Rejchrt S, Bures J (2009) Peutz-Jeghers syndrome: diagnostic and therapeutic approach. World J Gastroenterol 15:5397–5408
17. Levy AD, Remotti HE, Thompson WM, Sobin LH, Miettinen M (2003) Gastrointestinal stromal tumors: radiologic features with pathologic correlation. Radiographics 23:283–304
18. Chourmouzi D, Sinakos E, Papalavrentios L, Akriviadis E, Drevelegas A (2009) Gastrointestinal stromal tumors: a pictorial review. J Gastrointestin Liver Dis 18:379–383
19. Stamatakos M, Douzinas E, Stefanaki C, Safioleas P, Polyzou E, Levidou G et al (2009) Gastrointestinal stromal tumor. World J Surg Oncol 7:61
20. Ang YS, Farrell RJ (2006) Risk of lymphoma: inflammatory bowel disease and immunomodulators. Gut 55:580–581
21. Ghai S, Pattison J, Ghai S, O'Malley ME, Khalili K, Stephens M (2007) Primary gastrointestinal lymphoma: spectrum of imaging findings with pathologic correlation. Radiographics 27:1371–1388
22. Rubesin SE, Gilchrist AM, Bronner M, Saul SH, Herlinger H, Grumbach K et al (1990) Non-Hodgkin lymphoma of the small intestine. Radiographics 10:985–998
23. Ziech MLW, Stoker J (2010) MRI of the small bowel: enterography. In: Stoker J (ed) MRI of the gastrointestinal tract. Springer, Heidelberg, pp 117–134
24. Buckley JA, Fishman EK (1998) CT evaluation of small bowel neoplasms: spectrum of disease. Radiographics 18:379–392
25. Gore RM, Mehta UK, Berlin JW, Rao V, Newmark GM (2006) Diagnosis and staging of small bowel tumours. Cancer Imaging 6:209–212
26. Maglinte DD, Lappas JC, Sandrasegaran K (2008) Malignant tumors of the small-bowel. In: Gore R, Levine M (eds) Textbook of gastrointestinal radiology, 3rd edn. Saunders Elsevier, Philadelphia, pp 853–869
27. Masselli G, Gualdi G (2010) Evaluation of small-bowel tumors: MR enteroclysis. Abdom Imaging 35:23–30
28. Fork FT, Aabakken L (2007) Capsule enteroscopy and radiology of the small intestine. Eur Radiol 17:3103–3111

29. Gourtsoyiannis N, Papanikolaou N (2008) MR enteroclysis. In: Gore R, Levine M (eds) Textbook of gastrointestinal radiology, 3rd edn. Saunders Elsevier, Philadelphia, pp 765–774

30. Van Weyenberg SJ, Meijerink MR, Jacobs MA, Van der Peet DL, Van Kuijk C, Mulder CJ et al (2010) MR enteroclysis in the diagnosis of small-bowel neoplasms. Radiology 254:765–773

31. Gourtsoyiannis N, Ji H, Odze RD (2002) Malignant small intestinal neoplasm. In: Baert AL, Sartor K (eds) Radiological imaging of the small intestine. Springer, Berlin, pp 399–428

32. Fidler JL, Guimaraes L, Einstein DM (2009) MR imaging of the small-bowel. Radiographics 29:1811–1825